

**State of charge estimation  
for lithium-ion batteries with model-based algorithms**

Azizeh Lotfivand

A thesis submitted in partial fulfilment of the requirements of Liverpool John  
Moore's University for the degree of Master of Philosophy

May 2023

## **Abstract**

Electric vehicles have revolutionized automotive manufacturing in recent years. However, they are faced with some challenges that are essential to overcome to have an acceptable performance. Therefore, these kinds of vehicles need a safe, fast charging, and extended life cycle battery. Lithium-ion batteries have these characteristics and are used in different state-of-the-art industries. Having reliable data for the Lithium-ion batteries Battery Management System (BMS) is critical. They are required to monitor and control all parameters such as State of Charge and State of Health. These parameters cannot be measured directly, and the system should estimate them accurately and reliably. This study consists of 5 main parts: literature review, modelling, research methodology, data collection, and data analysis and interpretation. Firstly, the recent papers related to methods of SOC (State of Charge) estimation were reviewed to find out the existing algorithms' productivity and deeply realized in literature reviewing step.

Because of their inherent safety, fast charging capacity, and extended cycle life, lithium-ion batteries are preferred over other types of batteries in electric vehicle applications. It's critical to be able to determine state factors like state of charge and state of health to generate an accurate battery model. The state of charge estimation algorithms for generic Lithium-ion batteries were enhanced using LA92 drive cycle experiment data. To begin, a mathematical model for an analogous circuit battery was created with the goal of accurately imitating the behaviour of a lithium-ion battery. The Thevenin model is created by 2 RC branches and identifies the model parameters with the Coulomb Counting, Extended Kalman Filter (EKF) and Unscented Kalman Filter (UKF). The Hybrid Pulse Power Characterization (HPPC) test data obtained at 40°C, 25°C, 10°C, 0°C, and -10°C are used to calculate the OCV 3-dimensional curve as a function of SOC and T (Temperature). A comparison of the three methods is shown, indicating that the UKF method of battery SOC evaluation is more accurate than the Coulomb Counting method and EKF.

## **Acknowledgements**

First and foremost, I am extremely grateful to my supervisors, Dr. Barry Gomm and Prof. Dingli Yu for their invaluable advice, continuous support, and patience during my MPhil study. Their immense knowledge and plentiful experience have encouraged me in all the time of my academic research and daily life. I would also like to express my gratitude to my husband and my daughter. Without their tremendous understanding and encouragement in the past two years, it would be impossible for me to complete my study.

# Contents

<b>1.</b>	<b>Introduction</b> .....	8
1.1.	Batteries for electric vehicles.....	8
1.2.	Aims and Objectives.....	15
1.3.	Published papers.....	16
<b>2.</b>	<b>Literature review</b> .....	17
2.1	Introduction .....	17
2.2	First example for battery management system.....	21
2.3	Second example for battery management system.....	22
2.4	The third example for battery management system.....	26
2.5	Estimation Methods for State of Charge .....	43
2.6	Kalman Filter family .....	44
<b>3.</b>	<b>SOC Estimation Based on Kalman Filter</b> .....	66
3.1	Introduction .....	66
3.2	Battery modelling.....	66
3.3	Applying Extended Kalman Filter for the battery model .....	68
3.4	Applying Unscented Kalman Filter for the battery model .....	69
3.5	Conclusion .....	74
<b>4.</b>	<b>Analysis and interpretation of data</b> .....	74
4.1	Data Analysis for Extended Kalman Filter .....	74
4.2	RMSE values for Terminal Voltage and SOC in EKF .....	82
4.3	Data analysis for Unscented Kalman Filter .....	82
4.4	RMSE values for Terminal Voltage and SOC in UKF .....	91
<b>5.</b>	<b>Conclusion</b> .....	92
5.1	Further Work.....	92
<b>6.</b>	<b>References</b> .....	93
<b>7.</b>	<b>Appendix</b> .....	97
7.1	MATLAB CODES FOR EXTENDED KALMAN FILTER.....	97
7.2	MATLAB CODES FOR UNSCENTED KALMAN FILTER .....	108

## List of Tables

Table 1-1 Advantages and disadvantages of Nickel-metal hydride.....	9
Table 1-2 Advantage and disadvantage of Lithium-ion batteries.....	10
Table 1-3 Comparing Lithium batteries and Lead acid batteries.....	13
Table 2-1 Classification of models considered for battery. ....	32
Table 2-2 The classification of battery electrical model.....	33

## List of Figures

Figure 1-1 Working conditions created for SOC estimation. ....	15
Figure 2-1: Schematic of Battery Management System .....	18
Figure 2-2: Schematic diagram for first example of Battery Management System .....	21
Figure 2-3: Second example for Battery Management System .....	23
Figure 2-4: Block Diagram for the third example of battery management system C .....	26
Figure 2-5: Linear and Simple model for battery.....	34
Figure 2-6: Internal resistance varies with SOC.....	35
Figure 2-7: Internal resistance varies with temperature.....	36
Figure 2-8: Adding charging and discharging resistance to the simplest battery model.....	37
Figure 2-9: Power Fade (PF) considering in the simplest battery model.....	38
Figure 2-10: Model using voltage sources.....	39
Figure 2-11: The Dynamic RC models .....	40
Figure 2-12: OTC model.....	41
Figure 2-13: Thevenin model with 2RC pairs .....	42
Figure 2-14 Kalman filter algorithm.....	45
Figure 2-15 The estimation of the current state.....	46
Figure 2-16: EKF block diagram .....	52
Figure 2-17 Unscented Kalman Filter flowchart .....	61
Figure 2-18 The difference between actual sampling, Extended Kalman Filter and Unscented transformation.....	65
Figure 3-1 Battery Thevenin Model.....	67
Figure 4-1 Battery testing system .....	75
Figure 4-2 Dimensional OCV curve in line with State of Charge and temperature b. real points and fitted curve c. Error between real points and fitted curve. ....	76
Figure 4-3 SOC, V1, and V2 estimation curves a) SOC estimation by EKF and Coulomb Counting method b) V1 estimation by EKF c) V2 estimation by EKF.....	78
Figure 4-4 Measured and estimated battery terminal voltage.....	79
Figure 4-5 Estimation error of terminal voltage .....	80
Figure 4-6 Battery internal Resistances .....	81
Figure 4-7 Battery internal Capacities .....	82
Figure 4-8 dimensional open circuit voltage a) dimensional VOC curve related to SOC and temperature b) real points and fitted curve c) Error between real points and fitted curve .....	84
Figure 4-9 SOC, V1, and V2 estimation curves a) SOC estimation by UKF and formal Coulomb Counting method b) V1 estimation by EKF c) V2 estimation by EKF.....	88
Figure 4-10 Measured and estimated battery terminal voltage.....	88

Figure 4-11 Error of terminal voltage .....	89
Figure 4-12 Battery internal Resistances ( $\Omega$ ).....	90
Figure 4-13 Battery internal Capacities .....	90

## **Abbreviations**

SOC: state of charge

BMS: Battery Management System

SOD: State of Discharge

SOH: State of health

EV: electric vehicle

ECU: Electronic Control Unit

CAN: Control Area Network

OCV: Open-circuit voltage

DOD: Depth of discharge

SOF: State of Function

CCL: Charge Current Limit

OBD: On Board Diagnostics

DCL: Discharge Current Limit

UPS: Uninterruptible Power Supply

## **Keywords**

Electric vehicle, State of charge estimation, Battery management systems, Lithium-ion battery

# 1. Introduction

Nowadays, electric vehicles are the focus of attention because of the imperative to reduce emissions. Using electric vehicles will lead to less air pollution, less noise pollution, low costs, and using renewable energy tariffs. However, their performance is directly dependent on the battery's performance.

Perhaps the only weakness of the electric car is its batteries, resulting from the low energy density stored in the battery, many batteries must be used, which increases vehicle weight, additional energy is used to carry this weight, and the mileage is lower compared to combustion cars. Also, the charging of these batteries will take time and a high cost will be spent on buying batteries. If suitable batteries are made that do not have the current problems, of course, cars with internal combustion engines will be abandoned. Currently, Lithium-ion is so permanent and suitable. In the rest of this chapter the differences, pros and cons of several types of batteries will be thoroughly explained.

The electric vehicle industry is one of the most promising industries worldwide because of the rapid changes in manufacturing technology. It is one of the most important methods of development in the electric vehicle industry because of its advantages in low emission, high voltage, energy savings, and long service life. Lithium-ion batteries have become a basic source of energy due to their application fields, including electric cars, electric buses, underwater weapons, submarines, and space vehicles. Therefore, accurate state of charge (SOC) estimation is a crucial portion of electric vehicles. In these batteries, the problem is to prolong the lifetime of battery by preventing over charging, over discharging. Therefore, accurate estimation of state of charge of battery is essential to have more lifetime of the battery. In this study the main aim is proposing the best algorithm to SOC estimation and comparing existing methods for SOC estimation.

## *1.1. Batteries for electric vehicles*

These batteries have been made with different technology overing the last 20 years.

Lead-acid batteries

Until 1997, batteries for electric vehicle were lead-acid. The life of these batteries was three years, and they could withstand 300 to 500 cycles. They were the most common and cheapest hybrid car batteries in the past.

Two types of these batteries exist:

Batteries used for starting the motor starter: Car starter batteries should be able to charge quickly.

Batteries by Deep cycle: They are used for some special vehicles such as golf carts or forklifts.

Motor starter batteries are designed in a way that they have capability of fast charging. They are used for limited types of electric vehicles.

It is not appropriate to discharge the Lead-acid batteries at below half of their capacity, as this will shorten the battery life. It is common to use lead-acid batteries because of the maturity of the battery technology, their high availability and low cost (there are some exceptions: The first electric vehicles, like Detroit Electric, have used iron-nickel batteries).

Deep cycle lead batteries are not low cost, and their lifespan is shorter than the vehicle itself, and they need to be replaced every 3 years.

**Nickel–metal hydride batteries**

Lead-acid batteries have been replaced with nickel-metal hybrid ones. Recently their technology is going to be approximately mature.

Although their efficiency is less (60-70%) in discharging and charging than other batteries such as lead-acid batteries, their energy is higher approximately 30-80 watt-hours/kg (Wh/kg), more than lead-acid batteries. Nickel Metal hydride batteries have an incredibly long life if they are used correctly. For example, the TOYOTA RAV4 battery is of the nickel-metal type and has been shown to still work after 160,000 km (100,000 miles) and about 10 years. Table 1.1 shows the advantages and disadvantages of Nickel-metal hydride batteries. (Iwai, 2019)

*Table 1-1 Advantages and disadvantages of Nickel-metal hydride*

<b>Advantages</b>	<b>Disadvantages</b>
High stability and resistance	the ability to store up to 40% less energy than Li-ion batteries
Better safety due to less toxic substances	larger size and more weight
Lower recycling cost	high heating speed

**Lithium-ion batteries**

Lithium-ion batteries were first produced for use in laptops and electronic devices. These batteries have a long cycle life and high density of energy. Therefore, they became good candidates for using in electric vehicles. Table 1.2 explains this battery’s advantages and disadvantages. They were first used in electric vehicles in 1997. These batteries could withstand 1,000 battery cycles and the lifespan of these batteries was between 2 and 4 years. (Morita et al., 2021)

The technology of making these batteries has been improving all the time, until now these batteries can have 4,000 cycles. Also, you can use them for a lifespan of 10 years and 1 million miles. (Harlow et al., 2019) New electric cars are using new changes in the chemistry of their lithium-ion batteries that have less energy but are fire resistant, environmentally friendly, fast charging (as fast as a few minutes), and have a longer life. (Botsford and Szczepanek, 2009)

Currently, various automobile companies are testing and improving lithium-ion batteries. New data has proved that heating and charging fast causes lithium-ion batteries to deteriorate earlier

than their actual life span. For instance, the draining of the battery used in the Nissan LEAF will be twice as fast as Tesla's battery. The battery plays an important role in electric vehicles.

Table 1-2 Advantage and disadvantage of Lithium-ion batteries

<b>Advantages</b>	<b>disadvantages</b>
Better energy-to-weight ratio	high manufacturing cost
High charging speed	gradual reduction of capacity
No memory effect	high heating speed

**characteristics of batteries:**

Capacity is defined as the amount of stored energy in the battery and related to a lot of characteristics, the most important of which are:

- The surface area or physical size of the plates covered by the electrolyte.
- Weight and amount of material in plates
- The number of pages and the type of separator between them
- The amount of electrolyte and its specific mass
- Battery age
- Cell conditions - the amount of sediment at the bottom of the cell
- Temperature
- Low voltage limit
- Discharge rate

The battery capacity of an electric car is expressed in kilowatt-hours or KWh. By choosing a car with a higher battery capacity, you will have a greater range. This is like buying a gasoline car with a bigger tank. But it should be known that due to the way electric cars work, you will never have access to the battery's full capacity. The reason for this is related to the car's main management system, which prevents 100% charging and complete battery discharge to maintain efficiency and increase battery life. The capacity of current electric vehicles ranges from 17.6 kWh in the Smart EQ Fortwo to 330 kwh in the Tesla Model S. Battery capacity and other electric vehicle specifications can be Vc

**Lead acid batteries and lithium-ion - main differences**

The use of lithium-ion batteries in small devices such as laptops and smartphones has become commonplace. On the other hand, today the production of electric cars is very attractive for many companies, and as a result, the technology of lithium-ion batteries in large formats is expanding. (Horiba, 2014)

Usually, UPS (uninterruptible power supplies) batteries for emergency power devices are made of sealed (dry) lead acid batteries. These types of batteries are still preferred over lithium-ion batteries because of features such as final cost, energy storage, security, reliability, and considering the cost of these features. This battery is used for a long time in terms of rechargeability of the battery system that is. Lead acid is resistant, hard, and economical, but it holds little energy and has fewer cycles. Lead acid is used for golf carts, wheelchairs, personnel carriers, emergency power, and uninterruptible power supplies (UPS). Being toxic with Lead means they cannot be buried as waste.

Li-ion batteries are used in many tasks that were previously done with the help of nickel and lead batteries. Li-ion requires a protection circuit to maintain safety. This battery is more expensive than other types, but the low maintenance and high cycle count make it lower expense per cycle than other chemistries. Li-ion has different types that are named by their active ingredient, namely cobalt, manganese, phosphate, and titanate. (Mekonnen, Sundararajan and Sarwat, 2016)

Lead and lithium batteries may look quite similar. It can be an old marketing tactic to convince consumers of new technology. However, when you choose them, the difference between lithium and lead-acid batteries becomes more apparent. Lead acid batteries are older than lithium batteries and have been used for many years. With the passage of time and the advancement of science and technology, a new type of battery called lithium-ion emerged. Lead-acid batteries are larger than Lithium-ion batteries, have more odour and require more maintenance, are not as safe, and are less environmentally friendly.

### **The main differences between lithium and lead acid batteries are:**

#### **Chemical compounds:**

In the lead-acid battery, lead oxide is used as the anode and lead as the cathode, and sulfuric acid is also used as the electrolyte, but in the lithium-ion battery, graphite is used as the anode, and lithium oxide is used as the cathode. And salt is used as graphite. (Collins et al., 2010)

#### **Environmental effects:**

Lead-acid batteries contain 6% to 18% lead, which is considered a heavy and toxic metal, so they need more care in disposing, but because lithium is considered a safe material for nature, Lithium batteries are environmentally safe. (Zakiyya, Distya and Ellen, 2018)

#### **The price difference between Li-ion and Lead Acid batteries:**

Lithium-ion batteries are much more expensive than lead-acid batteries to manufacture due to having a protective circuit to monitor voltage and current.

### **The weight difference between lead and lithium**

Lead acid batteries are significantly heavier due to the presence of lead plates inside them.

### **The biggest difference is in chemical stability.**

Lead and lithium batteries have different chemical compositions. All types of lead acid batteries have stable chemical resistance. However, the dilute sulfuric acid inside the enclosure can cause skin irritation if there is a crack or crack in the battery. Some volatile hydrogen gas can escape during the charging of the target site. (Mirzaei, Leonardi and Neri, 2016)

Lithium-cobalt-oxide batteries, on the other hand, may catch fire when overcharged. Battery scientists have improved the technology by developing safer models of lithium-ion phosphate. However, this amount of development is still low and not always acceptable to inexperienced customers.

<b>Characteristic</b>	<b>Lithium battery</b>	<b>Lead acid batteries</b>
<i>Cycle life</i>	<i>1200 to 2000</i>	<i>500 to 900 times</i>
<i>tarting specific energy</i>	<i>40W · H / kg</i>	<i>150W · H / kg</i>
<b>Charging time</b>	<i>2~4h – fast charging 3~6h</i>	<i>slow charging in 8h or more</i>
<i>Energy for discharging and Charging</i>	<i>lithium-ion battery' efficiency in charging and discharging energy conversion efficiency can be more than 97%</i>	<i>discharging and charging energy conversion efficiency is about 80% in lead acid battery</i>
<i>Price</i>	<i>high</i>	<i>low</i>
<i>The volume and occupied space</i>	<i>small</i>	<i>big</i>
<i>Weight</i>	<i>less than 1/3 ~ 1/4 kg</i>	<i>heavy</i>
<i>Pollution</i>	<i>causing pollution during production</i>	<i>if it is not recycled, the presence of lead causes environmental pollution</i>
<i>Complex maintenance cost</i>	<i>high maintenance costs</i>	<i>Low maintenance costs</i>
<i>overcharge tolerance</i>	<i>high</i>	<i>low</i>
<i>The level of toxicity</i>	<i>very low</i>	<i>high</i>

Table 1-3 Comparing Lithium batteries and Lead acid batteries.

### Comparison of Lead acid batteries with lithium batteries

The biggest advantages of lead acid battery over lithium are:

- Its technology is known

Lead acid batteries have been known and used for about 25 to 30 years, and their production technology is very strong and advanced. (Li et al., 2018)

- **No internal electronic components**

Lead-acid batteries, unlike lithium batteries, do not have internal electronic components. Therefore, the lead-acid battery can withstand high electric current, temperature, and discharge, while the lithium battery cannot. In a lithium battery, these internal electronics shut down the battery under extreme conditions, which can cause problems for the user.

- **Stable and resistant**

The lead acid batteries are very resistant and hard. In difficult situations like high current and temperature, this battery maintains its performance. Sealed acid batteries are widely used in larger machines such as electric forklifts and electric motors that require high current. (Jang et al., 2006)

### **The biggest advantages of lithium batteries**

- **Spontaneous discharge is very limited.**

The lithium battery can maintain its charge level for long periods of time. For example, if you stop working with an electronic device on Friday evening with a 50% charge, on Monday morning, when you start working with the device again, you will see that it has retained almost 50% of the charge. This is a big advantage over lead-acid batteries where there is a spontaneous discharge. (Kamali-Heidari et al., 2018)

- **It weighs less.**

This type of battery is lighter and smaller than lead acid. This makes the user comfortable, and it can be used in small electronic devices.

- **It can be recharged very often.**

Lithium can be recharged about twice as often as a lead-acid battery.

### **Pros of lithium-ion batteries in comparison to lead acid.**

- Longer life of service in lithium-ion batteries and as a result reducing the frequency of changing UPS batteries and still more assurance that the batteries will not fail.
- The lightness of these types of batteries in the scale of a certain amount of stored energy
- The frequency of charging and discharging is almost 10 times higher.
- Much longer discharge time when not in use
- Shorter charging time up to 4 times or more

A lithium-ion battery is a nonlinear system that is a complex device. EKF is a nonlinear variant of the Kalman filter that linearizes the existing estimates of mean and covariance. It is an improvement of the traditional filter algorithm, which is developed by combining the conventional Kalman filter and the linearized based on Taylor series expansion and obtains the approximate linear space equation by discarding the second order and above-the-terms. This project has been done by several steps shown in following diagram. Several working conditions have been created for the errorless state of charge (SOC) estimation directive to ensure accurate results from the SOC estimate showed in figure 1-1..

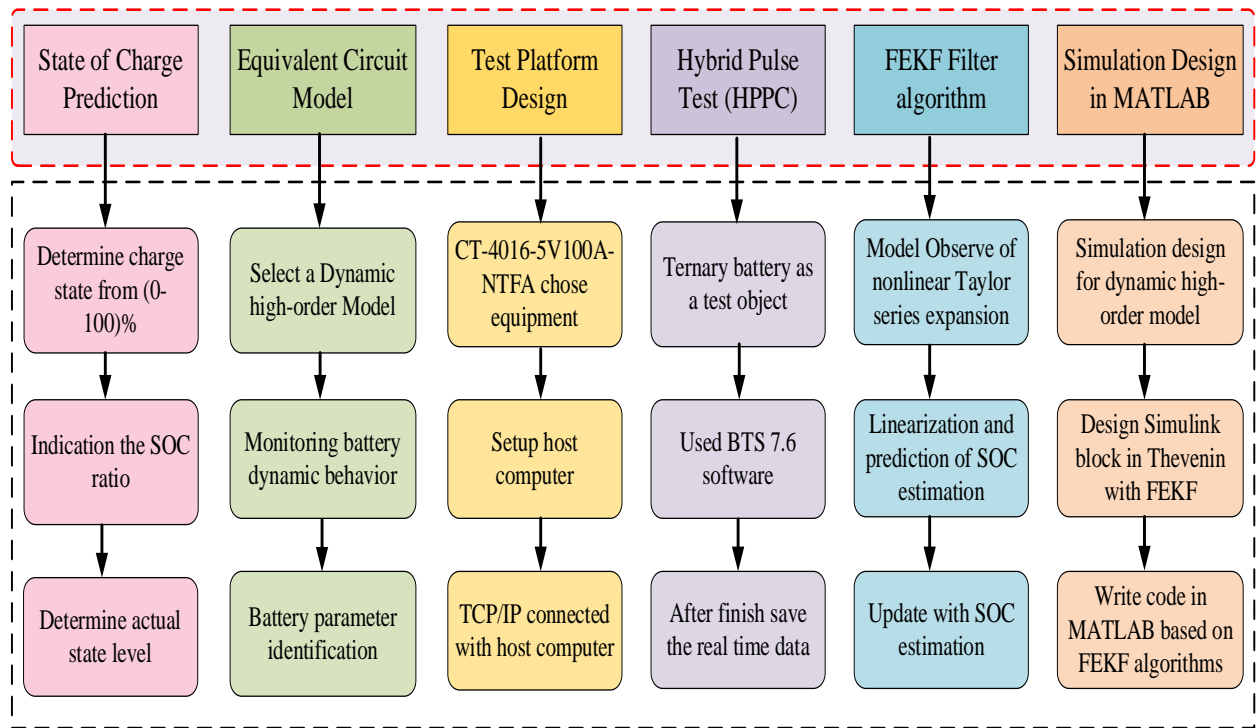


Figure 1-1 Working conditions created for SOC estimation.

## 1.2. Aims and Objectives

The main aims of this project are:

- To develop a method that can update model parameters online based on quantifiable factors under complex driven condition
- To exhibit better performance of SOC estimation in the presence of variable environmental temperature by tracking battery dynamics.

The main objective of this project is:

- To investigate the developed methods for SOC estimation of a li-ion battery.

### ***1.3. Published paperss***

This study resulted in two papers.

**1. Published:** A. Lotfivand, D. Yu and B. Gomm, "State of Charge estimation using Extended Kalman Filter in Electric Vehicles," 2022 27th International Conference on Automation and Computing (ICAC), 2022, pp. 1-5, doi: 10.1109/ICAC55051.2022.9911137.

**2. Accepted:** A. Lotfivand, D. Yu and B. Gomm, "State of Charge estimation using Unscented Kalman Filter in Electric Vehicles," 2023 28th International Conference on Automation and Computing (ICAC), 2023,

## 2. Literature review

### ***2.1 Introduction***

In this chapter, the details of the literature review are explained. By searching the important keywords, the related articles were found. These words are battery management system, state of charge estimation, lithium-ion batteries, electric vehicle, thermal management, fault diagnosing, equalizing the battery. In addition, the literature review helped in finding the gaps between the previous studies and the proposed project that can assist to ensure the novelty. **Introducing the**

#### **battery management system**

The battery management system includes monitoring the complete state of the software, hardware and imaging the battery performance in different working conditions of the vehicle.

One of the most important factors to show the status of the battery is its charge and discharge status. In addition, adjusting the amount of current voltage that is applied to the battery pack in different conditions is of vital importance. For these reasons, it is necessary to have a central control system to measure and adjust these important parameters on the battery, because according to the characteristics of each battery and its characteristic curves, these parameters change in different working situations and the absence of this system, or its incorrect operation, causes a sharp decrease in the useful life of the battery and sometimes causes unfortunate incidents such as battery explosion.

In general, it refers to a system that continuously monitors the status of the battery and displays it to the user, as well as the task of depicting various battery parameters, including the state of charge and discharge, the temperature, and environmental conditions of the battery. It is responsible for the parameters in different working conditions. In addition, it protects the battery against possible over currents and over voltages in the process of battery operation. (Shen and Gao, 2019)

- Sampling and monitoring system
- Central control system (calculations)
- security system

It is illustrated the main parts of Battery Management System in Figure 2-1 as follows:

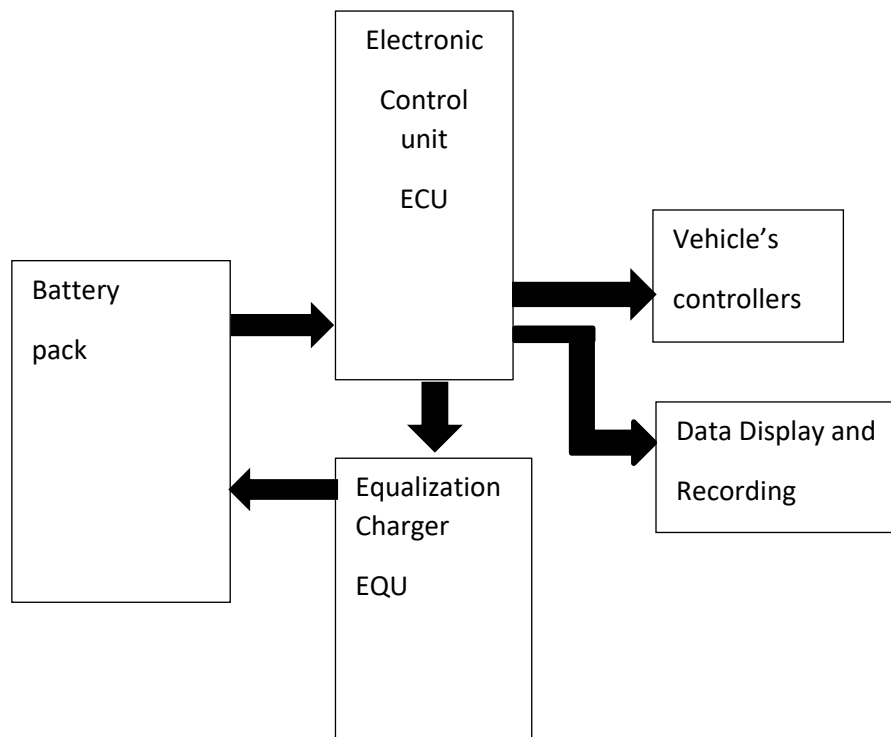


*Figure 2-1: Schematic of Battery Management System*

### **Sampling and monitoring system**

In this system, the following parameters are usually displayed for the user's information:

- The battery pack voltage and the voltage of each battery separately (in charging and discharging conditions)
- Current drawn (when discharging) or applied current (when charging) by the set of batteries
- The temperature of each battery permanently and in different working and environmental conditions
- Battery state of charge (SOC)
- Battery discharge rate (DOD) Depth of discharge
- Showing the state of health of the battery (SOH) both in terms of physical conditions and functional conditions

### **Protection system**

Another capability of BMS systems is to prevent the occurrence of causes and defects that endanger the health of the battery. The most important of these protections are:

- Protection against applying additional currents during charging or discharging by means of current limiters:
  - during charging - charge current limit (CCL)
  - during discharge - discharge current limit (DCL)
- Protection against overvoltage during charging
- Protection against voltage reduction over the permissible limit during discharge, especially in the case of lead-acid batteries (Acid-lead) and lithium-ion (Li-ion) must be observed.
- Protection when the temperature increases and decreases beyond the permissible limit of the battery
- Protection against pressure increase, which is mostly applicable to Nickel Metal Hydride (NIMH) batteries.

### **Central control system**

This part of BMS is the decision centre of the system, in such a way that the samples of parameters received by the sampling unit are transferred to this unit and compared with reference information and according to different conditions, the required calculations are done, and finally, control or protection commands are sent to different parts of the system. For instance, if the voltage of one of the cells is lower than the permissible limit, the central control system, after knowing about this and determining the amount of charge required for the battery, sends a command to the system balancer, and the balancer also applies voltage; this increases the battery until the charge reaches the optimal level. For another example, if the voltage of a battery exceeds the limit, in this case, the system adds a resistor (such as an inductor) to that battery and draws current, and the battery is brought to the optimal level. (Lelie et al., 2018)

### **Measurement and display systems**

#### **▪ Measurement systems**

In general, the decision of the control centre is based on the information that it receives from different parts of the system (specifically, the battery) and through the sampling system, and the more accurate the information, the more correct the controller's commands will be. It will increase the efficiency of the useful life of the battery and other electrical systems related to it.

The information on which the controller makes decisions is obtained in two ways:

- Information obtained through direct measurement of parameters including current, voltage, and battery temperature values.
- Information that is obtained indirectly by using the results of direct measurements and their analysis, such as the state of charge and discharge of the battery (SOC & SOD).

For parameters that can be measured directly, such as voltage, current, and temperature, the desired result can be achieved by using very simple measuring devices, including current, voltage, and battery temperature measuring devices. It is indirectly related to the performance accuracy of the measurement system. Temperature sensors can also be used to measure temperature.

But in the case of parameters of the second category, the story is different because the system is faced with a set of raw information and must combine the different pieces of information and finally, according to the obtained results, obtain detailed information about the battery condition. For this reason, it is necessary to have computational algorithms that can have a more detailed analysis of how the battery is doing. It is necessary to give a brief explanation of one of the important parameters in this section. (Chatzakis et al., 2003)

### **SOC curve**

The SOC curve is considered as an essential factor that shows the condition of the battery. This curve shows the amount of battery charge or, more precisely, the amount of energy remaining in the battery and is expressed as a percentage from zero to one hundred. (Haq et al., 2014)

To make the matter clearer, suppose the car battery is near the end of its life and has been discharged by 20%. Now, even if the battery is recharged and reaches 100%, the SOC curve will show 80%, which means that according to the useful life of the battery, 100% of its capacity can no longer be used, and the BMS system will make the car settings based on this 80% as if a new battery with 80% of the capacity of the previous battery is installed in the car. (Pop et al., 2008) Four factors are usually used to determine the state of charge curve in the battery, and in this section, these four factors are mentioned:

a) Battery voltage: as the efficiency of the battery decreases for various reasons such as increasing the battery life or frequent charging and discharging, the battery voltage also decreases, and even after recharging it does not return to its original value (so-called the battery does not charge more than this). As a result, the SOC percentage will show a lower value) Battery current: SOC percentage reduction shows that it is no longer possible to draw as much current from the battery as the nominal current (take a load from the battery).

c) Chemical compounds of battery electrolyte: Reducing the chemical compounds in the battery electrolyte reduces the ability of the battery to transfer electrons between the negative and positive poles of the battery and generally reduces the efficiency of the battery. This is shown in the SOC curve with a decrease in percentage.

d) Battery pressure: After a while this item will reduce the SOC.

### **Monitoring system**

As the name of this system suggests, its task is to display the information obtained from the measurement systems for the user and to inform them of the general state of the battery system and its accessories. Depending on the type of technology used, monitoring may only include the numerical values of voltage, current, temperature, pressure, and the state of the chemical composition of the battery, or in addition, it may provide the driver with SOC and SOD curves,

etc. Also, all the alarms related to BMS system protections such as voltage drops and over currents appear on the monitor.

## 2.2 First example for battery management system

The details of the operation of each block of BMS (A) are explained in Figure 2.2 as follows:

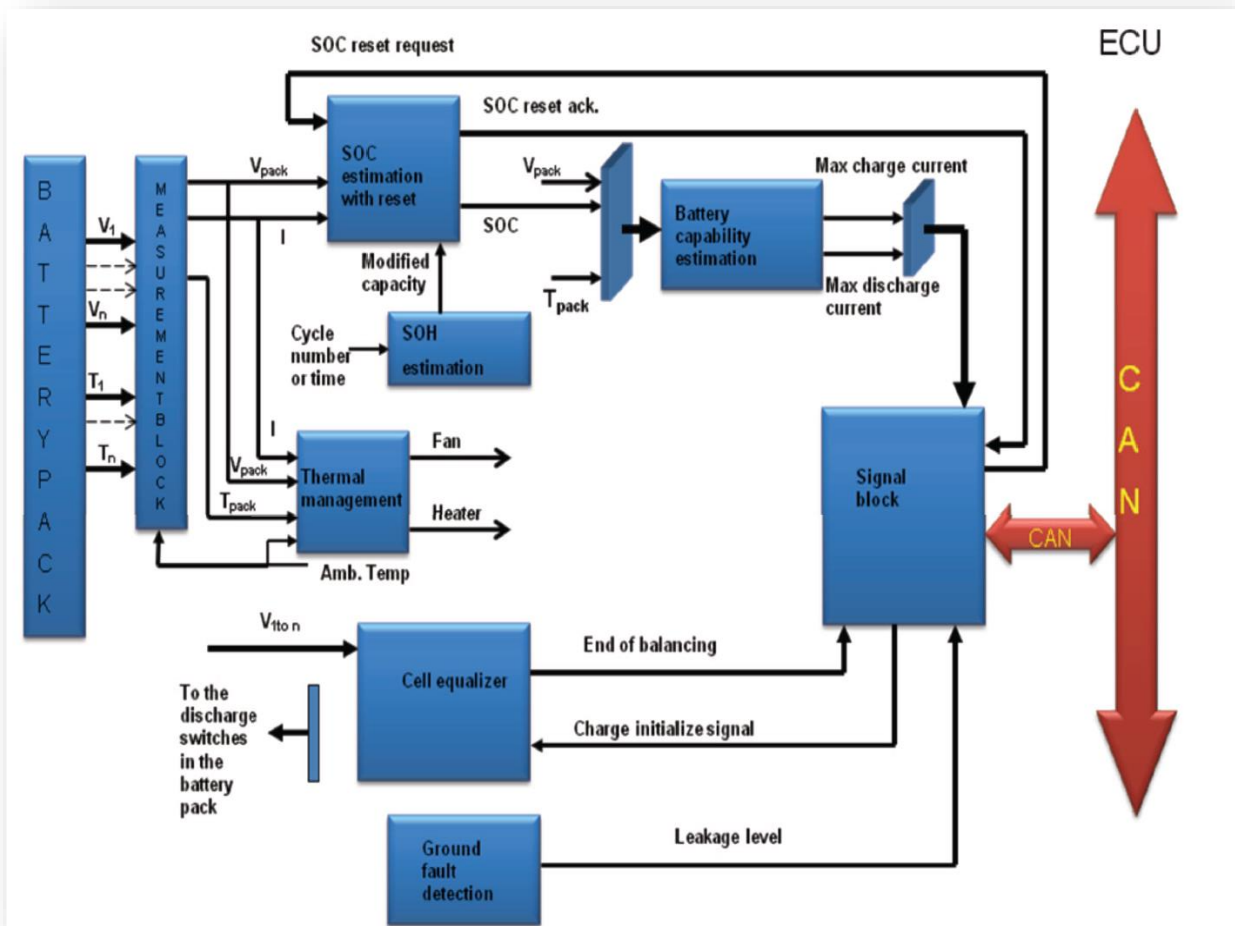


Figure 2-2: Schematic diagram for first example of Battery Management System

### Measuring block

This block converts the initial cell voltage, battery temperature, and battery current into digital values at various points in the battery pack. All these data are used to estimate the state of charge of the battery in the next steps.

### Battery algorithm blocks

The goal we are pursuing in this block is to estimate SOH and SOC by measuring battery parameters including voltage, current and temperature of battery. SOC is expressed as a percentage of a battery's capacity and can also be seen as a fuel gauge in HEVs and EVs.

### **Estimation capability blocks**

After determining the SOH and SOC, the BMS has the top amount of discharge and charge current at each moment according to the method. This block's output is required in the car's ECU and as a result charged or discharged, out of range is prevented.

### **Cell balancing block**

Because of the limitations of the manufacturing process, we cannot create all equally. Variations in cell capacity range from a few percent to 15% in normal circumstances. Differences like charging or discharging characteristics and internal resistance are inevitable. Cell balance is critical to maximizing battery pack capacity and battery life.

### **Ground fault detection block**

If the voltage of the battery pack is above 200-300V in HEV and EV, any leakage from the car chassis is very dangerous. Therefore, the effect of the detection system for ground fault is necessary to ensure the safety of the electric vehicle. Therefore, this block is essential for safety especially for high voltage DC. (Lelie et al., 2018)

### **Heat management block**

Temperature management needs to control and monitoring of the battery's temperature and then the battery's under or over temperature will not damage the battery. The result of this control block is the electric heater and fan that try to keep the battery temperature within desired limits. (Zhang et al., 2014)

### **CAN block**

It is a physical communication module that controls all output and input signals of the BMS. Given the amount of data being received and sent, the protocol of CAN which is high-speed should be applied because the amount of data allows up to 1 Mbps range.

## ***2.3 Second example for battery management system***

Figure 2.3 shows battery management system b as follows. It is consist of some parts like Battery Pack, Measurement, SOC estimation, Capability Estimation, Equalisation, SOH estimation, and signal blocks. (Bergveld et al., 2002)

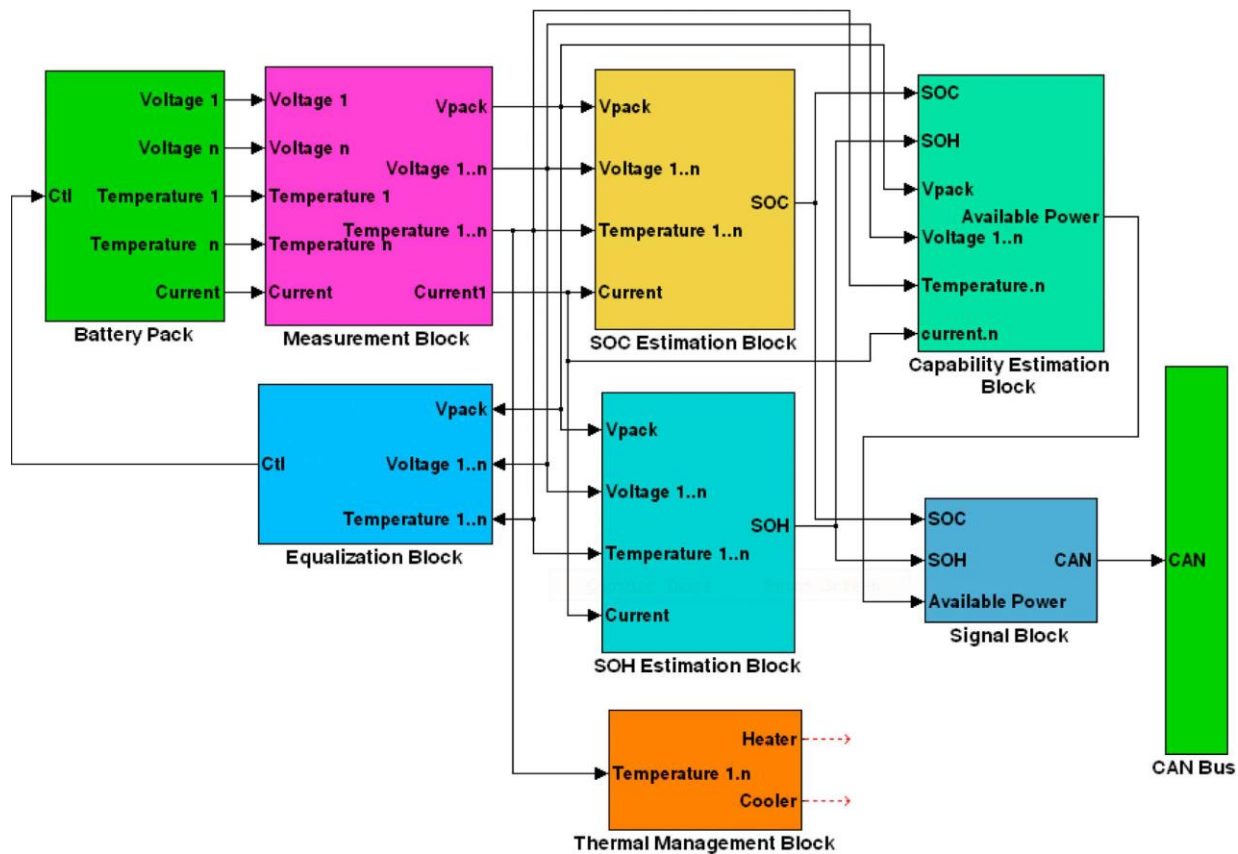


Figure 2-3: Second example for Battery Management System

### Measuring block

Cell voltage, battery current, battery temperature and ambient temperature at different parts of the battery pack are individually imaged and converted into digital amounts. The information is used to predict the battery's state in the next steps. Through each sampling step, just one value of the voltage of the cell is sent to the A to D converter in the centre of the processing unit. The pros of primary cell voltage measurement justify the additional equipment price since it can balance and protect the excess charge at the level of the cell. (Chan, 2007)

### Blocks of battery algorithm

The battery algorithm's block shows the status of the battery. Its main duty is to predict SOH and SOC by measuring battery parameters including battery temperature, current and voltage.

SOC is considered as a battery capacity or a percentage of the capacity range. This quantity looks like a fuel gauge in vehicles, but in a battery, it shows the energy being drained from the battery. SOC estimation is very important to understand the remaining usable battery's capacity while using the battery. This information allows estimating the distance travelled by the EV with the

available battery capacity. Temperature, duty cycle and range of discharge affect SOC estimation, so the BMS must use an appropriate model for the battery to consider these parameters to find an accurate SOC. The types of inputs of this method include temperature, current and voltage and these values achieved by the corresponding sensors. These kinds of sensors have analogue inputs that are digitized using an A/D converter. All the inputs should be continuously controlled by microprocessors at a regular peace.

The SOC indicator not only estimates the useful distance, but also maintains the battery at a certain SOC to transfer and accept charge not being over discharged or overcharged. In an EV type, mostly the cells undergo charge release related to regenerative braking, which allows excess charge to penetrate the cells, especially in the case of high SOC. In these conditions, the Battery Management System must monitor the SOC and control the release of charge during re-braking and prevent the cells from overcharging. Estimating an accurate SOC is BMS's most important task. We have several methods to obtain SOC using cell voltage, temperature and current. The easiest way is measuring directly. For example, measuring the OCV or voltage of the charged cell and then deriving the SOC using the discharge parameters.

This method has some problems with Li-ion batteries since in the Li-ion battery we have a smooth curve in the middle part of the discharge curve. So, we may have a large difference in SOC resulting from a small error in measurement. In direct measurement, temperature and age impacts must be considered.

### **The block for estimation of Capability**

When the SOC and SOH are determined, the BMS receives the limitation for discharge and charge current at any moment according to the algorithm. This block's output is sent to the car's ECU and the battery prevented from charging or discharging beyond its specific range. The estimation block's duty is sending information to the ECU that the charge and discharge levels of the battery are now safe. This information is critical to the safety of battery operation and accidental failure is preventable. (Beckmann et al., 2004)

The control rules for extracting the maximum charge and discharge current are according to the inputs. The maximum charge and discharge current time is expressed for different values of the battery parameters. (The maximum charge current percentage is the charge factor)

The BMS limits the current of charging based on the functions that depend on some parameters like SOC cell voltage, and temperature. For instance, the current of charging decreases when the temperature is between 30 and 40 degrees Celsius. Moreover, the maximum current that can charge the battery is dependent on SOC and cell voltage. It should be considered, based on the characteristics of the battery, that it is better to discharge the battery at a certain minimum temperature, for example below -20 °C. In practical cases, the C rate is very low. The maximum charge and discharge rate is stated in the data sheet of the battery manufacturers. C is the battery's nominal capacity.

### **Cell balancing block**

Because of the manufacturing limitations of the process, we cannot create all cells equally. Variations in the range of cell capacity range from a few percent to 15% in normal circumstances. Prominent differences like charging or discharging characteristics and internal resistance are inevitable. Cell balance is critical to maximizing battery pack capacity and battery life. (Cheng et al., 2010)

The above-mentioned block compares the voltage of the cells to achieve the difference between the higher voltage cell and the lower voltage cell. In the case of this amount being greater than a predetermined threshold, it stops charging and discharges the cell with a higher voltage through an external resistor. The discharge is finished after the difference is reduced. This balancing method of the cell is called dissipation.

The other algorithm for balancing the cell is balancing it actively, that is either through charging each cell separately or transferring the charge from a cell with a higher voltage to a cell with a lower voltage. This balancing is more efficient and clearly superior in performance; however, it is more expensive for the industries that are price sensitive.

### **Temperature management blocks**

The boundary of the temperature management block diagram in the BMS predicts the temperature of the battery. Estimating the temperature is done by some simple algorithms. Temperature management's duty is controlling and monitoring the temperature of the battery. Therefore, the battery will not be damaged at too low or too high temperatures. The output of this control block is the electric fan and heater that keep the temperature of the battery within the desired limits. The temperature management block detects the environment and battery temperatures and decides on heating or cooling operations and urgently sends a signal to the ECU if the temperature rises abnormally. Figure 2.4 shows the third Block Diagram for battery management system C. (Scavongelli et al., 2015)

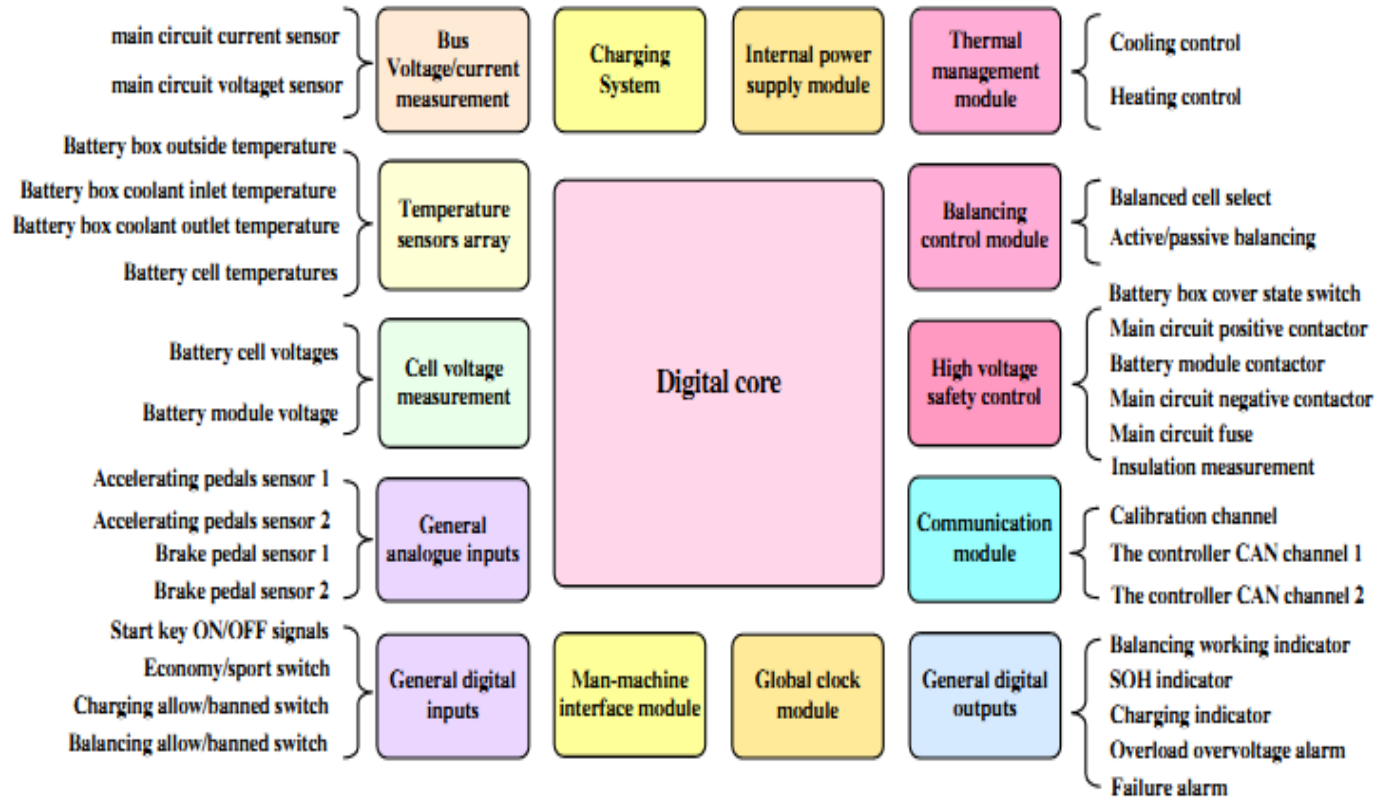


Figure 2-4: Block Diagram for the third example of battery management system C

## 2.4 The third example for battery management system

BMS consists of a variety of sensors, actuators and controls that have different signal wiring systems and methods. There are three important duties for Battery Management Systems in cars, which can be described below (Scavongelli et al., 2015)

- Protecting cells and battery packs from becoming damaged
- Creating batteries that work at the right voltage and temperature range and guaranteeing safety and if possible, service life.
- To maintain the battery so that it can work in a state to fully satisfy the needs of the drivers.
- Finally, the power of car batteries must have appropriate characteristics and standards. The general block diagram of the BMS hardware in the car was mentioned above.

The inputs to the BMS include the sensor for current, the sensor for voltage and their task is to measure the original voltage and current, sensors for temperature to measure cells' temperature, the ambient temperature and possibly the inside temperature of the battery cooler and the outlet. Usually, analogue input like accelerating the pedal sensor and the sensor of the brake and digital input like the start key signal (off or on) approves or prohibits the charging switch.

BMS outputs include temperature management module such as fan and electric heater that control heat and cold., balancing module such as capacitor switch adjustment and resistance loss to battery balancing and managing safety of voltage such as main current connector and module connector. Usually, digital outputs are like specific charge, error alarm and communication module. Moreover, BMS should contain global clock module internally and power storage module and possibly have a charging system and a module for interfacing with the machine. We should be confident of electromagnetic compatibility. The electric motor's working environment needs the BMS to have acceptable ability to combat anti-electromagnetic interference and transfer the wave to low output levels. BMS software covers these functions.

### **Detection of battery variables**

This function consists of systems for overall current, overall voltage, and initial cell detecting (preventing overcharge, over discharge, and anti-polarity), temperature detecting, insulation detecting, smoke detecting, impedance detecting, damage detecting, etc.

### **Estimation of battery condition**

This block consists of the SOC state of charge or the SOD discharge rate or the SOH health rate and the SOF performance state. The SOD or SOC of batteries is estimated based on the conditions that include voltage, current, and temperature. SOH is estimated based on the amount of improper use and reduction of battery performance. SOF is estimated based on SOH and SOC and the environments of the battery operating. (Lu et al., 2013)

### **On-board diagnostics (OBD)**

Errors consist of sensor failure, network failure, actuator failure, battery failure, over voltage (over charge), under voltage (over discharge), over current, over temperature, connections. It is baseless, due to combustible gas concentration, insulation failure, integrity failure, rapid and premature increase in temperature.

### **Controlling the battery safety and alarms**

Its function consists of controlling the thermal system and safety. When faults are detected, the vehicle control unit will either charge or be notified via the network and they will repair the faults to avoid damage, resulting from high temperature, overcharge, low temperature, overcurrent, over discharge, and electrical leakage etc., to the battery and people.

### **Control the charge**

Due to the characteristics of the battery and the level of charging power, the BMS has a duty to control the charging until it is completely charged.

### **Battery balance**

Based on the data belonging to every cell, BMS balances cells via balancing algorithms such as cell balance, loss balance, non-loss balance to make SOC compatible and possible between cells.

### **Temperature managing**

Based on distributing the temperature in the battery pack and the regulation of charging or discharging, the BMS makes the decision to start cooling or heating and has power for heating and cooling.

## **Networks**

As it is inappropriate to implement a BMS in a car and the car also needs network functionality, it is suitable for performing linear calibration and monitoring and automatically generating code and downloading the program linearly (updating the program without sample isolation) for BMS without disassembly. Usually, the CAN network is adopted. (Controller Area network)

## **Information storage**

One of BMS's duties is to store important information like SOH and SOC and the total number of charges and discharges, failure codes, coordination, etc. An actual BMS in a car may just have some of the software and hardware listed above. For each cell we need a sensor for voltage and a sensor for temperature. For a system of a battery that has a small number of cells, it is possible that the BMS control or even the BMS function will be integrated into the vehicle main control, and for a battery system that has many cells, there may be a main control and several sub-controls just to manage one battery module. Each module of battery with a lot of cells, can have circuits as connector module and module for balancing and sub-control. The battery module will manage voltage, current and control connector measurements, balanced cells, and communication with the main control. According to the data reported by the secondary control, the central control estimates the battery condition, diagnoses the failure, manages the temperature, etc.

## **Introducing the proposed battery management system**

### **Ground fault detection block**

Since the battery pack voltage is above 200-300V in HEV and EV, any leakage from the car chassis is very dangerous. Therefore, the effect of the system for detecting ground faults is necessary to be confident of the safety of the electric vehicle. It is used for safety and is essential for high DC voltage.

### **Temperature management block**

Temperature management is based on the monitoring and control of the temperature of the battery and ensuring the battery is not damaged by high or low temperature. The output of this control block is the electric cooling and heating that tries to control the temperature within the desired limits.

### **Measurement block**

Cell voltage, battery current, battery temperature and ambient temperature at different points of the battery pack are individually imaged and converted into digital signals. All this information is required to estimate the state of the battery in the next steps. The block that measures cell voltage shown in the figure below consists of a relay matrix. Each time, just an analogue-to-digital converter of the central processing unit is connected to the cell voltages. The advantage of primary

cell voltage measurement justifies the additional hardware price because it can balance and protect the excess charge at the cell level.

### **Blocks for algorithm of battery**

This block shows the battery's status. This block contains SOC state of charge or DOD discharge rate or SOH health rate. DOD or SOC of batteries is estimated based on situations that include current, voltage and temperature. SOH is predicted based on the amount of improper use and reduction of battery performance.

SOC is defined as a battery capacity or a percentage of the capacity range. This quantity looks like a fuel gauge in vehicles, but in a battery, it shows the energy being drained from the battery. SOC estimation is beneficial to understand the amount of battery capacity that remains in the situation that the battery is empty. Therefore, using this information, the driver can estimate the distance travelled by the EV with the remaining battery capacity. Temperature can affect SOC estimation, duty cycle and discharge range, so the BMS must use an appropriate model to affect these factors to find SOC. The types of inputs of this method include voltage, current and temperature and the values obtained by the corresponding sensors. It is sensors' duty to obtain analogue inputs that are converted to digital with an A-D converter. Inputs are continuously monitored by microprocessors regularly.

More than just the estimation of distance, the SOC indicator maintains the battery at a certain SOC to transfer and can be charged without the risk of over discharging or overcharging the cell.

In an EV type, the cells often undergo charge release due to regenerative braking, which allows excess charge to penetrate the cells, especially in the high amount of battery SOC. In such events, the BMS must monitor the SOC and control the release of charge during re-braking and prevent the cells from overcharging. Therefore, we can assume SOC as an important output of BMS. There are several methods to determine SOC based on cell voltage, current and temperature. The simplest algorithm is measuring them directly. For example, measuring the OCV or voltage of the charged cell and then deriving the SOC from the discharge characteristics.

This method is inappropriate for Li-ion batteries because the middle part of the Li-ion battery discharge curve is completely smooth. A small error in measurement will cause a large change in SOC. In directly measuring temperature and age, impacts must be considered.

### **Block for capability estimation**

After determining the SOH and SOC, the BMS receives the discharge current and maximum charge at any moment according to the algorithm. This block's output is provided to the car's ECU and the battery cannot be charged or discharged beyond its specific range. The estimation block's duty is to send data to the ECU that the charge and discharge levels of the battery are now safe. This information is critical to the safety of battery operation and prevents accidental failure of battery specifications.

The control rules for extracting the maximum charge and discharge current are based on the inputs. The maximum discharge and charge current time are expressed for different amounts of the

variables of the battery. (The value of the maximum charge current is defined as the charge factor in percentage)

It limits the current of charging based on functions that depend on SOC, temperature, and cell voltage. For instance: the charging current decreases if the temperature is in the range of 30 to 40 degrees Celsius. Moreover, the battery charging maximum current depends on cell voltage and SOC. Note that, according to the characteristics of the battery, it is better to discharge the battery at a certain minimum temperature, for example below  $-20^{\circ}\text{C}$ . In real cases, we have very low C rate. The maximum charge and discharge rate is stated in the data sheet of the battery manufacturers. C is the nominal battery capacity.

### **Cell balancing blocks**

Because of the limitations of the production process, the cells will not be equal; the capacity of the cell will be varied from a few percent to 15% commonly. Other differences such as charging or discharging characteristics and internal resistance are inevitable. Cell balance is critical to maximizing the battery pack capacity and battery life.

This module has the duty of comparing the voltage of the cells and finds the difference between the cell having higher voltage and the cell having lower voltage. In case of the difference being greater than a predetermined threshold, it stops charging and discharges the cell with a higher voltage through an external resistor. The discharge is finished after the difference is reduced. This balancing method of the cell is called dissipation.

The other method for balancing the cell is active balancing, that is either through charging each cell separately or transferring the charge from a cell with a higher voltage to a cell with a lower voltage. This method is obviously superior in performance and energy utilization, but it is expensive for the price-sensitive automotive industry. (Manenti et al., 2010) Many hybrids balancing circuits use fast capacitors, a dc-dc converter with a single dc converter, and several secondary windings that could charge the weakest cell of the battery pack. The method cost is related to the balancing time that in turn, is related to the auxiliary power supply's power.

### **Existing battery models for electric vehicles**

Nowadays, Electric vehicles are the focus of attention because of the imperative to reduce emissions, however, their performance is directly dependent on the battery's performance. Currently, Lithium-ion is so permanent and suitable. Nickel-manganese-Cobalt (NMC) and nickel-cobalt-aluminium (NCA) seem more suitable among them. Therefore, acting as a suitable model for simulation of battery behaviour for obtaining SOC (state of charge), the capacity State of health (SOH) is essential. We can use several existing models and the impedance electric equivalent model is more appropriate, attractive, and its performance is better in real-time simulation. (Kroeze and Krein, 2008)

Batteries are the most important storage systems. Namely, when hydrogen storage is used, we need for a battery for stabilizing DC voltage. There are some drawbacks to EVs such as lifetime, being expensive, and limited environmental temperature. So, concentrating on batteries used in EVs (electric Vehicles) seems essential. There are some advantages for Li-ion batteries that make them

stand out, such as low self-discharge ratio, high energy, and power density. On the other hand, the tolerance overcharging is low. Therefore, we need a high-performance charging system for this battery.

Between 8 and 10 years is the average lifetime for EV's batteries, and it is 20% to 30% degradation in comparison to first capacity. (Severson et al., 2019). However, in practical cases, because of braking and acceleration that is approximately more than ten times average power, the lifetime will be reduced. To sort this issue, we need a technology to increase the amount of energy and control and optimizing the energy is needed. Therefore, a reliable model is essential for technical and economic efficiency of the battery. It is notable that BMS (Battery Management System) is directly responsible for stored energy in the battery and indirectly responsible for passengers' safety. There are several models that are appropriate for related studies such as State of Charge (SOC), State of Health (SOH), Thermal analysis, and mechanical stress studies. . (Lelie et al., 2018)

Mostly the models are called electrochemical models and they show their reaction in electrochemical terms. These models are detailed and there is a high price for developing them, and high-level computing is their characteristic. Electrical models have the circuits that are equivalent to the battery to imitate their behaviour under operation. These models neglect some details, so they are faster than electrochemical and are more common. There are other models that are based on second order or higher mathematical complex equations to predict a batteries performance for methods such as artificial intelligence. The accuracy of these models is closely related to the amount of data applied in the training step. (Ren et al., 2020)

Table 2-1 illustrates several models for electric vehicle batteries and compare them in terms of Ability for physical interpreting Data, Being Complex, Accuracy, and suitability for some application.

Category of model	Model	Ability for physical interpreting	Data	Being Complex	Accuracy	Appropriate for
Analytical model	State-Space Sheperd other rations Rakhmatov and Vrudhula Peukert's model	Low Medium Medium Low	E SE SE E	Medium Medium Medium Medium	Medium Medium Medium Medium	ESTIMATION
Electro-chemical	ECM/Reduced order Electro- Chemical Pure Electro- Chemical		SE P	Medium High	High Very High	Designing battery
Impedance	Frequency domain	Low- Medium	SE	Medium	Medium	real time operation and Characterization
Fatigue/ Mechanical	Fatigue/ Mechanical	High		High		Designing
Thermal	ECM Thermal Analytical Thermal	Medium High	SE P-SE	Medium High	Medium High	Real Time
Combination of models	Thermo- Mechanical Thermo- electrochemical Electro-Thermal	High High Medium	SE P SE	High High Medium	Low- High	Real Time
Abstract model	Artificial Intelligence	Low	E	Medium	Medium	Analysing Offline
Electrical Noshin			SE	Medium	Medium	SoC estimation
Electrical Neural nets			S	High	High	SoC estimation
Electrical PNGV	1st, 2nd, nth order	Medium- Low	SE	Low- High	Low- High	SoC estimation
Electrical ECM Thevenin	1st, 2nd, nth order	Medium	SE	Low- High	Low- High	SoC estimation

Table 2-1 Classification of models considered for battery.

E: Empirical, SE: Semi-Empirical, VH: Very High

Therefore, in analysing electromobility, combination models or electrical models are usable. However, mathematical models are complex and are not appropriate for real-time systems. Since they use complex formulas, computing values takes a lot of time and cost. Too simple models may not be suitable for steady-state analysis. PNGV (partnership for a new generation of vehicles) and Thevenin models are appropriate for simulations in transient state. Models based on Impedance show the battery's AC reaction. On the other hand, runtime models show the battery's DC reaction. Table 2.2 explains the classification of battery electrical models.

Ability to predict	Models based on Runtime-Combined	Models based on Impedance	PNGV or Thevenin models
Runtime	Able	Not Able	Not Able
Transient	Limiting ability	Limiting ability	Able
AC	Not Able	Able	Limiting ability
DC	Able	Not Able	Not Able

*Table 2-2 The classification of battery electrical model*

### **Models based on Equivalent circuits:**

This section explains several ECMs (Equivalent Circuit Models) which are suitable for electromobility systems and are arranged from the simplest one to the most complex.

#### **Less Complex models:**

##### **The model of Ideal Battery**

The first model proposed by Hageman is used in nickel-cadmium, (Jongerden and Haverkort, 2008) Pb-acid, and alkaline batteries. After a while another model was proposed by Gold for the most common batteries, Li-Ion, that has errors of up to 12%.

This model (ideal model) has only voltage source and neglects the other parameters. However, this model neglects the load variation, and the changes of other parameters such as SOC.

The important characteristics of this model are voltage (V) and capacity (Ah). Therefore, the amount of energy that is stored in the battery is (WH). In this model it is considered that the battery maintains the constant amount of voltage that is not dependent on other important factors until the battery runs out of charge. Nevertheless, in real situations the open loop voltage directly depends on main factors such as SOC and the capacity and load are indirectly dependent.

This model is usable for steady-state application and does not consider the behaviour of the battery. The updating for this model is done by replacing the voltage source by another voltage source that can be controlled by SOC. It is obvious that voltage changes by SOC with a look-up table. This will lead to improving the accuracy of the model.

### Linear model of battery

In this model an internal resistance ( $R_{int}$ ) is added to the model to have IR (Internal Resistant model) shown in Figure 2.5. Therefore, in this model we have a voltage source and a resistance.

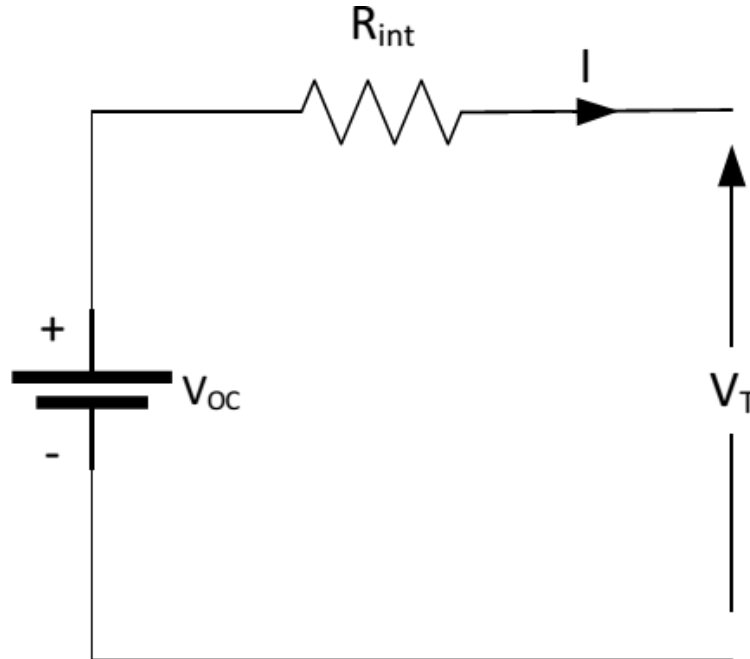


Figure 2-5: Linear and Simple model for battery

$R_{int}$  is losing energy and causes the battery to heat up and  $V_T$  shows the voltage depending on the Open Circuit voltage and its equation is as follows:

$$V_T = V_{OC} - IR_{int} \quad 2-1)$$

With this model we can emulate the instant dropped voltage that is dependent on the circuit current. If the resistance increases, the power loss will be increased, and the power availability will decrease. The main disadvantage of this method lies in its independence from the SOC, terminal voltage, open circuit voltage, and other important parameters of the battery. Internal resistance is completely dependent on parameters such as SOH, SOC, and temperature. However, in this model it does not depend on the parameters. By decreasing temperature, SOH, and SOC the resistance will increase. This is shown in Figure 2.6 and Figure 2.7 as follows. (Chiang, Sean and Ke, 2011)

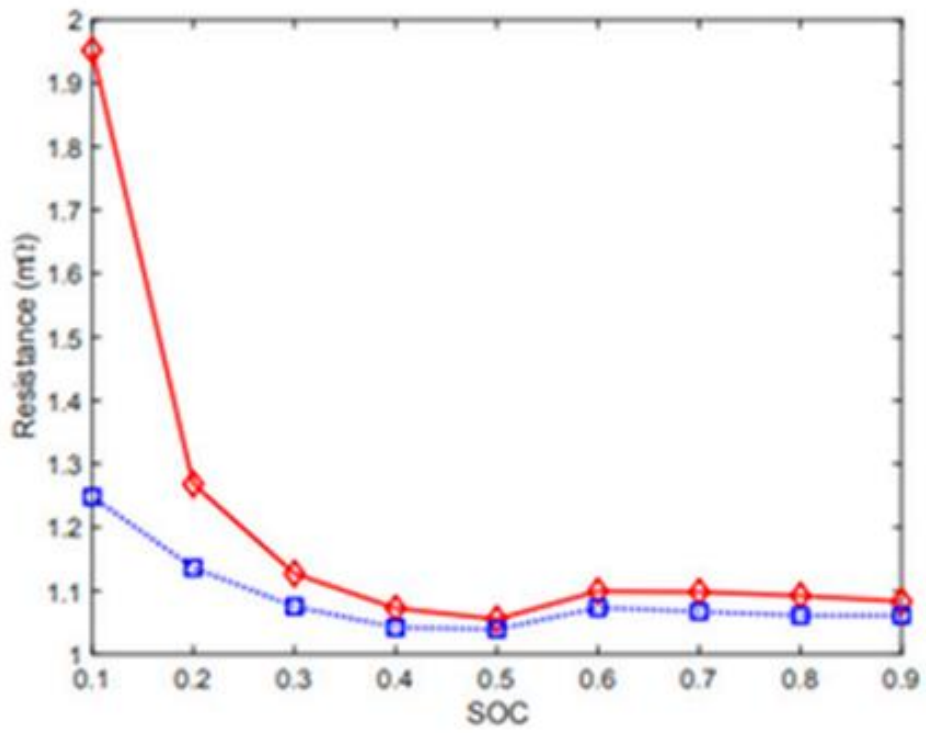


Figure 2-6: Internal resistance varies with SOC.

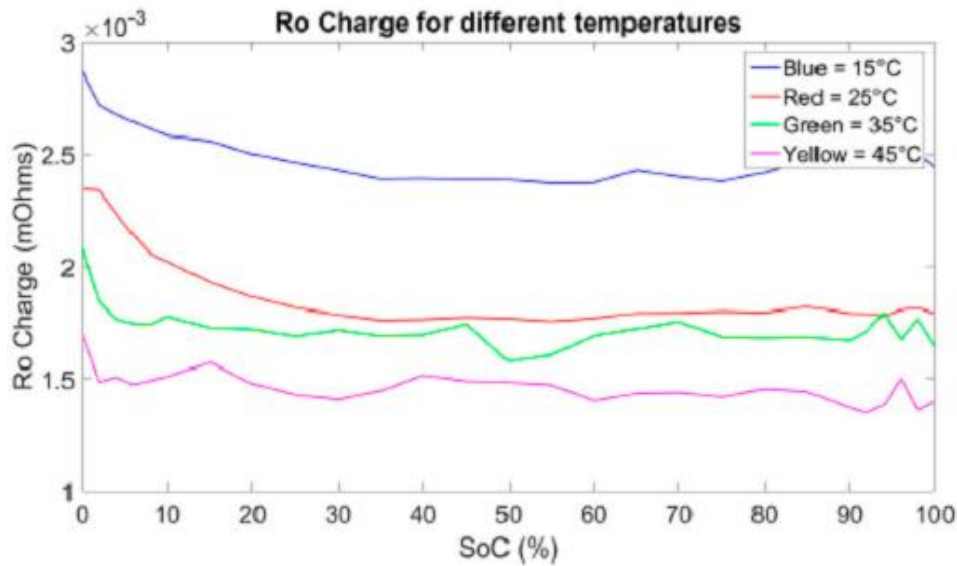


Figure 2-7: Internal resistance varies with temperature.

Figure 2-7 shows the internal resistance for 4 different temperatures. This model is only used in cases where the battery operates in the SOC's middle range. Because just in this part, internal resistance is approximately constant. We can use this model in studies related to maintenance and the model can be improved by having a voltage source dependent on SOC. (Chiang, Sean and Ke, 2011)

Moreover, internal resistance changes through charging and discharging time. So, we can add a separate resistance for charging and discharging time in Figure 2.8 as follows. (Dürr et al., 2006)

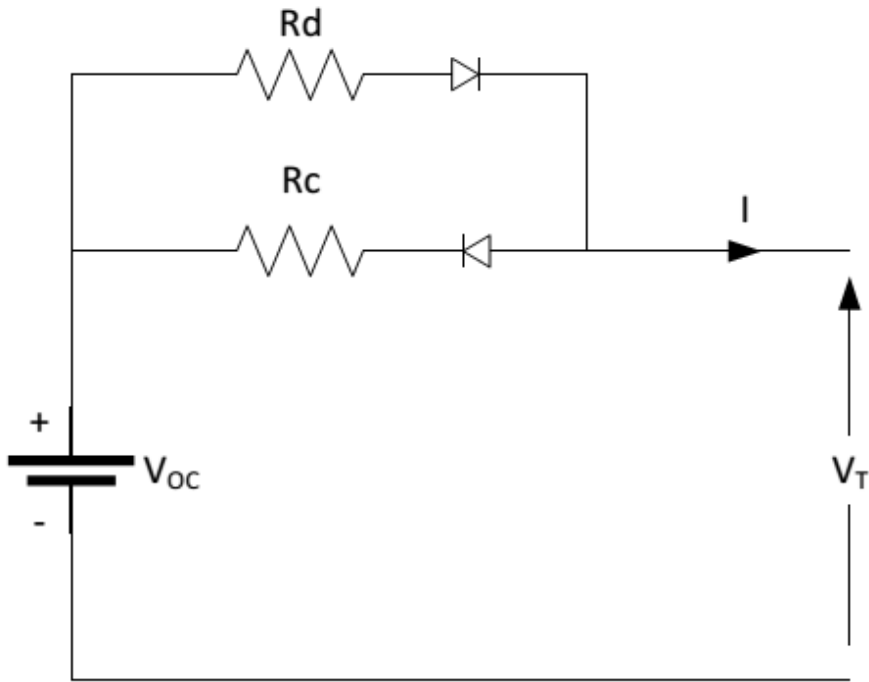


Figure 2-8: Adding charging and discharging resistance to the simplest battery model.

*Charging:*  $V_T = V_{OC} + R_C \cdot I$

*Discharging:*  $V_T = V_{OC} + R_d \cdot I$  2-2)

In charging time  $R_c$  associated diode will polarize directly and will conduct, however the other diode will polarize indirectly and will not let the current circulate. In this model accuracy will be improved but the drawback of the previous mode exists. This model is shown in Figure 2.9.

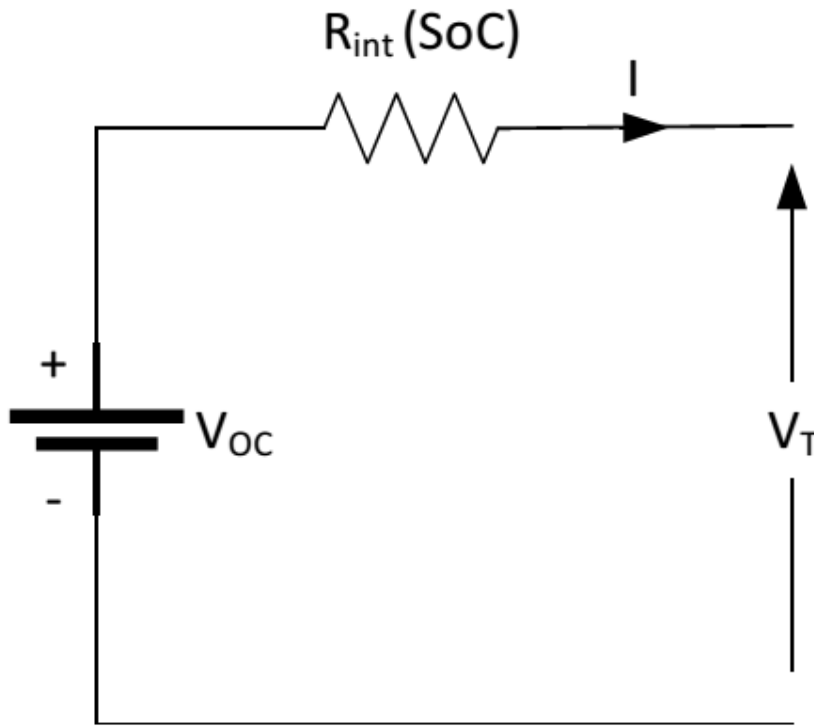


Figure 2-9: Power Fade (PF) considering in the simplest battery model.

$$R_{int}(SOC) = \frac{R_0}{SOC^k} \quad (2-3)$$

$$V_T = V_{OC} - R_{int}(SOC) \cdot I \quad (2-4)$$

$R_0$  shows the starting resistance,  $k$  is the factor of capacity that can be obtained from the curve of load that the manufacturer provides, and  $SOC$  shows the current  $SOC$ .

So, the recent value of  $SOC$  is as follow:

$$SOC = 1 - \frac{A \cdot h}{C_{10}} \quad (2-5)$$

' $A$ ' shows the current that is demanded, ' $h$ ' shows the time in Hours, and  $C_{10}$  shows the amount of capacity in 10 hours. Nevertheless, in some studies another resistance is added to the internal resistance, which is not linear as follows:

$$R_{int}(SOC) = R_{int} + \frac{k}{SOC} \quad 2-6$$

k shows a constant value for polarization and  $R_{int}(SOC)$  is a non-constant resistor.

So, this model has been widely used in stationary stages by a lot of battery producers. It is suitable for Pb-acid batteries. Moreover, in Li-ion batteries it can be used, as well. In the case of increasing the load, this model does not reduce the capacity. Therefore this model cannot be used in systems working dynamically or transient cases. The other drawback of the model is that the resistance does not vary with temperature. We can upgrade this model by adding  $V_{oc}$  that is controlled by SOC as follows:

$$V_T = V_{OC}(SOC) - R_{int}(SOC).I \quad 2-7$$

$$V_{OC}(SOC) = V_o - k.SOC \quad (2-8)$$

$$R_{int}(SOC) = R_{int} - k_R SOC \quad (2-9)$$

In the above equations  $V_{OC}$  is dependent on SOC and the internal resistance  $R_{int}(SOC)$  is dependent on SOC, as well.  $V_o$  is fully charged  $V_{OC}$ .

However, this model is not suitable for transient analysis. Its accuracy can be improved by considering SOH and temperature.

### Battery model using voltage sources:

This model is based on connecting several voltage sources that each show several things. It can be shown as follows in Figure 2.10: (Nikdel, 2014)

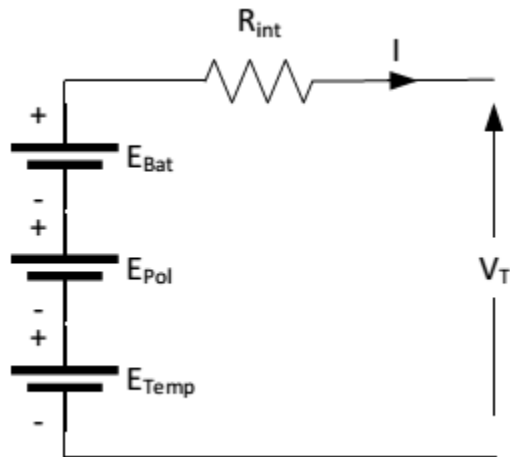


Figure 2-10: Model using voltage sources.

Terminal voltage can be written as follows:

$$V_T = E_{bat} + E_{pol} + E_{Temp} - R_{int} \cdot I \quad (2-10)$$

$E_{pol}$  shows polarizations resulted from active substances,  $E_{bat}$  represents the internal battery voltage,  $E_{Temp}$  shows the effect of temperature, and internal resistance is shown by  $R_{int}$ . The voltage sources can be obtained using practical measurement of the effect of each phenomenon in each SOC value. This is suitable for Li-ion, Pb-acid, and Ni-cd and applied for Hybrid automotive and EVs simulations.

### Electrical Dynamic Model RC (Resistor and Capacitor) Model:

This model was first developed by SAFT battery Company and is shown in Figure 2.11. (Chiang, Sean and Ke, 2011)

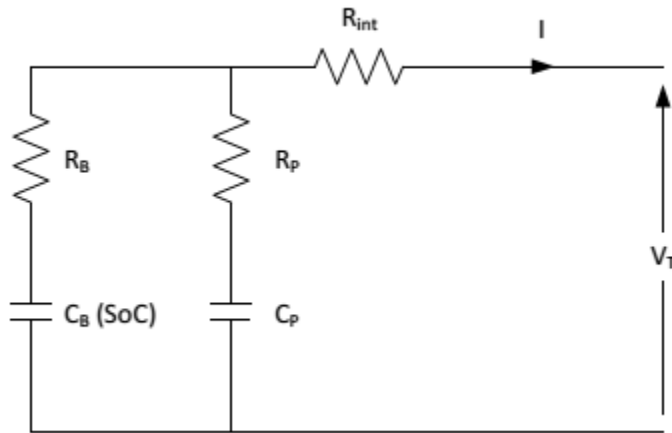


Figure 2-11: The Dynamic RC models

$C_p$  and  $R_p$  shows the polarization effects,  $C_p$  shows the capacitor for storage, propagation is shown by  $R_b$ ,  $R_{int}$ , shows internal resistor is so small, and  $C_b$  is very large. Moreover, in Li-ion batteries the resistance allocated for self-charging is negligible. The variation in voltage through the  $C_b$  is SOC.

This simple model is preferable in SOC estimation because it is accurate enough.

$$V_T = V_{OC} - R_b \cdot I_b - R_{int} \cdot I \quad (2-11)$$

$$V_T = V_{CP} - R_p \cdot I_p - R_{int} \cdot I \quad (2-12)$$

## Battery Thevenin Models:

This first model in the Thevenin models was called OTC (One time Constant). This model consists of an RC Serie,  $V_{OC}$  (open-source voltage), and internal resistance ( $R_{int}$ ). Figure 2.12 shows this model.

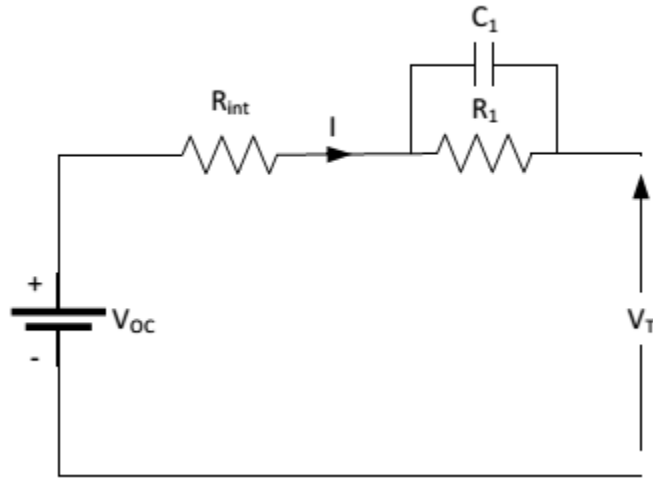


*Figure 2-12: OTC model*

To have good performance in transient mode we added an RC Serie to the simple model. The downside of the model is that it is assumed that all parameters are constant. All parameters in the model completely depend on SOH, SOC, temperature, and C rate. Therefore, improving the model can be considered as the effect of SOC on  $V_{oc}$ . It can improve the transient simulating results.

## Second Order Thevenin Model

In this model, there are two pairs of RCs. Therefore, the second time constants (TTC) are larger in comparison to the first order. RC pair ( $R_2$  and  $C_2$ ) with a larger time constant (Figure 2.13) to the previous model. Thus, it is possible to accurately represent the terminal voltage when the current is zero, which was not possible for the OTC. For representing transient conditions in the short-term the first RC is required, and for representing transient conditions in long-term the second RC is required. The main advantage of Li-ion batteries is that the hysteresis effect is low. So, we need a model considering temperature, SOC, and hysteresis. On the other hand, the second order Thevenin model surpasses these models that have good accuracy concerning hysteresis effect. By precisely adjusting the main parameters, we will have a precise model and we can use this model in several tests. A group of pulses consisting of charge-discharge are used, and the PEM algorithm (prediction error-minimization) was considered. Using the neuro-fuzzy method, SOC is obtainable discretely but using this model we have a fast enough algorithm for estimating the SOC in real-time operations. (Cai, Du and Liu, 2003)

In this model, there are two time-constants, and another R and C are added to the first order model. This model is shown in Figure 2.13. Via this model, we can terminal voltage in the case of zero current. However, in the first order model it is impossible.

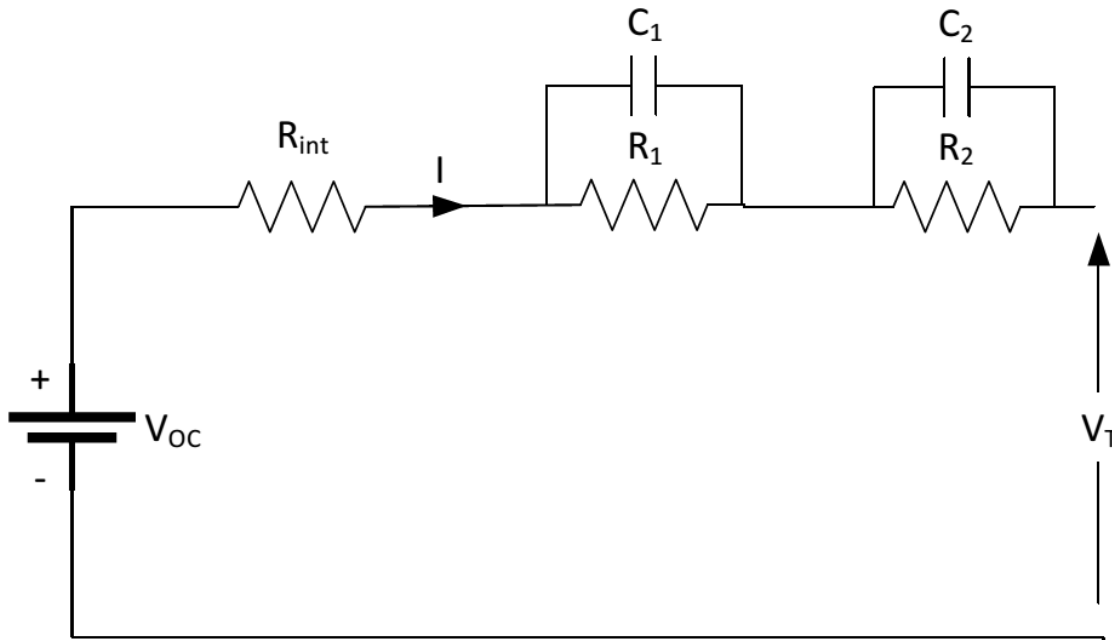


Figure 2-13: Thevenin model with 2RC pairs

So, the first RC pair shows transient effects in the short-term transient condition, and the second pair shows the long-term transient characteristic and has a larger time constant and consists of concentration polarization and electrochemical effects. These effects consist of diffusion, charge transfer effect. We have the following equations:

$$V_T = V_{OC} - R_{int} \cdot I - V_{C1} - V_{C1} \quad (2-13)$$

$$V_{C1} = -\frac{1}{R_1 \cdot C_1} \cdot V_{C1} + \frac{1}{C_1} \cdot I \quad (2-14)$$

$$V_{C2} = -\frac{1}{R_2 \cdot C_2} \cdot V_{C2} + \frac{1}{C_2} \cdot I \quad (2-15)$$

A more precise model is by adding  $R_{int}$  to the model and this has two parts, R series and R cycling showing cycling of the cell. In this model all the parameters are defined considering SOC and temperature.

## Noise and its types

Everywhere we go there is noise around us. For example, in the street, car, office, etc. Noise exists in different forms in our daily life. Noises can be stationary while their statistical characteristics do not change over time. Noises can also be non-stationary. Removing noise for non-stationary mode is much more difficult than for stationary mode.

Another characteristic of noise types is their spectrum mode, especially the distribution of noise energy in the frequency domain. The following are some of the noise types in their spectrum mode:

### **White Noise**

It is a random signal that assigns energy to each frequency band equal to the other bands in the frequency spectrum. This feature produces a flat spectrum in the frequency domain.

### **Pink noise**

Pink noise has smooth graph when the scale is logarithmic. It means that pink noise in each frequency band has the same power as other bands in a logarithmic scale.

### **Brown noise**

If the power density of our noise decreases by 6 decibels per octave in the frequency domain and does not include DC frequency, our noise is brown or red.

### **Industrial noise**

In this section, we consider the audio sample recorded from the operation of a drill as industrial noise. This noise is considered as a non-stationary noise.

To observe the state variables of a dynamic system from measurements with noise, methods based on the Kalman filter can be used, which will be discussed further.

## ***2.5 Estimation Methods for State of Charge***

Some methods have been proposed to estimate the SOC, such as the ampere-hour (Ah) counting, Kalman filter (KF), sliding mode observer (SMO), particle filter (PF), artificial neural network (ANN) and fuzzy logic (FL) methods. In this project Kalman Filter family has been applied for estimating the SOC. Some other methods are explained as follows:

### **Coulomb Counting Method**

This method is called, amper hour and current integration. This method is the most used method for SOC estimation. In this definition, the state of charge at any moment is the result of subtraction the initial value and the integral of the battery current (according to the current direction). SOC is calculated according to equation.

$$SOC = SOC_0 + \frac{1}{C} \int_0^t \eta i(\tau) \cdot d\tau \quad (2-16)$$

where C is the battery capacity in Farads,  $\eta$  is the coulombic discharge efficiency. Its value is usually taken as 99.0. This method depends on the amount of  $SOC_0$  and if its value is assumed to

be wrong; the whole estimate will be wrong. The effectiveness of the above system reduces with the noise that is also considered as one of the disadvantages of the above method. (Ng et al., 2009). In this definition, the state of charge is defined as the open circuit voltage of the battery (OCV). They are proportional and they have a linear relationship. There are some problems with this method:

- The initial SOC should be accurate.
- The current should be accurately measured.
- The error of current integration
- The accurate capacity of battery
- Timing error

## **Kalman Filter and its family**

Kalman filter is one of the most important types of Wiener filters that can adapt to changing conditions with time. It also covers estimation of states belongs to all the time and in the situation of an unrecognized model it has acceptable performance. Estimation is done by mathematics that in the right way it can reduce the RMSE (Root Mean Square Error) efficiently. (Shrivastava et al., 2019)

Estimation of a situation is done by probability density functions (pdf) and full pdf explanation requires a Bayesian optimal solution to solve the problem. This observation only applies to some systems because the pdf structure is unbounded and hence cannot be accounted for using a finite number of parameters. To solve this problem an optimal state estimator for linear estimation of dynamic systems designed using the concept of state space, which is known as the Kalman filter. That is very powerful for several reasons:

The Kalman filter is the best observer in the sense that it produces estimates with minimum variance of the system states. For example, the expected value of the error between the estimates of the filters and the real state of the system is zero, and the expected value of the squared error between the estimated states and the actual is minimum. For a discrete-time dynamic model when distributing the state space with the inputs with Gaussian noise, the Kalman filter provides a real-time recursive algorithm to estimate the state vectors by using only the available noisy data.

This filter is a productive recursive algorithm that is excellent in estimating noisy systems that are not statistic with minimum RMSE. This filter family works like a low pass matched digital filter IIR (Infinite Impulse Response) with a cut-off frequency, which relies on the ratio between the measured or observed noise as well as the estimated covariance.

### ***2.6 Kalman Filter family***

This filter was provided in 1960 and afterward many algorithms were introduced. Therefore, this fact shows the importance of this family. This Filter estimates using the last state estimation and the observation that is done now to obtain the current state estimate. This filter is a very powerful in combination of data in uncertainties presence. This filter has been used as the best solution for having precise prediction in some cases.

Wherever we have uncertain information about a dynamic system, we can use the Kalman filter to provide a good estimate of the system's future changes. Kalman filters are ideal for systems that are constantly changing. The advantage of Kalman filters is that they require little memory because they do not need memory except to store the information of previous states. Also, these filters are very fast and therefore suitable for real-time problems and embedded systems.

At first glance, the mathematics of the Kalman filter seem intimidating and obscure. But it is quite the opposite and if we learn it properly, it will be very simple to understand.

**Kalman filter algorithm:**

At the beginning, the system state variables are estimated in some time, subsequently the value of noise is achieved as feedback. We have two types of Equations:

- **Predictive equations (time update)**

By these equations we can produce recent state and estimate error covariance to have prior information used for the coming step.

- **Correction equations (measurement update)**

By these equations we can have feedback. For example, to combine a recent value with a previous prediction to achieve better final value. Figure 2-14 shows Kalman filter algorithm that V and W are applied to the system as process noise and measurement noise.

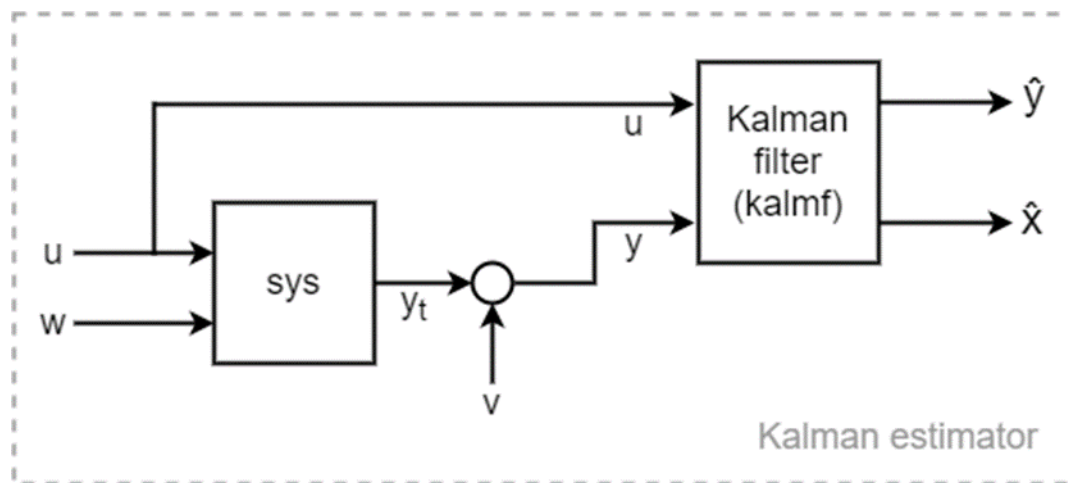


Figure 2-14 Kalman filter algorithm

Figure 2-15 shows the equation for the estimation of the current state that is completely related to predicted value and measurement value and Kalman gain.



Figure 2-15 The estimation of the current state

**Limitations of the Kalman filter algorithm:**

Some Kalman filter design methods were reviewed for systems with uncertainty and three scenarios were presented in which the Kalman filter is not well used:

- **Poor observation**

If the process is poorly visible, the sensors should be changed, or a new sensor should be added.

- **Numerical instability**

The covariance matrices may become asymmetric, which leads to divergence in the regression calculation.

- **Blind spot**

The error-covariance estimation situation decreases rapidly when both the measurement noise and the process noise covariance matrices are assumed to be very small.

**Extended Kalman Filter (EKF)**

*Extended Kalman Filter (EKF) is a nonlinear type in the Kalman filter family, that is linearized around a mean and covariance estimate. In the case of well-defined transient models, the EKF is proposed. (Huang, Mourikis and Roumeliotis, 2008)*

**Process dynamics**

Consider the following nonlinear system, which includes a differential equation and an observer model accompanied noise:

$$x_k = w_{k-1} + f(x_{k-1}) \tag{2-17}$$

$$z_k = v_k + h(x_k) \tag{2-18}$$

where  $x_0$  is the first coition of a random vector and its mean is  $\mu_0 = E[x_0]$  and covariance

$$P_0 = E [ (x_0 - \mu_0) (x_0 - \mu_0) T ] \tag{2-19}$$

Below we consider  $W_k$  as the random vector that is the model’s unpredictability and  $V_k$  represents the noise of measurement. They are not related to each other (noise) temporarily and

both are temporally, mean free random sequences by certain covariance. None of them is related to start state  $x_0$ .

$$E[w_k] = 0 \quad E[w_k w_k^T] = Q_k \quad E[w_k x_0^T] = 0 \text{ for all } k \quad E[w_k w_j^T] = 0 \text{ for } k \neq j \quad (2-20)$$

$$E[v_k] = 0 \quad E[v_k v_k^T] = R_k \quad E[v_k x_0^T] = 0 \text{ for all } k \quad E[v_k v_j^T] = 0 \text{ for } k \neq j \quad (2-21)$$

Also, these two vectors  $W_k$  and  $V_k$  are random, and they are not related to each other:

$$E[w_k v_j^T] = 0 \text{ for all } j \text{ and } k$$

Numbers of columns, rows and distribution of parameters are as follows:

$x_k$	is	$n \times 1$	– State vector
$w_k$	is	$n \times 1$	– Process noise vector
$z_k$	is	$m \times 1$	– Observation vector
$v_k$	is	$m \times 1$	– Measurement noise vector
$f(\cdot)$	is	$n \times 1$	– Process nonlinear vector function
$h(\cdot)$	is	$m \times 1$	– Observation nonlinear vector function
$Q_k$	is	$n \times n$	– Process noise covariance matrix
$R_k$	is	$m \times m$	– Measurement noise covariance matrix

Assuming nonlinear system dynamics and observing the simplified model,  $h(x_k)$  and  $f(x_k)$  can be expanded in the Taylor series, and this is an uncertain method of predicting and estimating the next  $x_k$ .

In the initial stage of model prediction, since the data we have is the mean,  $\mu_0$  and covariance,  $p_0$ , from the initial conditions of the states, and therefore the first and best estimate  $X_a^0$  and the error covariance are calculated as follows:

$$x_0^a = \mu_0 = E[x_0] \quad (2-22)$$

$$P_0 = E[(x_0 - x_0^a)^T (x_0 - x_0^a)] \quad (2-23)$$

Suppose that the estimate of  $x_{k-1}^a \equiv E[x_{k-1}|Z_{k-1}]$  is the best with covariance  $P_{k-1}$  at time  $k-1$ .  $x_k$  has a part that we can predict as follows:

$$x_k^f \equiv E[x_k|Z_{k-1}] = E[f(x_{k-1})|Z_{k-1}] = E[f(x_{k-1}) + w_{k-1}|Z_{k-1}] \quad (2-24)$$

$f(0)$  is expanded in the Taylor series around  $x_{k-1}^a$ , the following expression is obtained:

$$f(x_{k-1}) \equiv f(x_{k-1}^a) + J_f(x_{k-1}^a)(x_{k-1} - x_{k-1}^a) + H.O.T \quad (2-25)$$

$J_f$  represents  $f(x)$ 's Jacobian and higher order terms (H.O.T) are very small. Hence, we can assume EKF first order filter. Definition of Jacobian is as follows:

$$J_f \equiv \begin{bmatrix} \frac{\partial f_1}{\partial x_1} & \frac{\partial f_1}{\partial x_2} & \dots & \frac{\partial f_1}{\partial x_n} \\ \vdots & \vdots & \ddots & \vdots \\ \frac{\partial f_n}{\partial x_1} & \frac{\partial f_n}{\partial x_2} & \dots & \frac{\partial f_n}{\partial x_n} \end{bmatrix} \quad (2-26)$$

where  $f(x) = (f_1(x), f_2(x), \dots, f_n(x))^T$  and  $x = (x_1, x_2, \dots, x_n)^T$ . The equation becomes :

$$f(x_{k-1}) \approx f(x_{k-1}^a) + J_f(x_{k-1}^a)e_{k-1} \quad (2-27)$$

where  $e_{k-1} \equiv x_{k-1} - x_{k-1}^a$ . The expected value of  $f(x_{k-1})$  conditioned by  $Z_{k-1}$

$$E[f(x_{k-1})|Z_{k-1}] \approx f(x_{k-1}^a) + J_f(x_{k-1}^a)E[e_{k-1}|Z_{k-1}] \quad (2-28)$$

where  $E[e_{k-1}|Z_{k-1}] = 0$ . Thus the forecast value of  $x_k$  is

$$x_k^f \approx f(x_{k-1}^a) \quad (2-29)$$

Substituting (2 – 28) in the forecast error equation results :

$$\begin{aligned} e_k^f &\equiv x_k - x_k^f & (2-30) \\ &= f(x_{k-1}) + w_{k-1} - f(x_{k-1}^a) \\ &\approx J_f(x_{k-1}^a)e_{k-1} + w_{k-1} \end{aligned}$$

The covariance of the prediction error is given by:

$$\begin{aligned} P_k^f &\equiv E[e_k^f (e_k^f)^T] = J_f(x_{k-1}^a)E[e_{k-1}e_{k-1}^T]J_f^T(x_{k-1}^a) + E[w_{k-1}w_{k-1}^T] \\ &= J_f(x_{k-1}^a)P_{k-1}J_f^T(x_{k-1}^a) + Q_{k-1} \end{aligned} \quad (2-31)$$

### Data integration stage:

At every time for example  $k$ , there are two main knowledge: the predicted  $x_k^f$  value accompanied with covariance  $P_k^f$  and the  $z_k$  value accompanied with covariance  $R_k$ . The main purpose is to approximate the optimum least-squares predict of  $x_k^a$  from  $x_k$ . The proposed way is to believe that the estimate is a linear mixture of  $z_k$  and  $x_k^f$ .

$$x_k^a = a + K_k z_k \quad (2-32)$$

In Unbiasedness conditions:

$$\begin{aligned} 0 &= E[x_k - x_k^a | Z_k] \quad (2-33) \\ &= E[(x_k^f + e_k^f) - (a + K_k h(x_k) + K_k v_k) | Z_k] \\ &= x_k^f - a - K_k E[h(x_k) | Z_k] \\ a &= x_k^f - K_k E[h(x_k) | Z_k] \quad (2-34) \end{aligned}$$

By placing 2-34 in 2-33, we have:

$$x_k^a = x_k^f + K_k (z_k - E[h(x_k) | Z_k]) \quad (2-35)$$

Following the same steps as the step of predicting the model and expanding  $h(x_k)$  in the Taylor series around  $x_k^f$  we have:

$$h(x_k) \equiv h(x_k^f) + J(x_k^f)(x_k - x_k^f) + H.O.T \quad (2-36)$$

where  $J_h$  is the Jacobian  $h(x_k)$  and (H.O.T) terms of higher order are considered negligible. Jacobian  $h(x_k)$  is defined as follows:

$$J_h \equiv \begin{bmatrix} \frac{\partial h_1}{\partial x_1} & \frac{\partial h_1}{\partial x_2} & \dots & \frac{\partial h_1}{\partial x_n} \\ \vdots & \vdots & \ddots & \vdots \\ \frac{\partial h_m}{\partial x_1} & \frac{\partial h_m}{\partial x_2} & \dots & \frac{\partial h_m}{\partial x_n} \end{bmatrix} \quad (2-37)$$

where  $h(x) = (h_1(x), h_2(x), \dots, h_m(x))^T$  and  $x = (x_1, x_2, \dots, x_n)^T$  2-40

are obtained from expanding both sides of 2-36 by subjecting to  $z_k$ :

$$E[(x_k - x_k^a) | Z_k] \equiv h(x_k^f) + J_h(x_k^f) E[e_k^f | Z_k] \quad (2-38)$$

Since we have  $E[(x_k - x_k^a) | Z_k] = 0$  by placing in 2-39, the estimation of the state is:

$$x_k^a \approx x_k^f + K_k (z_k - h(x_k^f)) \quad (2-40)$$

The error in  $x_k^a$  estimation is as follows

$$e_k \approx x_k^f - x_k^a = f(x_{k-1}) + w_{k-1} - x_k^f - K_k (h(x_k) - h(x_k^f)) \quad (2-41)$$

$$\begin{aligned} &\approx f(x_{k-1}) - f(x_{k-1}^a) + w_{k-1} - K_k (h(x_k) - h(x_k^f) + v_k) \\ &\approx J_f(x_{k-1}^a) e_{k-1} + w_{k-1} - K_k (J_h(x_k^f) e_k^f + v_k) \\ &\approx J_f(x_{k-1}^a) e_{k-1} + w_{k-1} - K_k J_h(x_k^f) (J_f(x_{k-1}^a) e_{k-1} + w_{k-1}) - K_k v_k \end{aligned}$$

$$\approx \left( I - K_k J_h(x_k^f) \right) J_f(x_{k-1}^a) e_{k-1} + \left( I - K_k J_h(x_k^f) \right) w_{k-1} - K_k v_k$$

So, the covariance after the new estimate is as follows:

$$\begin{aligned} P_k &\equiv E[e_k e_k^T] & (2-42) \\ &= \left( I - K_k J_h(x_k^f) \right) J_f(x_{k-1}^a) P_{k-1} J_f^T(x_{k-1}^a) \left( I - K_k J_h(x_k^f) \right)^T \\ &\quad + \left( I - K_k J_h(x_k^f) \right) Q_{k-1} \left( I - K_k J_h(x_k^f) \right)^T + K_k R_k K_k^T \\ &= \left( I - K_k J_h(x_k^f) \right) P_k^f \left( I - K_k J_h(x_k^f) \right)^T + K_k R_k K_k^T \\ &= P_k^f - k_k J_h(x_k^f) P_k^f - P_k^f J_h^T(x_k^f) k_k^T + k_k J_h(x_k^f) P_k^f J_h^T(x_k^f) k_k^T + K_k R_k K_k^T \end{aligned}$$

The next covariance formula is preserved for each  $k_k$ . As with the standard Kalman filter, we obtain  $k_k$  by minimizing the (Pk)

$$\begin{aligned} 0 &= \frac{\partial \text{tr}(P_k)}{\partial K_k} = -\left( J_h(x_k^f) P_k^f \right)^T - P_k^f J_h^T(x_k^f) + \\ &2K_k J_h(x_k^f) P_k^f J_h^T(x_k^f) + \\ &2K_k R_k \end{aligned} \quad (2-43)$$

As Kalman gain is as following:

$$K_k = P_k^f J_h^T(x_k^f) \left( J_h^T(x_k^f) P_k^f J_h^T(x_k^f) + R_k \right)^{-1} \quad (2-44)$$

By substituting in 25 will have:

$$\begin{aligned} P_k &= \left( I - K_k J_h(x_k^f) \right) P_k^f - \left( I - K_k J_h(x_k^f) \right) P_k^f J_h^T(x_k^f) K_k^T + \\ &K_k R_k K_k^T & (2-45) \\ &= \left( I - K_k J_h(x_k^f) \right) P_k^f - \left( P_k^f J_h^T(x_k^f) - K_k J_h(x_k^f) P_k^f J_h^T(x_k^f) - K_k R_k \right) K_k^T \\ &= \left( I - K_k J_h(x_k^f) \right) P_k^f - \left[ P_k^f J_h^T(x_k^f) - K_k \left( J_h(x_k^f) P_k^f J_h^T(x_k^f) + R_k \right) \right] K_k^T \\ &= \left( I - K_k J_h(x_k^f) \right) P_k^f - \left[ P_k^f J_h^T(x_k^f) - P_k^f J_h^T(x_k^f) \right] K_k^T = \left( I - K_k J_h(x_k^f) \right) P_k^f \end{aligned}$$

### EKF in a glance:

Model and Observations:

$$w_{k-1} \quad x_k = f(x_{k-1}) + \quad (2-46)$$

$$= h(x_k) + v_k \quad (2-47)$$

Initialization:

$$x_0^a = \mu_0 \text{ with error covariance } P_0 \quad (2-48)$$

Model Forecast step/Predictor:

$$x_k^f \approx f(x_{k-1}^a) \quad (2-49)$$

$$P_k^f = J_f(x_{k-1}^a)P_{k-1}J_f^T(x_{k-1}^a) + Q_{k-1} \quad (2-50)$$

Data assimilation step/Corrector:

$$x_k^a \approx x_k^f + K_k(z_k - h(x_k^f)) \quad (2-51)$$

$$K_k = P_k^f(x_k^f)(J_h(x_k^f)P_k^f J_h^T(x_k^f) + R_k)^{-1} \quad (2-52)$$

$$P_k = (I - K_k J_h(x_k^f))P_k^f \quad (2-53)$$

### Limitations of the EKF algorithm:

EKF block diagram is shown in Figure 2.14 as follows. (Lin, 1996). Although EKF is a computationally efficient recursive form of the Kalman filter, it has some serious limitations:

- EKF does not guarantee that the estimates it makes are unbiased. Moreover, there is the possibility that the obtained error covariance is not correct.
- Linearization can only be used if there is a Jacobian matrix. In some cases, obtaining the analytical Jacobian matrix is so hard. For these applications, it is required to obtain the numerical approximation of the Jacobian matrix.
- In standard EKF divergency of the system heavily depends on the estimation of the first conditions of the system states, and therefore the scaling of the filter parameters is a critical step for estimation.

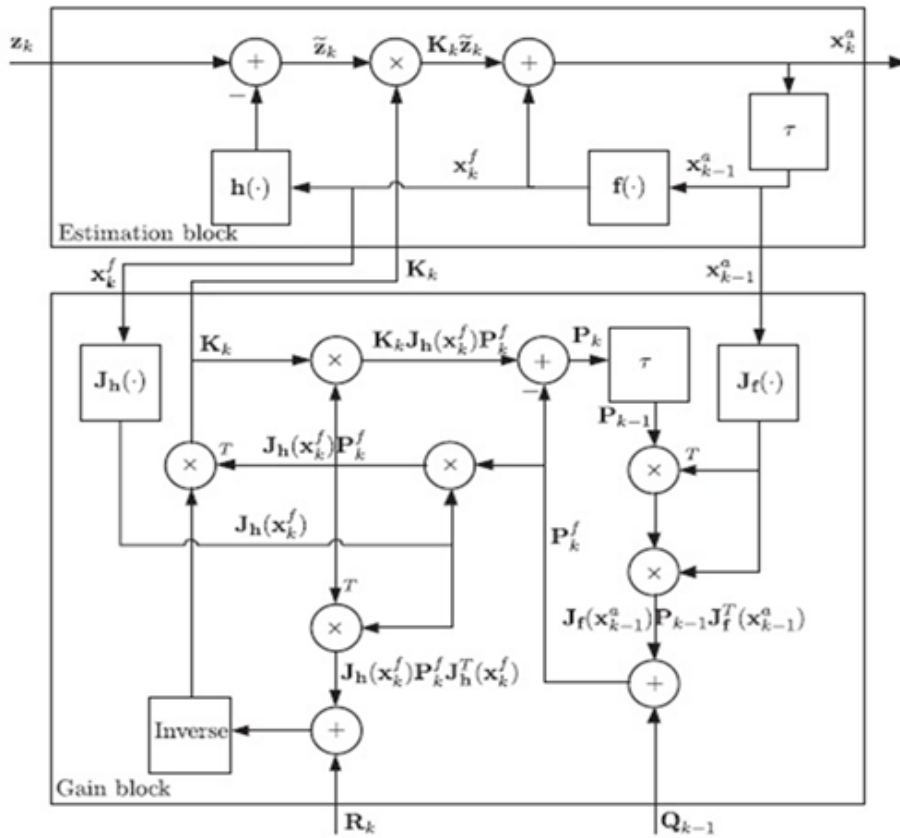


Figure 2-16: EKF block diagram

Figure 2-16 shows the main steps and equations for Extended Kalman Filter. This block diagram contains all steps for linearization of EKF.

### Iterative Extended Kalman Filter (IEKF)

In the EKF,  $h(0)$ , is linearized around the predicted state estimate  $x_k^f$ . IEKF tries to linearize it around the last estimate made.

This is obtained by calculating  $X_{k,0}^a$ ,  $k_k$ ,  $p_k$  in each iteration. The meaning of  $X_{k,i}^a$  is the estimate at time  $k$  and the  $i$ -th iteration. The iteration process starts with  $X_{k,0}^a = X_k^f$ , then the step of updating the measurement for each  $i$  is as follows:

$$x_{k,i}^a \approx x_k^f + K_k \left( Z_k - h(x_{k,i}^a) \right) \quad (2-54)$$

$$K_{k,i} = P_k^f J_h^T(\hat{x}_{k,i}) \left( J_h(x_{k,i}^a) P_k^f J_h^T(x_{k,i}^a) + R_k \right)^{-1} \quad (2-55)$$

$$P_{k,i} = \left( I - K_{k,i} J_h(x_{k,i}^a) \right) P_k^f \quad (2-56)$$

If this is a small improvement between two consecutive iterations, then the iteration process stops. The accuracy obtained by this method increases with the increase in the calculation time.

### Particle Filter:

The algorithm of the particle filter method is based on the following Monte Carlo method, for example, a sampling method to approximate a spreading that causes it to be used in a temporal structure. In the spread of  $P(x_t|z_{0:t})$ ,  $x_t$  presents the state that is not observed at time  $t$  and  $z_{0:t}$  shows the series of observations starting at time zero and ending at time  $t$ . If linear Gaussian guess about the transmitters and sensor modellings,  $P(x_{t+1}|x_t)$  will be in complicated form, on the other hand it will be shown with  $N$  samples with weights or  $N$  elements.  $\{x_t^{(i)}, \Pi_t^{(i)}\}_{i=1}^N$  where  $\Pi_t^{(i)}$  is the weight of the element  $x_t^{(i)}$ ,  $a$ .

$$P(x_t|z_{0:t}) \approx \sum_i \Pi_{t-1}^{(i)} \delta(x_t - x_{t-1}^{(i)}) \quad (2-57)$$

To perform each filtering step, it is necessary to take the integral:

$$P(x_t|z_{0:t}) = \alpha P(z_t|x_t) \quad (2-58)$$

We obtain filter spread  $P(x_t|z_{0:t})$  by using the recursive definition obtained by the spread of  $P(x_{t-1}|z_{0:t-1})$ . By using the elements determined for  $P(x_{t-1}|z_{0:t-1})$ , previous formula will be approximately as follows:

$$P(x_t|z_{0:t}) \approx \alpha P(z_t|x_t) \sum_i \Pi_{t-1}^{(i)} \delta(x_t - x_{t-1}^{(i)}) \quad (2-59)$$

How can the set of elements representing the distribution of  $P(x_t|z_{0:t})$  be achieved? One answer is to use purposive sampling. The particle filter method can perform the observation operation as a special sampling vector on this distribution. Sampling technique is a method to generate relatively good samples of a  $p(x)$  distribution. Assume  $p(x)$  shows a concentration that is difficult to graph, but checking  $p(x_i)$  for some specific  $x_i$  is straightforward. So an estimation for  $p(x)$  is determined as follows:

$$P(x) \approx \sum_{i=1}^N \pi^{(i)} \delta(x - x^{(i)}) \quad (2-60)$$

$$\pi^{(i)} = \frac{P(x)}{q(x^{(i)})} \quad (2-61)$$

The point is that each  $q(x)$  shows a propositional spread and is applied in this equation, in specific a single sampling of the  $x$  as state space. Nevertheless, when we are sampling uniquely, lots of samples with small values of  $\pi^i$  will be wasted. However, we use a lot of proposed spread, the estimation for  $P(x_t|z_{0:t-1})$  (in whole Eq. 2). Due to proposed spread, the weight matrices  $\pi^i$  eventually become approximately simple resulting in cancellation. Specifically, the particle filter method includes 3 main steps:

1. Draw  $N$  samples  $x_t^{(j)}$  from the proposal distribution  $q(x_t)$ :

$$x_t^{(j)} \sim q(x_t) = \sum_i \pi_{t-1}^{(i)} P(x_t | x_{t-1}^{(i)}) \quad (2-62)$$

By randomly choosing a number  $r$  between 0 and 1 selecting the related element  $i$  and by sampling  $P(x_t|x_{t-1}^{(i)})$ , this transient model is considered as a linear Gaussian model, but every model that can be drawn from those samples will be sufficient.

2. set the weight  $\pi_t^{(j)}$  as the likelihood:

$$\pi_t^{(j)} = P(y_t | x_t^{(j)}) \quad (2-63)$$

The examples of  $\{x^{(i)}_t\}$  above are relatively good examples of  $P(x_t|z_{0:t-1})$ .

3. Normalize the weights  $\{\pi_t^{(j)}\}$ :

$$\pi_t^{(j)} = \frac{\pi_t^{(j)}}{\sum_k \pi_t^{(k)}} \quad (2-64)$$

The other important thing is that there is a better suggested distribution that is unused here. The optimal proposed distribution of variance minimization is found in the weights  $\pi^i$  in  $p(x_t|x_{t-1}, z_t)$ . We can consider particle filter's capability to cope with the non-simple multi-model non-Gaussian feature as its most prominent feature. Nevertheless, in some cases where  $x_t$  is large it will be difficult. Basically, the number of  $N$  elements requires a distribution approximation that increases exponentially with the dimensions of the state space. This may cause difficulties for some cases like human body limb tracking or SLAM.

### Unscented Kalman Filter (UKF) Method

The UKF method is one of the larger filters' family named sigma-point Kalman filters or inverse linear Kalman filters.

We can utilize this algorithm for linearizing a non-linear system consisting of a random variable through a linear regression between  $n$  points drawn from the first distribution of the random variable. Dealing with the extended random variable, this method is more reliable and accurate than Taylor series linearizing methods (Sun et al., 2011).

First order linearization is applied in the EKF method and states of non-linear systems since there is the possibility the next mean and covariance are not correct. In the UKF method we do not use derivation such as EKF, so it is the method, which is a free derivative alternative to EKF, and overcomes this problem by using a certain sampling approach.

The mode distribution is represented using a minimum set of carefully selected points called sigma points. Like EKF, UKF consists of the same two steps: model prediction and data assimilation. It is expected that there will now be another step for selecting sigma points.

### UKF algorithm

In the UKF method it is important to understand that approximating is simpler than a probability spread and is close to a linear transformation or system.

We select Sigma points until their covariance and mean are the same as  $x_{k-1}^a$  and  $P_{k-1}$ . Therefore, every sigma point is then propagated via non-linear submitting after the transformed point stack. The last estimate of mean and covariance are calculated using their statistical index. It is named as unscented conversion. By the unscented transformation we can obtain the statistical indices of a random variable that is propagated through nonlinear transformation and change. We can explain a nonlinear function by two differential equation and the observation plus noise equations:

$$x_k = f(x_{k-1}) + w_{k-1} \quad (2-65)$$

$$z_k = h(x_k) + v_k \quad (2-66)$$

$x_0$  represents a first state and is a random vector with unknown mean  $\mu_0 = E[x_0]$  and covariance  $P_0 = E[(x_0 - \mu_0)(x_0 - \mu_0)]^T$ . for the noiseless system and the measurement noise, the unscented transformation method is used for the enhanced mode.

$$x_k^{aug} = [x_k^T \ w_{k-1}^T \ v_k^T]^T \quad (2-67)$$

### Choosing sigma points:

$X_{k-1}$  exists in a group consists of  $2n + 1$  sigma points ( $n$  shows the state space dimension) and its relation to the weights:

$$X_{k-1} = \{ (x_{k-1}^j, W^j) | j = 0 \dots 2n \} \quad (2-68)$$

The following sigma point selection introduces higher order information into the chosen points.

$$X_{k-1}^0 = x_{k-1}^a \quad (2-69)$$

$$-1 < w^0 < 1 \quad (2-70)$$

$$x_{k-1}^i = x_{k-1}^a + \left( \sqrt{\frac{n}{1-w^0} P_{K-1}} \right)_i \text{ for all } i = 1 \dots n \quad (2-71)$$

$$x_{k-1}^{i+n} = x_{k-1}^a - \left( \sqrt{\frac{n}{1-w^0} P_{K-1}} \right)_i \text{ for all } i = 1 \dots n \quad (2-72)$$

$$W^j = \frac{1-w^0}{2n} \text{ for all } j = 1 \dots 2n \quad (2-73)$$

$$\sum_{j=0}^{2n} W^j = 1 \quad (2-74)$$

And  $\sqrt{\frac{n}{1-w^0} P_{K-1}}$  represents the column or row belonging to the square matrix of squares  $\frac{n}{1-w^0} P_{K-1}$ .  $W^0$  adjusts sigma points' location:

Points  $w^0 > 0$  want to be further from the main, points  $w^0 \leq 0$  want to be closer to the main. The algorithm for choosing sigma points called scaled unscented transformation is explained in detail in (Dunik, Simandl and Straka, 2012).

### Model prediction stage

All sigma points are expanded via the non-linear trend function:

$$x_k^{f,j} = f(x_{k-1}^j) \quad (2-75)$$

The transformed points are utilized to calculate the predicted value covariance and mean. The new sigma points are required to calculate the predicted value  $x_k$ 's covariance and mean of:

$$x_k^f = \sum_{j=0}^{2n} W^j x_k^{f,j} \quad (2-76)$$

$$P_k^f = \sum_{j=0}^{2n} W^j (x_k^{f,j} - x_k^f)(x_k^{f,j} - x_k^f)^T + Q_{k-1} \quad (2-77)$$

In the next step the sigma points are obtained via the non-linear observation model:

$$z_{k-1}^{f,j} = h(x_{k-1}^j) \quad (2-78)$$

By observing the transformations, their mean and covariance (creative covariance) are calculated:

$$z_{k-1}^f = \sum_{j=0}^{2n} W^j z_k^{f,j} \quad (2-79)$$

$$\text{cov}(\tilde{z}_{k-1}^f) = \sum_{j=0}^{2n} W^j (z_k^{f,j} - z_{k-1}^f)(z_k^{f,j} - z_{k-1}^f)^T + R_k \quad 2-80)$$

$$\text{cov}(\tilde{x}_k^f, \tilde{z}_{k-1}^f) = \sum_{j=0}^{2n} W^j (x_k^{f,j} - x_{k-1}^f)(z_k^{f,j} - z_{k-1}^f)^T \quad (2-81)$$

### Data integration stage

It is desirable to mix the information achieved in the prediction stage with the recently observed  $z_k$  value, such as KF, it is assumed that the estimate has the following forms:

$$x_k^a = x_k^f + K_k(z_k - z_{k-1}^f) \quad 2-82$$

$$K_k = \text{cov}(\tilde{x}_k^f, \tilde{z}_{k-1}^f) \text{cov}^{-1}(\tilde{z}_{k-1}^f) \quad (2-83)$$

$$P_k = P_k^f - K_k \text{cov}(\tilde{z}_{k-1}^f) K_k^T \quad (2-84)$$

### UKF square method

The point in computing another group of sigma points is that the squared matrix of the prior covariance is required at each time ( $P_k = S_k S_k^T$ ) and new information is used to achieve new covariance. We can use the method change to the direct expansion of the squared matrix,  $s_k$ . The sigma points scheme is selected as follows:

$$x_{k-1}^0 = x_{k-1}^a \quad 2-85)$$

$$-1 < w^0 < 1 \quad 2-86)$$

$$x_{k-1}^i = x_{k-1}^a + \left( \sqrt{\frac{n}{1-w^0} S_{k-1}} \right)_i \quad \text{for all } i = 1 \dots n \quad (2-87)$$

$$x_{k-1}^{i+n} = x_{k-1}^a - \left( \sqrt{\frac{n}{1-w^0} S_{k-1}} \right)_i \quad \text{for all } i = 1 \dots n \quad (2-88)$$

$$W^j = \frac{1-w^0}{2n} \quad \text{for all } j = 1 \dots 2n \quad 2-89)$$

The filter starts by calculating the initial squared matrix by Cholesky factorization of the covariance matrix with the highest error value:

$$S_0 = \text{chol}(E[(x_0 - \mu_0)(x_0 - \mu_0)^T]) \quad (2-90)$$

$w^j > 0$  for all  $i \geq 0$  in the next time, the covariance prediction matrix will be as follows:

$$\begin{aligned}
P_k^f &= \sum_{j=0}^{2n} W^j (x_k^{f,j} - x_k^f)(x_k^{f,j} - x_k^f)^T + Q_{k-1} \quad (2-91) \\
&= \sum_{j=0}^{2n} \sqrt{W^j} (x_k^{f,j} - x_k^f) \sqrt{W^j} (x_k^{f,j} - x_k^f)^T + \sqrt{Q_{k-1}} \sqrt{Q_{k-1}}^T \\
&\quad + W^0 (x_k^{f,0} - x_k^f)(x_k^{f,0} - x_k^f)^T \\
&= [\sqrt{W^j} (x_k^{f,j} - x_k^f) \sqrt{Q_{k-1}} \begin{bmatrix} \sqrt{W^j} & (x_k^{f,j} - x_k^f)^T \\ 0 & \sqrt{Q_{k-1}}^T \end{bmatrix} \\
&\quad + [W^0 (x_k^{f,0} - x_k^f)(x_k^{f,0} - x_k^f)^T] \quad \text{for } j = 1 \dots 2n
\end{aligned}$$

which  $\sqrt{Q_{k-1}}$  square matrix is the noise processing of the covariance matrix. This form is computationally unfavourable. Since the number of columns is three.

$$[\sqrt{W^j} (x_k^{f,j} - x_k^f) \quad \sqrt{Q_{k-1}}] \in R^{n \times 3n} \quad \text{for } j = 1 \dots 2n \quad (2-92)$$

$$[\sqrt{W^j} (x_k^{f,j} - x_k^f) \quad \sqrt{Q_{k-1}}]^T \in Q_k (S_k^f)^T \quad \text{for } j = 1 \dots 2n \quad (2-93)$$

$$\begin{aligned}
P_k^f &= S_k^f O_k^T O_k (S_k^f)^T + W^0 (x_k^{f,0} - x_k^f)(x_k^{f,0} - x_k^f)^T \quad (2-94) \\
&= S_k^f (S_k^f)^T + W^0 (x_k^{f,0} - x_k^f)(x_k^{f,0} - x_k^f)^T
\end{aligned}$$

To have the final term effect in the square matrix, it is required to apply a rank 1 update for the Cholesky factorization:

$$S_k^f = \text{cholupdate} (S_k^f, (x_k^{f,0} - x_k^f), \text{sgn}\{W^0\} \sqrt{W^0}) \quad (2-95)$$

*cholupdate* returns the cholesky factor of

$$S_k^f (S_k^f)^T + W^0 (x_k^{f,0} - x_k^f)(x_k^{f,0} - x_k^f)^T \quad (2-96)$$

Therefore, the prediction of the covariance matrix can be written  $P_k^f = S_k^f (S_k^f)^T$ . The same method, the next covariance could be written as  $P_k = S_k (S_k)^T$  and the original covariance can be expressed as:

$$\text{Cov}(z_{k-1}^{-f}) = S_{k-1}^{-f} S_{k-1}^T \quad (2-97)$$

Time update summary:

$$x_k^{f,j} = f(x_{k-1}^j) \quad (2-98)$$

$$x_k^f = \sum_{j=0}^{2n} W^j x_k^{f,j} \quad (2-99)$$

$$S_k^f = qr[\sqrt{W^j}(x_k^{f,j} - x_k^f) \quad \sqrt{Q_{k-1}}] \in R^{n \times 3n} \quad \text{for } j = 1 \dots 2n \quad (2-100)$$

$$S_k^f = \text{cholupdate}(S_k^f, (x_k^{f,0} - x_k^f), \text{sgn}\{W^0\}\sqrt{W^0}) \quad (2-101)$$

The sigma points are redrawn under the influence of unifying the noise process:

$$x_k^{f,0} = x_k^f \quad (2-102)$$

$$x_k^{f,i} = x_k^f + \left( \sqrt{\frac{n}{1-w^0} S_k^f} \right)_i \quad \text{for all } i = 1 \dots n \quad (2-103)$$

$$x_k^{f,i+n} = x_k^f + \left( \sqrt{\frac{n}{1-w^0} S_k^f} \right)_i \quad \text{for all } i = 1 \dots n \quad (2-104)$$

Expansion of new sigma points through measurement model:

$$h(x_{k-1}^j) \quad z_{k-1}^{f,j} = \quad (2-105)$$

$$z_{k-1}^f = \sum_{j=0}^{2n} W^j z_k^{f,j} \quad 2-106$$

$$S_{\tilde{z}_{k-1}^f} = qr[\sqrt{W^j}(z_{k-1}^{f,j} - z_{k-1}^f) \quad \sqrt{R_k}] \quad \text{for } j = 1 \dots 2n \quad 2.2-107$$

$$S_{\tilde{z}_{k-1}^f} = cholupdate \left( S_{\tilde{z}_{k-1}^f}, (z_{k-1}^{f,0} - z_{k-1}^f), \text{sgn}\{W^0\}\sqrt{W^0} \right) \quad 2-108$$

$$cov(\tilde{x}_k^f, \tilde{z}_{k-1}^f) = \sum_{j=0}^{2n} W^j (x_k^{f,j} - x_{k-1}^f)(z_k^{f,j} - z_{k-1}^f)^T \quad 2-109$$

The function returns only the lower order triangular matrix.

Measurement update summary:

$$x_k^a = x_k^f + K_k(z_k - z_{k-1}^f) \quad 2-110$$

$$K_k = cov(\tilde{x}_k^f, \tilde{z}_{k-1}^f)cov^{-1}(\tilde{z}_{k-1}^f) \quad (2-111)$$

$$S_k = cholupdate K_k cov(\tilde{x}_k^f, \tilde{z}_{k-1}^f), -1) \quad 2-112$$

which is defined as reverse placement function. This is a better replacement to matrix inversion. Since the Cholesky factor is a lower-order triangular matrix, Kk can be achieved by substituting in the following equation.

$$K_k \begin{pmatrix} S_{\tilde{z}_{k-1}^f} & S_{\tilde{z}_{k-1}^f}^T \\ S_{\tilde{z}_{k-1}^f}^T & S_{\tilde{z}_{k-1}^f} \end{pmatrix} = cov(\tilde{x}_k^f, \tilde{z}_{k-1}^f) \quad (2-113)$$

In equation (114), since the argument of the mean is the Cholesky update function  $\epsilon R^{n \times n}$  of the matrix, the result is n successive updates of the Cholesky factor with n columns in the matrix.

Since Cholesky factorization and QR decomposition want to better control round-off errors and the inverse term of the matrix does not exist, SR-UKF has better numerical properties and guarantees the fundamental state of the covariance as positive semi-definite.

Repeated Unscented Kalman filter method (IUKF)

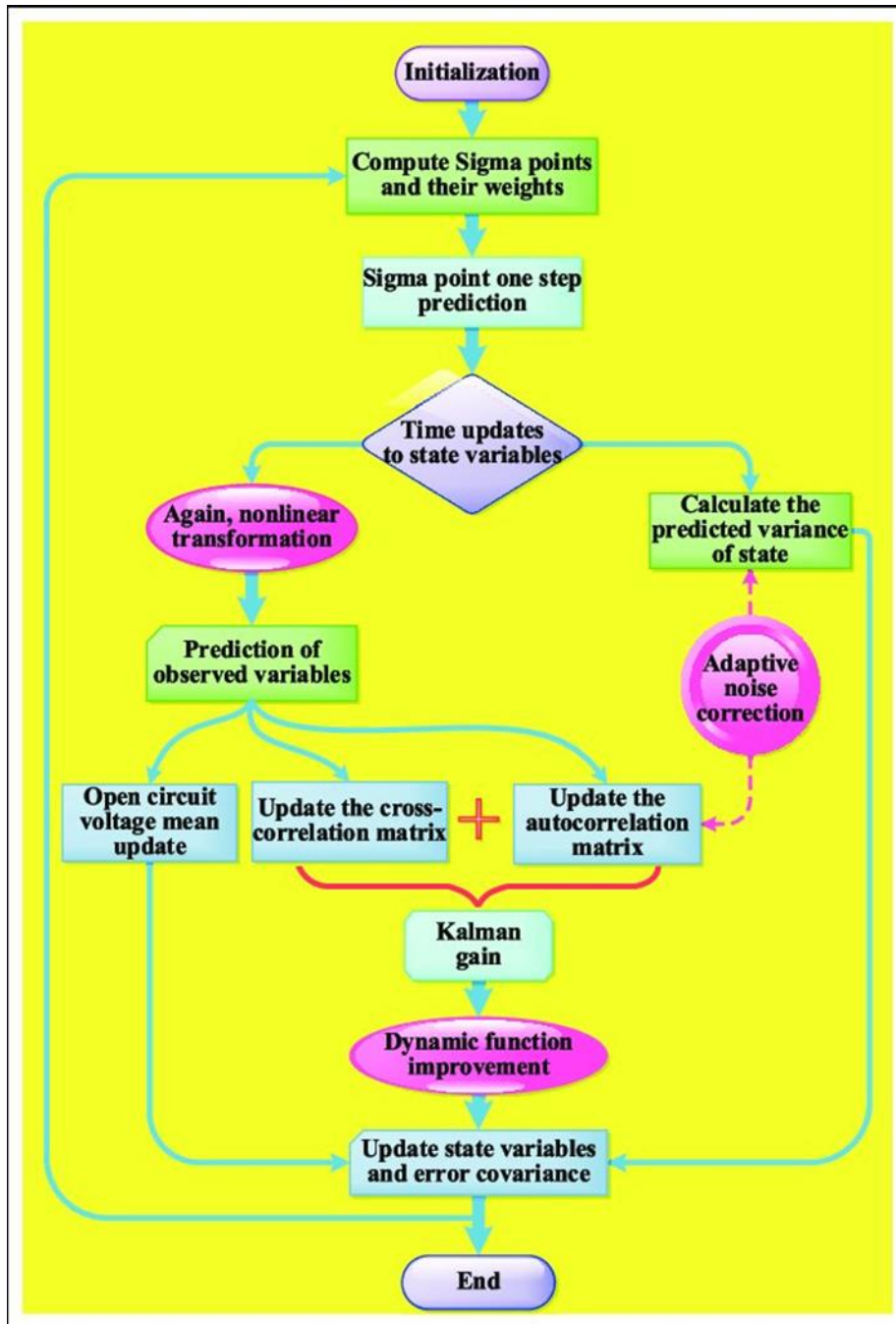


Figure 2-17 Unscented Kalman Filter flowchart

Figure 2-17 shows the main steps of estimation by Unscented Kalman Filter (UKF). It is consist of initializing, selecting sigma points, nonlinear transformation, calculating variance and Kalman gain, and repeating the steps.

$$X_0(K|K) = \hat{X}(K|K) \quad 2-114)$$

$$W_0 = \frac{K}{(n+k)} \quad (2-115)$$

$$x_i(k|k) = (\sqrt{(n+k)p(k|k)})_i + \hat{X}(k|k) \quad i = 1, \dots, n \quad 2-116)$$

$$W_i = \frac{1}{2(n+k)} \quad 2-117$$

$$x_i(k|k) = \hat{X}(k|k) + (\sqrt{(n+k)p(k|k)})_i \quad i = n + 1, \dots, 2n \quad 2-118$$

$$W_i = \frac{1}{2(n+k)} \quad 2-119)$$

The group of samples selected by (1) have the same sample covariance, mean, and all odd ranks of the central moment as  $x(k)$  spread.  $K$  and the square matrix are affected by the sampled moments of the fourth order and higher orders of the sigma point. The following nonlinear filtering problem is defined as:

$$X(K+1) = F_K(X(K), W(K)) \quad (2-120)$$

$$Z(K) = h_{k+1}(x(k)) + v(k) \quad (2-121)$$

So,  $x(k)$  shows the state vector of the function at time step  $k$ ,  $w(k)$  is the process noise vector, created by modelled troubles and errors,  $z(k)$  shows the observation vector and  $v(k)$  is the added measurement noise. The noise vector  $V(K)$  and  $W(K)$  have zero mean.

$$[W(i)W^T(j)] = \delta_{ij}c_w(i) \quad (2-122)$$

$$E[V(i)V^T(j)] = \delta_{ij}c_v(i) \quad \forall i, j \quad 2-123)$$

$$E[V(i)W^T(j)] = 0 \quad 2-124)$$

It is assumed that the probability density of the next moment in time  $K$  is Gaussian, for example  $p(x_k|z_k) = N(x_k; \hat{x}_k, P(k|k))$ . The first step is to present this density function with a set of  $x_i^{(k|k)}$   $2n$  sample points and their weights  $W_k^i, i = 0, \dots, 2n$ . Each sigma point of a sample in the middle of the model process is the product of a set of transformed samples:

$$X_{k+1|k}^i = f_k(x_i(k|k)) \quad (2-125)$$

The prediction stage is then performed as follows:

$$\hat{X}(K + 1|K) = \sum_{i=0}^{2n} W_K^i X_{K+1|k}^i \quad (2-126)$$

And the predicted covariance matrix is calculated as follows:

$$P(K + 1|K) = \sum_{i=0}^{2n} W_K^i [X_{K+1|k}^i - \hat{X}(K + 1|K)][X_{K+1|k}^i - \hat{X}(K + 1|K)]^T \quad (2-127)$$

The covariance matrix and mean vector are obtained with matrix and standard vector functions, the mean algorithm is suitable for each step of choosing to advance the model process. This implementation is simply because it does not require the Jacobian analysis required in EKF. This method is more advantageous when its product has a more accurate prediction than the analytical linearization method. The next step is the updating. The information comes from observation of  $z(k)$  measurement and is applied to correct the probability density system. The use of Bayes theorem on the conditional probability density for memory sensor systems is as follows:

$$\begin{aligned} P(X(K)|Z(K)) &= P(X(K)|Z(K - 1), Z(K)) \quad (2-128) \\ &= \frac{1}{c} P(Z(K)|X(K), Z(K - 1)) P(X(K)|Z(K - 1)) \\ &= \frac{1}{c} P(Z(K)|X(K)) P(X(K)|Z(K - 1)) \end{aligned}$$

where  $z(k)$  is the set of observations achieved from  $z(1)$  to  $z(k)$  and  $c$  is the nonlinearization factor:

$$c = \oint X(K) \in XP(Z(K)|X(K))P(X(K)|Z(K - 1))dX(K) \quad (2-129)$$

The approximation produces both the measurement noise and the predicted state that are relevant to the normal distribution. Therefore,  $P(Z(K)|X(K))$  the probability function of the next moment is that the result includes two and one Gaussian result. So, the MMSE estimate coincides with the MAP estimate, and so the task now is to obtain the maximum of  $P(Z(K)|X(K))$ . Equivalently and simultaneously, we can maximize its logarithm. After removing inappropriate constants and relevant items, it all resulted in minimizing the following equation:

$$\bar{X}_p) \underbrace{f(X) = \frac{1}{2} (X - \bar{X}_p)^T C_p^{-1} (X - \bar{X}_p)}_{\text{due to } p(x(k)|z(k - 1))} \quad (2-130)$$

due to  $p(x(k)|z(k - 1))$

$$+ \frac{1}{2} \underbrace{(Z - h(x))^T C_v^{-1} (z - h(x))}_{\text{due to } p(z(k)|x(k))}$$

In short, the following points are used:

$$\bar{X}_p = \hat{X}(K + 1|K) \quad (2-131)$$

$$C_p = P(K + 1|K) \quad 2-132$$

$$Z = Z(K) \quad 2-133$$

$$C_v = C_v(K) \quad 2-134$$

The way of finding the minimum is to use the Newton-Raphson iteration, which uses  $\bar{X}_0 = \hat{X}(K + 1|K)$  in the L iteration step, we already have an estimate  $\bar{X}_{l-1}$  obtained from the previous step. For approximation, we use the second order Taylor series for expanding f(x):

$$\begin{aligned} f(X) &= (X - \bar{X}_{l-1})^T \frac{\partial f(\bar{X}_{l-1})}{\partial X} + f(\bar{X}_{l-1}) \\ &+ \frac{1}{2} (X - \bar{X}_{l-1})^T \frac{\partial^2 f(\bar{X}_{l-1})}{\partial X^2} (X - \bar{X}_{l-1}) \end{aligned} \quad (2-135)$$

which  $\frac{\partial f}{\partial X}$  shows the gradient (slope) and  $f(x) \frac{\partial^2 f}{\partial X^2}$  is Hessian. The estimate  $\bar{X}_l$  is the minimum approximation that is obtained by equating the slope of the approximation to zero.

Differentiating from (8) gives us the following expression:

$$\frac{\partial f(\bar{X}_{l-1})}{\partial X} + \frac{\partial^2 f(\bar{X}_{l-1})}{\partial X^2} (X - \bar{X}_{l-1}) = 0 \quad 2-136$$

$$\bar{X}_l = \bar{X}_{l-1} - \left[ \frac{\partial^2 f(\bar{X}_{l-1})}{\partial X^2} \right]^{-1} \frac{\partial f(\bar{X}_{l-1})}{\partial X} \quad 2-137$$

Hessian and Jacobian f(x) in simple and obvious form is obtained from 2-139 as follows:

$$\frac{\partial f(\bar{X}_{l-1})}{\partial X} = C_p^{-1} (\bar{X}_{l-1} - X_p) - H_l^T C_v^{-1} (Z - h(\bar{X}_{l-1})) \quad 2-138$$

$$\frac{\partial^2 f(\bar{X}_{l-1})}{\partial X^2} = C_p^{-1} + H_l^T C_v^{-1} H_l \quad (2-139)$$

which  $H_l = H(\bar{X}_{l-1})$  is the Jacobian matrix h(x) obtained in  $\bar{X}_{l-1}$   
Substituting (10) into (9) is seen in the following iteration:

$$\bar{X}_l = \bar{X}_{l-1} - (C_p^{-1} + H_l^T C_v^{-1} H_l)^{-1} [C_p^{-1} (\bar{X}_{l-1} - X_p) - H_l^T C_v^{-1} (z - h(\bar{X}_{l-1}))] \quad 2-140$$

The number needed for more iterations is related to converges speed. This is a general element to fix the number of iterations in the L number in a practical and practical way. The result is the last iteration set, for example  $\hat{X}(K|K) = \bar{X}_L$  (2-141)

The factor  $(C_p^{-1} + H_l^T c_v^{-1} H_l)^{-1}$  in (2-141) can be considered as the error covariance matrix related to  $\bar{X}(K|K)$ :

$$p(k|k) = (c_p^{-1} + H_l^T C_v^{-1} H_l)^{-1} \quad 2-142$$

It makes another connection and continuity in the last part in 2-143 and in fact the part of  $p(k|k)H_l^T C_v^{-1}$  could be the Kalman obtained in the matrix k1 in iteration.

Figure 2-18 shows the difference between EKF and UKF in a simple way. The EKF uses linearization and UKF as mentioned before uses some points (Sigma points) to obtain real mean and covariance.

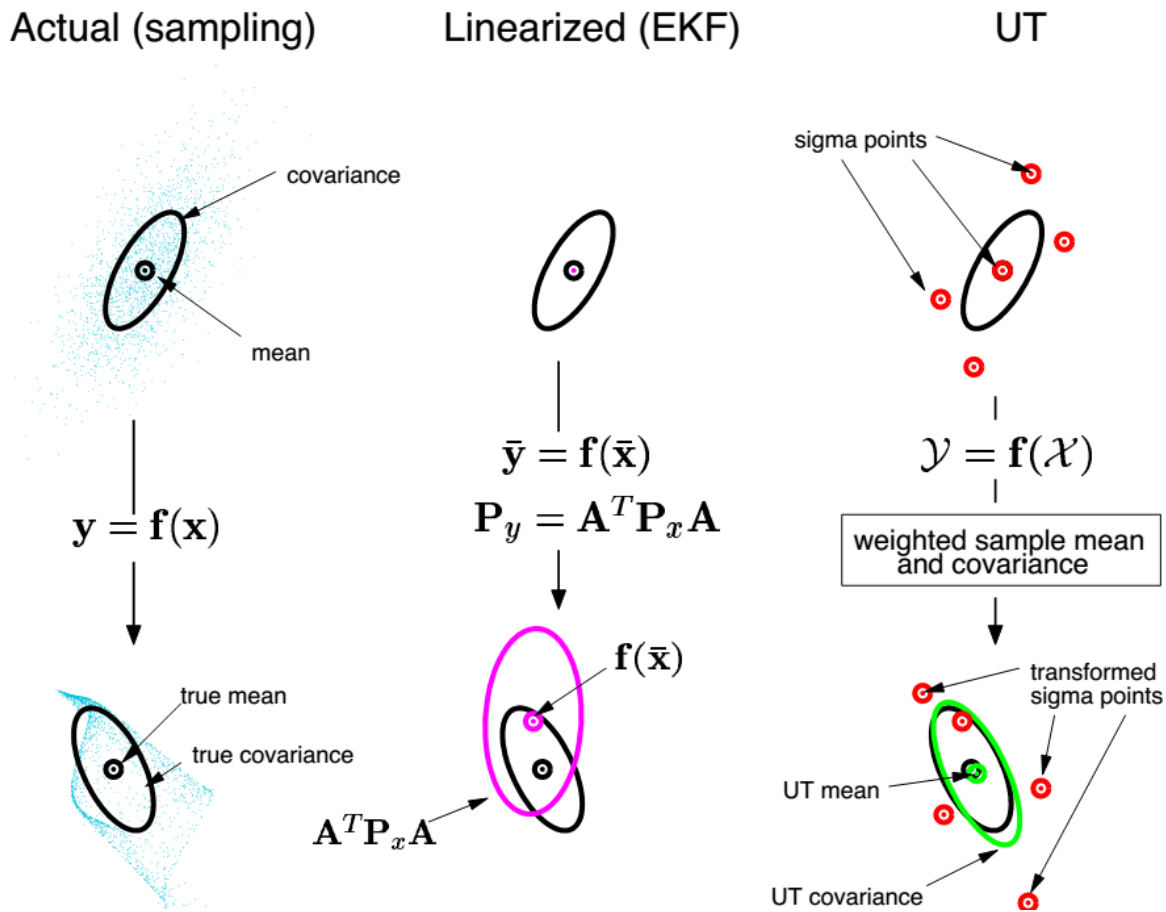


Figure 2-18 The difference between actual sampling, Extended Kalman Filter and Unscented transformation

## 3. SOC Estimation Based on Kalman Filter

### 3.1 Introduction

The statistical characteristics of measurement noise were corrected. Moreover, adaptively the matrix of error covariance was corrected and updating of model parameters online consequently was done using the measurable parameters, in the presence of uncertainty in model variables and matrix of noise covariance initial value. The battery's internal chemical chemistry is quite complex. The performance of various types of batteries varies. Even identical lithium-ion batteries from the same brands have a wide range of performance (Seaman, Dao and McPhee, 2014). Due to the nonlinear properties, performance can be strongly influenced by environmental factors and load conditions. The electrochemical model and the equivalent circuit model are the two types of battery models now in use. To describe the electrochemical model, an electrochemical approach is used (He, Xiong and Fan, 2011).

This method requires a lot of computing power and is better suited to research in electrolyte and electrode fields. The equivalent circuit model simulates the battery's dynamic voltage characteristics by using circuit elements like capacitors and resistors to construct a model consisting of resistors and capacitors. This method is easier to use than the electrochemical model, and it accurately captures the battery's dynamic reaction. Because the comparable circuit model is better suited for simulating purposes, it is used for battery status updating. In this study the lithium-ion battery's equivalent circuit model consists of a second-order RC network topology, which was used for simulating the polarisation effect during the charging stage and discharging.

A first-order functional state space equation was employed as an analogous circuit model for the second-order RC network topology since it is balanced in terms of processing complexity and accuracy. The root means square error (RMSE) was utilised as the assessment index to quantify the estimation error of techniques. Model-based approaches consisting of the Standard Kalman Filter, Extended Kalman Filter (EKF), and Unscented Kalman Filter (UKF) for battery state estimation were thoroughly investigated. The fundamental constraints and challenges of various types of Kalman filter families were discussed, as well as the advantages and disadvantages of existing SOC estimate approaches. In the presence of uncertainty in model parameters, the precise initial value of the noise covariance matrix is unknown, for example, EKF cannot produce reliable estimation results. To address these flaws, a unique approach for improving the accuracy and resilience of the EKF was proposed. In the meantime, the EKF was adaptively corrected using a unique technique that can update model parameters online based on the measurable variables and error covariance matrix.

### 3.2 Battery modelling

Battery modelling is an essential and tricky issue in the Battery management system. So far, there are several models for batteries. It has been reported that they are generally divided into four categories consisting of ideal model, behavioural model, electrochemical model, and electrical

equivalent model. Equivalent circuit models include ordered RC networks is used to recommend the dynamic characteristics of the battery(Gu and Wang, 2000). In this study, it is required to be more accurate and precise, low calculation, so the second order RC model is used, which is shown in Figure 3.1. (Lotfivand, Yu and Gomm, 2022)

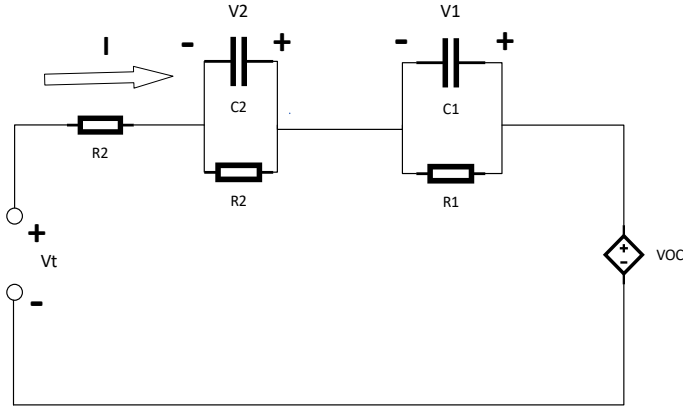


*Figure 3-1 Battery Thevenin Model*

The following equations are derived from the figure using KVL:

$$V_1(t) = \frac{-V_2(t)}{R_1 C_1} + \frac{I(t)}{C_1} \quad (3-1)$$

$$V_2(t) = \frac{-V_1(t)}{R_2 C_2} + \frac{I(t)}{C_2} \quad 3-2$$

$$SoC = \frac{\eta I(t)}{Q} \quad (3-3)$$

$$V_t(t) = V_{OC}(SoC(t)) + V_1(t) + V_2(t) + I(t)R_0 \quad 3-4$$

The state and measurement equations are as follows:

$$\dot{x}(t) = \frac{dx}{dt} = Bu(t) + Ax(t) \quad (3-5)$$

$$Y(t) = Du(t) + Cx(t) \quad (3-6)$$

$$A = \begin{bmatrix} \frac{-1}{R_1 C_1} & 0 & 0 \\ 0 & \frac{-1}{R_2 C_2} & 0 \\ 0 & 0 & 0 \end{bmatrix} \quad (3-7)$$

$$B = \begin{bmatrix} \frac{1}{C_1} \\ \frac{1}{C_2} \\ \frac{\eta}{Q} \end{bmatrix} \quad C = \begin{bmatrix} 1 & 1 & \frac{dV_{OC}}{dSOC} \end{bmatrix} \quad D = [R_0]$$

$$\text{State Vector} = x(t) = \begin{bmatrix} V_1(t) \\ V_2(t) \\ SoC(t) \end{bmatrix} \quad (3-8)$$

### 3.3 Applying Extended Kalman Filter for the battery model

The state matrix is A, the input matrix is B, the output matrix is C, and the feedthrough matrix is D. EKF approach uses a discrete state space model. This is because data will be updated after each time step. The following is the discrete state space model:

$$V_1(k+1) = e^{\frac{-\Delta T}{R_1 C_1}} V_1(k) + R_1 (1 - e^{\frac{-\Delta T}{R_1 C_1}}) \quad (3-9)$$

$$V_2(k+1) = e^{\frac{-\Delta T}{R_2 C_2}} V_2(k) + R_2 (1 - e^{\frac{-\Delta T}{R_2 C_2}}) \quad (3-10)$$

$$A = \begin{bmatrix} e^{\frac{-\Delta T}{R_1 C_1}} & 0 & 0 \\ 0 & e^{\frac{-\Delta T}{R_2 C_2}} & 0 \\ 0 & 0 & 0 \end{bmatrix} \quad B = \begin{bmatrix} R_1 (1 - e^{\frac{-\Delta T}{R_1 C_1}}) \\ R_2 (1 - e^{\frac{-\Delta T}{R_2 C_2}}) \\ \frac{\eta \Delta T}{Q} \end{bmatrix} \quad (3-11)$$

$$C = \begin{bmatrix} 1 & 1 & \frac{dV_{OC}}{dSOC} \end{bmatrix} \quad D = [R_0]$$

The prominent and forthright method for estimating SOC is the Coulomb counting method. However, there are two problems using these algorithms: the first is the amount of SoC and sensor noise. SoC estimation will be erroneous if the starting SoC is incorrect because the CC method is not a closed loop control method, so sensor noise will be added at each time step.

Closed loop approaches such as EKF are employed to solve these shortcomings. The suggested methodology employs the EKF method to estimate SOC and Terminal voltage.

The Hybrid Pulse Power Characterization (HPPC) test data achieved in 4 temperatures from 40°C to -10°C are used to calculate the SOC 3-dimensional curve as a function of SOC and T. In the proposed methodology, a four-order polynomial to the entirety of the SOC-OCV data fitted with thermal effects on Open Circuit Voltage (OCV).

$$OCV=f(SOC, Temperature) \quad (3-12)$$

It can be written as a function of SOC and temperature as follows:

$$OCV_{fit}=p00+p10*SOC+p11*SOC*T+p20*SOC^2+p11*SOC*T+p02*T^2+P30*SOC^3+p21*SOC^2*T+p12*SOC*T^2+p03*T^3+p40*SOC^4+P31*SOC^3*T+p22*SOC^2*T^2+P13*SOC*T^3+p04*T^4$$

Derivative of OCV with respect to SOC is: (3-14)

$$\frac{dOCV}{dSOC} = 4*p40*SOC^3 + 3*p31*SOC^2*T + 3*p30*SOC^2 + 2*p22*SOC*T^2 + 2*p21*SOC*T + 2*p20*SOC + p13*T^3 + p12 * T^2 + p11 * T + p10$$

Derivative of OCV with respect to SOC is:

$$df\_OCV\_T=p31*SOC^3+2*p22*SOC^2*T+p21*SOC^2+3*p13*SOC*T^2+2*p12*SOC*T+p11*SOC+4*p04*T^3+ \quad (3-15)$$

$$3*p03*T^2+2*p02*T+p01$$

### 3.4 Applying Unscented Kalman Filter for the battery model

$$SoC = \frac{\eta(t)}{Q} \quad (3-16)$$

$$V_t(t) = V_{OC}(SoC(t)) + V_1(t) + V_2(t) + I(t)R_0 \quad (3-17)$$

The state and measurement equations are as follows:

$$\dot{x}(t) = Bu(t) + Ax(t) \quad (3-18)$$

$$Y(t) = Du(t) + Cx(t) \quad (3-19)$$

$$A = \begin{bmatrix} \frac{-1}{R_1 C_1} & 0 & 0 \\ 0 & \frac{-1}{R_2 C_2} & 0 \\ 0 & 0 & 0 \end{bmatrix} \quad (3-20)$$

$$B = \begin{bmatrix} \frac{1}{C_1} \\ \frac{1}{C_2} \\ \frac{1}{Q} \end{bmatrix}$$

$$C = \begin{bmatrix} 1 & 1 & \frac{dV_{OC}}{dSoC} \end{bmatrix} \quad D = [R_0]$$

$$\text{State Vector} = x(t) = [V_1(t) \quad V_2(t) \quad SoC(t)] \quad (3-21)$$

The state matrix is A, the input matrix is B, the output matrix is C, and the feedthrough matrix is D. (He, Xiong and Guo, 2012)

EKF approach uses a discrete state space model. This is because data will be updated after each time step. The following is the discrete state space model:

$$V_1(k+1) = e^{\frac{-\Delta T}{R_1 C_1}} V_1(k) + R_1 \left(1 - e^{\frac{-\Delta T}{R_1 C_1}}\right) \quad (3-22)$$

$$V_2(k+1) = e^{\frac{-\Delta T}{R_2 C_2}} V_2(k) + R_2 \left(1 - e^{\frac{-\Delta T}{R_2 C_2}}\right) \quad (3-23)$$

$$A = \begin{bmatrix} e^{\frac{-\Delta T}{R_1 C_1}} & 0 & 0 \\ 0 & e^{\frac{-\Delta T}{R_2 C_2}} & 0 \\ 0 & 0 & 0 \end{bmatrix} \quad (3-24)$$

$$B = \begin{bmatrix} R_1(1 - e^{\frac{-\Delta T}{R_1 C_1}}) \\ R_2(1 - e^{\frac{-\Delta T}{R_2 C_2}}) \\ \frac{\eta \Delta T}{Q} \end{bmatrix}$$

$$C = \begin{bmatrix} 1 & 1 & \frac{dV_{OC}}{dSOC} \end{bmatrix} \quad D = [R_0]$$

The most popular and straightforward method for estimating SOC is the Coulomb Counting method. Nevertheless, this algorithm has two main drawbacks: the first value of SoC and sensor noise. SoC estimation will be erroneous if the starting SoC is incorrect. Because the CC method is not a closed loop algorithm, sensor uncertainty accumulates at each time step. Closed loop approaches such as EKF are employed to solve these shortcomings. The second issue with Coulomb Counting method is that in Li-ion batteries middle part of Open Circuit Voltage graph is flat and small measurement error will lead to a big error in estimation.

The EKF needs to linearize both equations consisting of state and measurement equations. It leads to have lower order nonlinear systems and less precise at the same time. It assumes this is a drawback for the EKF method and so the UKF method is preferable. Using UKF Jacobians and Hessians is not required, and this method is ‘derivative-free’ among the Kalman filter family. The EKF algorithm uses one spot that is called mean, however in UKF we have several points known as sigma points consisting of mean. As in UKF we need few sigma points, it needs moderate computation (Sun et al., 2011) . We use sigma points to find two main parameters consisting of mean and covariance of main data. There will be 2n+1 sigma points. Choosing sigma points is described as follows:

$$X_{k-1}^{[0]} = X_{k-1}^+ \quad (3-25)$$

$$X_{k-1}^{[i]} = (\sqrt{(n + \lambda)P_{k-1}}) + X_{k-1}^+ \text{ for } i=1,2,\dots,n \quad (3-26)$$

$$X_{k-1}^{[i]} = -(\sqrt{(n + \lambda)P_{k-1}}) + X_{k-1}^+ \text{ for } i=n+1,\dots,2n \quad (3-27)$$

Then these points go through equations (3-28) to (3-30) and their weights are as follows:

$$\frac{\lambda}{n+\lambda} w_m^{[0]} = \quad (3-28)$$

$$w_c^{[0]} = (1 - \alpha^2 + \beta) + w_m^{[0]} \quad (3-29)$$

$$w_m^{[i]} = w_c^{[i]} = \frac{1}{2(n+\lambda)} \text{ for } i = 1, 2, \dots, 2n \quad (3-30)$$

$$\lambda = \alpha^2(n + k) - n \quad (3-31)$$

Since weights are normalized, the sum of them is one.

$X_{k-1}^+$  is supposed as the mean of the selected points,  $P_{k-1}$  is the covariance matrix of state variables,  $n$  is the number of state variables,  $k$  is another scaling factor and normally it is  $3-n$ ,  $\alpha$  shows the stretch of sigma points,  $\beta$  shows prior knowledge of  $x$  distribution [9] and it is 2 for gaussian noises.

The number of columns is  $i$ , computing mean weight is  $w_m^{[i]}$ , computing covariance weight is  $w_m^{[i]}$ .

So, the Unscented Kalman Filter algorithm is as follows:

We can assume the nonlinear system as:

$$x(n+1) = f(w(n), u(n), x(n)) \quad (3-32)$$

$$Y(n) = h(v(n), x(n)) \quad (3-33)$$

prediction:

- By propagating sigma points via transition equation, we have:

$$x_k^i = f(X_{k-1}^{[i]}, u_k) \text{ for } i = 0, 1, \dots, 2n \quad (3-34)$$

- Getting priori covariance matrix:

$$x_k^- = \sum_{i=0}^{2n} w_m^{[i]} x_k^i \quad (3-35)$$

$$P_k^- = \sum_{i=0}^{2n} w_c^{[i]} (x_k^i - x_k^-)(x_k^i - x_k^-)^T + Q \quad (3-36)$$

Updating:

- Computing propagated sigma point measurements through measurement equation:

$$y_k^i = h(x_k^i, u_k) \text{ for } i = 0, 1, \dots, 2n \quad (3-37)$$

- Computing measurement mean:

$$y_k = \sum_{i=0}^{2n} w_m^{[i]} y_k^i \quad (3-38)$$

- Computing measurement covariance matrix:

$$P_k^y = \sum_{i=0}^{2n} w_c^{[i]} (y_k^i - y_k)(y_k^i - y_k)^T + R \quad (3-39)$$

- Computing cross covariance matrix:

$$P_k^{xy} = \sum_{i=0}^{2n} w_c^{[i]} (x_k^i - x_k^-)(y_k^i - y_k)^T \quad (3-40)$$

- UKF Gain:

$$K_k = P_k^{xy} (P_k^y)^{-1} \quad (3-41)$$

- Updating the state variables:

$$x_k^+ = x_k^- + K_k (Y_k - y_k) \quad (3-42)$$

- Updating the state covariance:

$$P_k^+ = P_k^- + K_k P_k^y K_k^T \quad (3-43)$$

### 3.5 Conclusion

To estimating output, sigma points should be handed over measurement function. The results are used for obtaining cross covariance  $P_k^{xy}$  between measurement and state estimation. Estimate d measurement at  $k^{th}$  iteration is  $y_k^i$  and  $y_k$  and  $P_k^y$  are its mean and covariance respectively.  $Y_k$  is the measurement signal from the sensor.

## 4. Analysis and interpretation of data

### 4.1 Data Analysis for Extended Kalman Filter

The Hybrid Pulse Power Characterization (HPPC) test data achieved at 5 degrees from 40°C to -10°C are used to calculate the SOC 3-dimensional curve as a function of SOC and T. There are 59 samples to be fitted. In the proposed methodology, a four-order polynomial to the entirety of the SOC-OCV data with thermal effects on Open Circuit Voltage is fitted as shown in figure 4.1. This system consists of a temperature test chamber, a Lithium-ion battery, and a PC. (Lotfivand, Yu and Gomm, 2022)

$$OCV=f(SOC, Temperature) \quad (4-1)$$

In the previous studies the effect of temperature was neglected and OCV was assumed as a function of SOC. Therefore, the accuracy will be improved by adding the temperature term in OCV equation.

It can be written as follows:

$$OCV_{fit}=p00+p10*SOC+p11*SOC*T+ p20*SOC^2+p11*SOC*T+p02*T^2 \quad (4-2)$$

$$+P30*SOC^3+p21*SOC^2*T +p12*SOC*T^2+p03*T^3+p40*SOC^4$$

$$+P31*SOC^3*T+p22*SOC^2*T^2+P13*SOC*T^3+p04*T^4$$

Figure 4.1 illustrates dimensional open circuit voltage that is related to State of Charge and temperature, the curve fitted and real points, and error between them. It is shown that fitting four-

order polynomial equation is a good compromise of complexity and accuracy of approximation. It is shown in 4-1 figure, the error of fitting is less than %0.04 and considered as a good approximation.

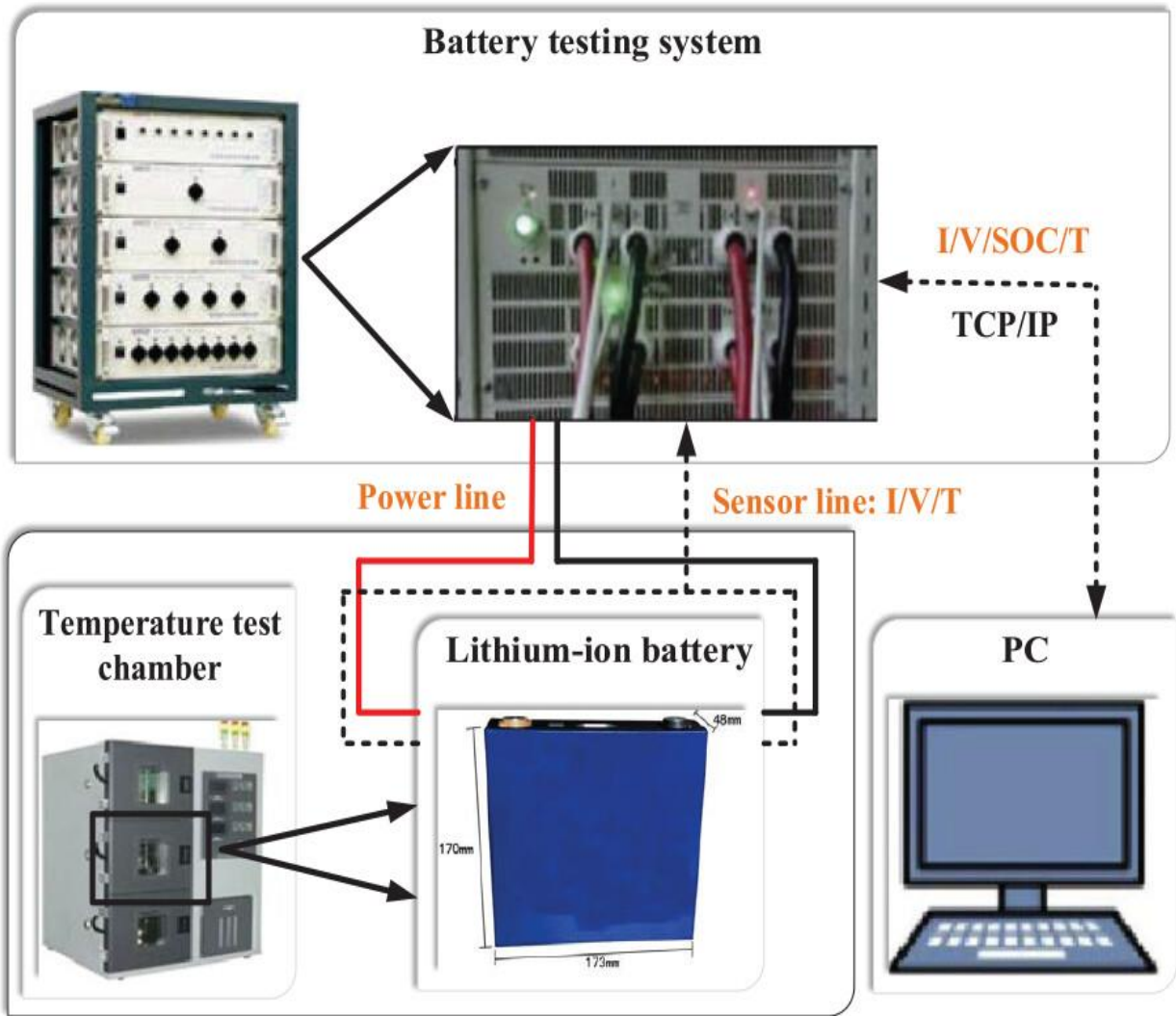


Figure 4-1 Battery testing system

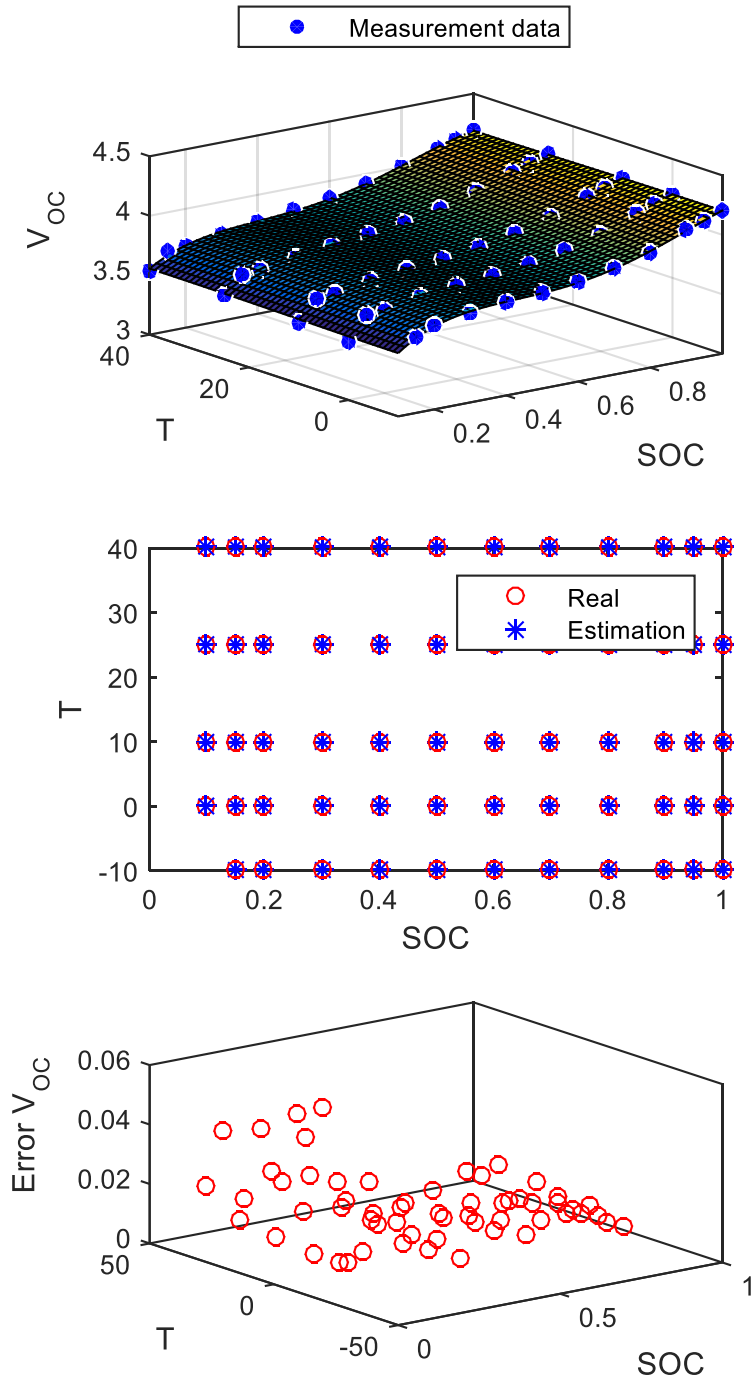


Figure 4-2 Dimensional OCV curve in line with State of Charge and temperature b. real points and fitted curve c. Error between real points and fitted curve.

The most popular and straightforward method for estimating SOC is the Coulomb Counting method. Nevertheless, this algorithm has two main drawbacks: the first value of SoC and sensor noise. SoC estimation will be erroneous if the starting SoC is incorrect. Because the CC method is not a closed loop algorithm, sensor uncertainty accumulates at each time step. Closed loop approaches such as EKF is employed to solve these shortcomings. The EKF needs to linearize both equations consist of state and measurement equations. It leads to have lower order nonlinear systems and less precise at the same time.

The nonlinear system's equations are as follow:

$$x(n+1)=f(w(n), u(n),x(n) ) \quad (4-3)$$

$$y(n)=h(v(n),x(n) ) \quad (4-4)$$

**(a) Prediction stage:**

$$x_a(n+1)=f(u(n),x_e(n) ) \quad (4-5)$$

$$M(n+1)=W(n) \sum_w W(n)^T + F(n) P(n)F(n)^T \quad (4-6)$$

**(b) Correction stage:**

$$K(n+1)=V(n) \sum_v V(n)^T]^{-1}+M(n+1)H(n)^T.[H(n)M(n+1)H(n)^T] \quad (4-7)$$

$$P(n+1)=-H(n)K(n+1)M(n+1) +M(n+1) \quad (4-8)$$

$$x_e(n+1)= x_a(n+1)+ K(n+1)[-h(x_a(n+1),0)+y(n+1)] \quad (4-9)$$

For predicting the next state, the transition equation is required. The related covariance matrix M is constructed by Jacobians with  $x_e(n)$ ,  $w(n)$  assessment:

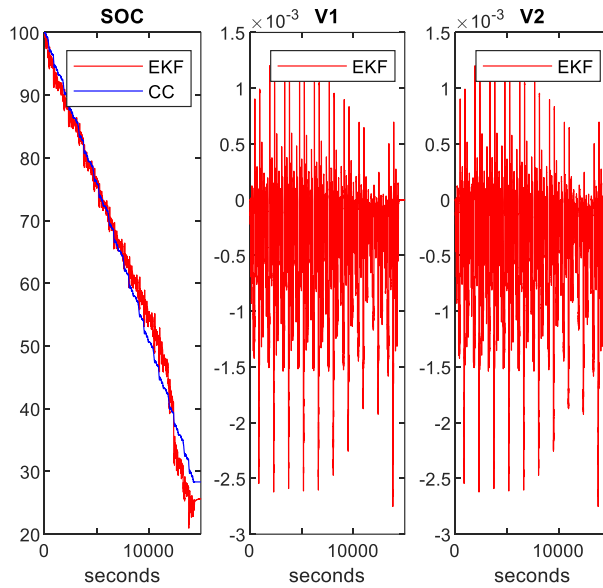
$$H(n)=\frac{dh(v,x)}{dx} \quad F(n) = \frac{df(w,x)}{dx} \quad (4-10)$$

Covariance matrix P is updating by the following Jacobians that is evaluated at  $x_a(n+1)$ ,  $v(n)$ :

$$V(n)=\frac{dh(x,v)}{dv} \quad W(n) = \frac{df(x,w)}{dw} \quad (4-11)$$

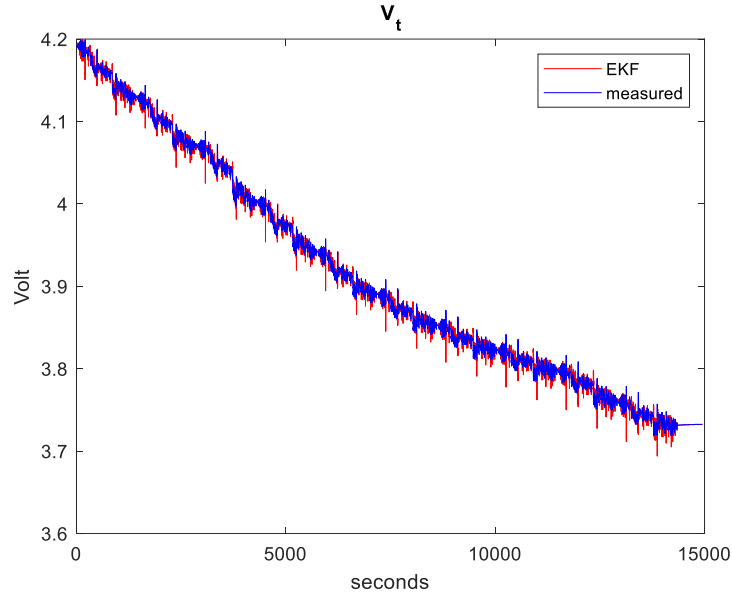
Comparing the prediction and update step equations in Standard Kalman Filter with these steps in EKF, we can say that the Jacobian F(n) is said to serve the role of the A matrix, while the C matrix is the Jacobian H(n). P is the state covariance, W is the process noise covariance matrix, and V is assumed as the measurement noise covariance matrix. Using data taken from sensor (y) and Kalman gain, the Kalman filter will decide to rely on estimation or measurement. As a result, Kalman filter will update the estimation While, y is the measurement taken from the sensor. (Lotfivand Yu and Gomm, 2022)

Figure 4.3 shows estimated SoC by Coulomb Counting and Extended Kalman filter (as we do not have the real SOC, the SOC achieved by Coulomb Counting considered as real SOC) , estimated V1 and V2 by Extended Kalman filter. There are 14951 experimental data for voltage, current, temperature, and time of driving cycle. Since it is impossible to directly measure the SOC, Coulombe counting SOC assumed as real SOC. Then it compared to EKF estimated SOC. Figure 4.3.a shows the SOC estimated by EKF compared to Coulomb Counting (assumed as a real SOC). 4.3.b and 4.3.c show the voltage of two network illustrating dynamic characteristics of the battery.



*Figure 4-3 SOC, V1, and V2 estimation curves a) SOC estimation by EKF and Coulomb Counting method b) V1 estimation by EKF c) V2 estimation by EKF.*

Figure 4. 4 illustrates measured terminal voltage and estimated terminal voltage has calculated by the Extended Kalman filter. Due to the large amount of data, resampling will be done from 1 Hz to 10 Hz. The nominal capacity provided by battery manufacturer can be used or the 25C C/20 calculated capacity. The capacity used in this study as nominal here is 4.8 Ah from data.

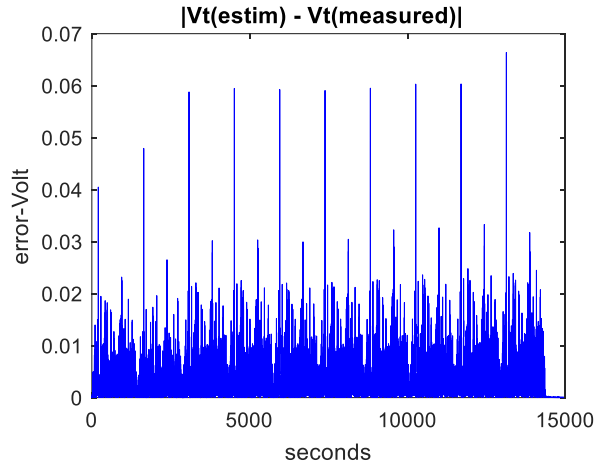


*Figure 4-4 Measured and estimated battery terminal voltage*

The Kalman Filter has 2 main parameters  $S_v$  and  $S_w$  defined as Observation noise and process noise and directly affect errors and RMSE. The best ways for tuning them are manually or by using optimization algorithm.  $S_v$  is defined as error square of the battery test equipment. So, after setting the  $S_v$  value, we cannot change the  $S_w$  anymore. In this study the LA92 drive cycle used and  $S$  and  $S_w$  is set for it as follows. If US06, HWFET, or UDDS cycles were utilized, those parameters should be changed. Therefore, by tuning the values the best amount for them is set as follows:

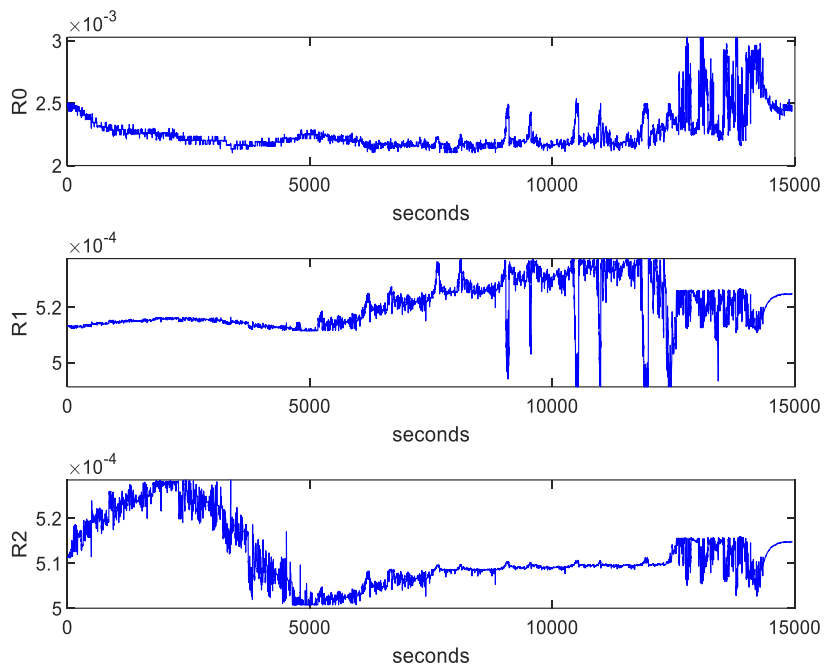
$$S_w = \begin{bmatrix} 1.0e^{-6} & 0 & 0 \\ 0 & 1.0e^{-5} & 0 \\ 0 & 0 & 1.0e^{-5} \end{bmatrix} \quad S_v = 10^{-5} \quad (4-31)$$

Figure 4.5 shows the error of terminal voltage that is defined as the estimated terminal voltage take away measured terminal voltage. (Lotfivand, Yu and Gomm, 2022)



*Figure 4-5 Estimation error of terminal voltage*

As shown in figure 4-5, the EKF is an acceptable method for estimating terminal voltage of Li-ion batteries and the highest error of this estimation error is less than 0.07 volt. It is more reliable than Coulomb Counting method. Figure 4.6 illustrates 3 resistances included in battery second order Thevenin model obtained from HPPC and consists of the SOC,  $R_0$ ,  $R_1$ ,  $C_1$ ,  $R_2$ ,  $C_2$ , and T samples. In the data set there are more than 14951 samples taken every second.



*Figure 4-6 Battery internal Resistances*

Figure 4.7 illustrates 2 capacities included in battery second order Thevenin model obtained from HPPC cycle. In the data set there are more than 15000 samples taken every second.

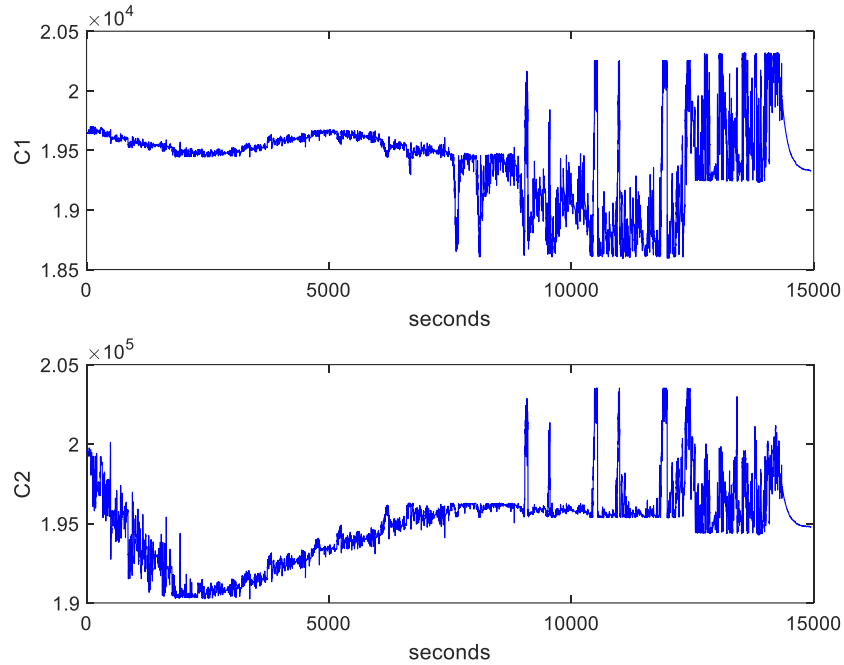


*Figure 4-7 Battery internal Capacities*

## ***4.2 RMSE values for Terminal Voltage and SOC in EKF***

In this study, SOC and terminal voltage estimation is carried out with the EKF algorithm Li-ion batteries. The state space analysis is done by applying related equations on the 2 RC branch battery model. The Hybrid Pulse Power Characterization (HPPC) test data obtained at several temperatures from 40°C to -10°C are used to calculate the SOC 3-dimensional curve as a function of SOC and T. The simulation results show that the EKF is more productive and precise than C\_C (Coulomb Counting). As a result, this method is more reliable. The inaccuracy in the EKF results is less than 1%, indicating that EKF is a trustworthy method for estimating battery states. Moreover, RMSE is utilized for the assessment index to quantify the estimation error of techniques. RMSE values for Terminal Voltage and SOC are 5% and 1.7% respectively. (Lotfivand, Yu and Gomm, 2022)

## ***4.3 Data analysis for Unscented Kalman Filter***

The Li-ion battery has highly nonlinear and time varying properties. The battery's OCV-Soc characteristic curve, for example, is not linear. Furthermore, due to changing operating conditions, some essential EECM (Equivalent electrical circuit model) metrics, such as resistance and capacitance vary with time and are not linear. Therefore, the Linear Kalman Filter is not able to estimate the SOC of a Li-ion battery. OCV-Soc curve and other characteristics must be linearized

in every point they are applied. Nevertheless, because the OCV of most Li-ion batteries does not settle to its ultimate value immediately, long time it needs to obtain correct value for having correct OCV-SOC relationship, which is not possible in many applications.

Figure 4.7 illustrates dimensional open circuit voltage that is related to State of Charge and temperature, the curve fitted and real points, and the error between them.

The Hybrid Pulse Power Characterization (HPPC) test data achieved at 5 degrees from 40°C to -10°C are used to calculate the SOC 3-dimensional curve as a function of SOC and T. There are 59 samples to be fitted. In the proposed methodology, figure 2 is resulted by fitting a four-order polynomial to the entirety of the SOC-OCV data with thermal effects on Open Circuit Voltage. (Lotfivand, Yu and Gomm, 2022)

$$OCV=f(SOC, Temperature) \quad (4-32)$$

In the previous studies the effect of temperature was neglected and OCV was assumed as a function of only SOC. Therefore, the accuracy will be improved by adding the temperature term in OCV equation.

It can be written as follows:

$$OCV_{fit}=p00+p10*SOC+p11*SOC*T+ p20*SOC^2+p11*SOC*T+p02*T^2 \quad (4 - 33)$$

$$+P30*SOC^3+p21*SOC^2*T +p12*SOC*T^2+p03*T^3+p40*SOC^4$$

$$+P31*SOC^3*T+p22*SOC^2*T^2+P13*SOC*T^3+p04*T^4$$

Figure 4.8 illustrates dimensional open circuit voltage that is related to State of Charge and temperature, the curve fitted and real points, and error between them. It is shown that fitting four-order polynomial equatin is a good compromise of complexity and accuracy of approximation. It is shown in 4-8 figure, the error of fitting is less than %0.04 and cosidered as a good approximation.

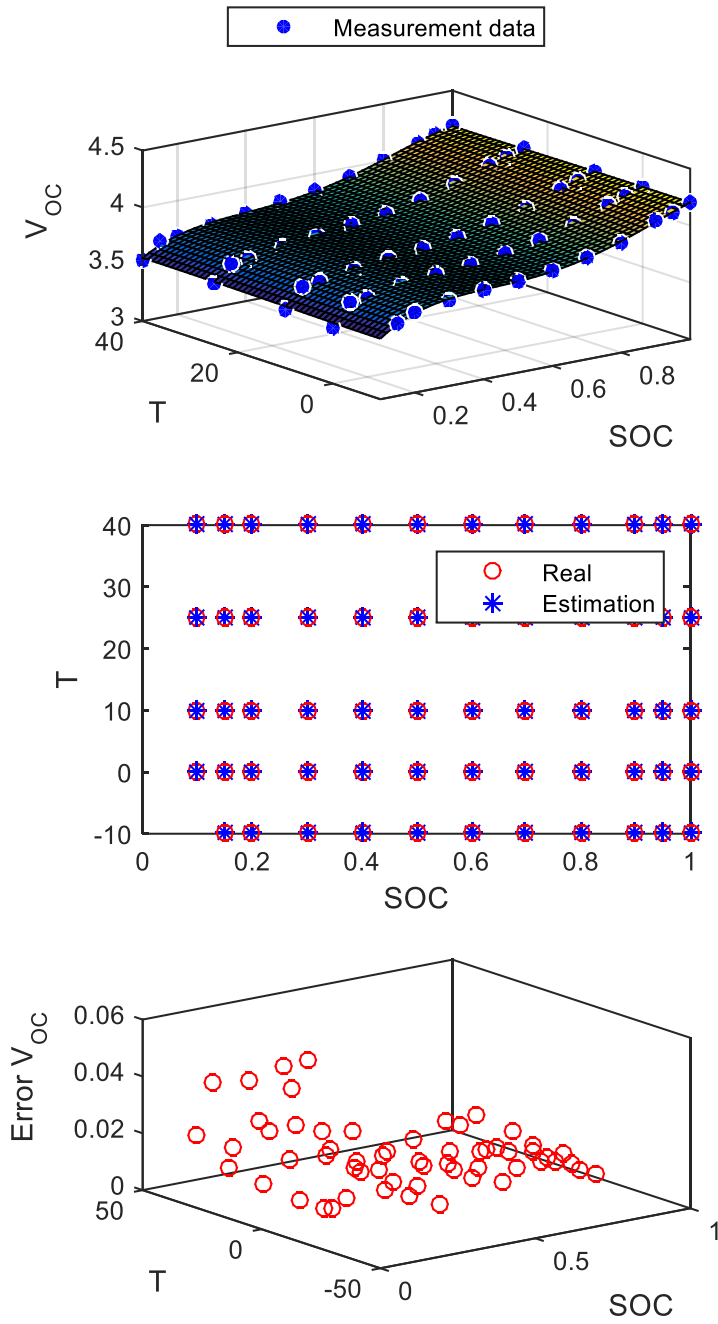


Figure 4-8 dimensional open circuit voltage a) dimensional  $V_{OC}$  curve related to SOC and temperature b) real points and fitted curve c) Error between real points and fitted curve

It assumes as a drawback for the EKF method and so the UKF method is preferable. Using UKF Jacobians and Hessians are not required, and this method is ‘derivative-free’ among Kalman filter family. EKF algorithm uses one spot that is called mean, however in UKF we have several points known as sigma points consist of mean (Sun et al., 2011). As in UKF we need few sigma points, it needs moderate computation. We use sigma points to find two main parameters consist of mean and covariance of main data. There will be  $2n+1$  sigma points. Choosing sigma points is described as follows:

$$X_{k-1}^{[0]} = X_{k-1}^+ \quad (4-12)$$

$$X_{k-1}^{[i]} = (\sqrt{(n + \lambda)P_{k-1}}) + X_{k-1}^+ \text{ for } i=1,2,\dots,n \quad (4-13)$$

$$X_{k-1}^{[i]} = -(\sqrt{(n + \lambda)P_{k-1}}) + X_{k-1}^+ \text{ for } i=n+1,\dots,2n \quad (4-14)$$

Then these points go through equations 4-6 to 4-9 and their weights are as follows:

$$w_m^{[0]} = \frac{\lambda}{n+\lambda} \quad (4-15)$$

$$w_c^{[0]} = (1 - \alpha^2 + \beta) + w_m^{[0]} \quad (4-16)$$

$$w_m^{[i]} = w_c^{[i]} = \frac{1}{2(n+\lambda)} \text{ for } i = 1,2,\dots,2n \quad (4-17)$$

$$\lambda = \alpha^2(n + k) - n \quad (4-18)$$

Since weights are normalized, the sum of them is one.

$X_{k-1}^+$  is supposed as mean of the selected points,  $P_{k-1}$  is covariance matrix of state variables,  $n$  is number of state variables,  $k$  is another scaling factor and normally it is  $3-n$ ,  $\alpha$  shows the stretch of sigma points,  $\beta$  shows prior knowledge of  $x$  distribution and it is 2 for gaussian noises.

The number of columns is  $i$ , computing mean weight is  $w_m^{[i]}$ , computing covariance weight is  $w_m^{[i]}$ .

So, the Unscented Kalman Filter algorithm is as follows:

We can assume the nonlinear system as:

$$x(n+1)=f w(n) (u(n), x(n)) \quad (4-19)$$

$$Y(n)=h(v(n), x(n)) \quad (4-20)$$

**prediction:**

- By propagating sigma points via transition equation, we have:

$$x_k^i = f \left( X_{k-1}^{[i]}, u_k \right) \text{ for } i = 0, 1, \dots, 2n \quad (4-21)$$

- Getting priori covariance matrix:

$$x_k^- = \sum_{i=0}^{2n} w_m^{[i]} x_k^i \quad (4-22)$$

$$P_k^- = \sum_{i=0}^{2n} w_c^{[i]} (x_k^i - x_k^-)(x_k^i - x_k^-)^T + Q \quad (4-23)$$

**Updating:**

- Computing propagated sigma point measurements through measurement equation:

$$y_k^i = h(x_k^i, u_k) \text{ for } i = 0, 1, \dots, 2n \quad (4-24)$$

- Computing measurement mean:

$$y_k = \sum_{i=0}^{2n} w_m^{[i]} y_k^i \quad (4-25)$$

- Computing measurement covariance matrix:

$$P_k^y = \sum_{i=0}^{2n} w_c^{[i]} (y_k^i - y_k)(y_k^i - y_k)^T + R \quad (4-26)$$

- Computing cross covariance matrix:

$$P_k^{xy} = \sum_{i=0}^{2n} w_c^{[i]} (x_k^i - x_k^-)(y_k^i - y_k)^T \quad (4-27)$$

- UKF Gain:

$$K_k = P_k^{xy} (P_k^y)^{-1} \quad (4-28)$$

- Updating the state variables:

$$x_k^+ = x_k^- + K_k (Y_k - y_k) \quad (4-29)$$

- Updating the state covariance:

$$P_k^+ = P_k^- + K_k P_k^y K_k^T \quad (4-30)$$

To estimating output, sigma points should be handed over measurement function. The results are used for obtaining cross covariance  $P_k^{xy}$  between measurement and state estimation. Estimated measurement at  $k^{th}$  iteration is  $y_k^i$  and  $y_k$  and  $P_k^y$  are it's mean and covariance respectively.  $Y_k$  is measurement signal from sensor. Figure 4.9 shows estimated SoC by formal coulomb Counting and Unscented Kalman filter, estimated V1 and V2 by Unscented Kalman filter.

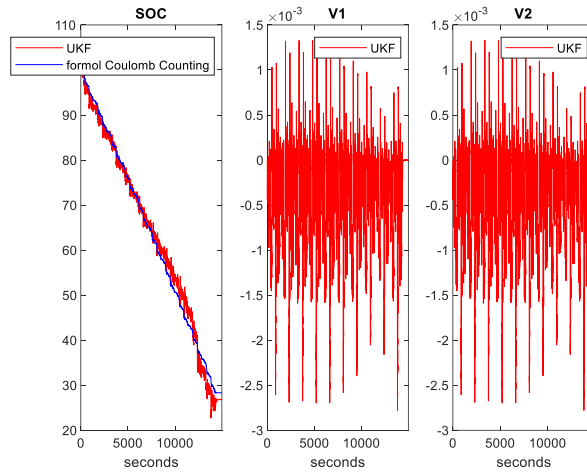


Figure 4-9 SOC, V1, and V2 estimation curves a) SOC estimation by UKF and formal Coulomb Counting method b) V1 estimation by EKF c) V2 estimation by EKF

Figure 4.10 illustrates measured terminal voltage and estimated terminal voltage as done by Unscented Kalman filter. Figure 4.11 illustrates the error values for estimation. It can be seen that the amount of error for UKF is considerably lower than EKF. So in conclusion UKF is better method for deeply nonlinear system of Li-ion batteries.

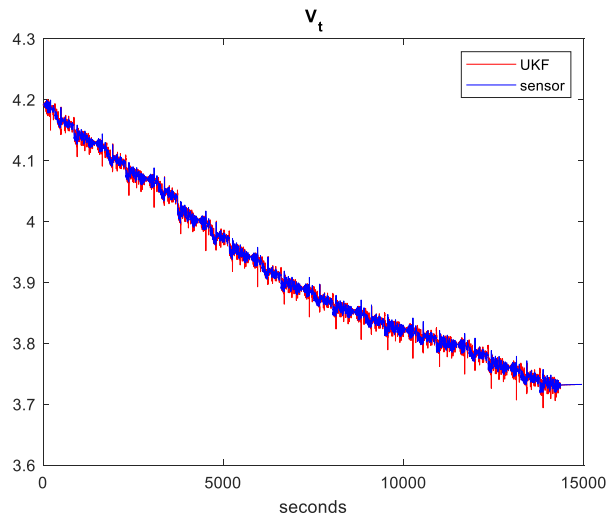


Figure 4-10 Measured and estimated battery terminal voltage

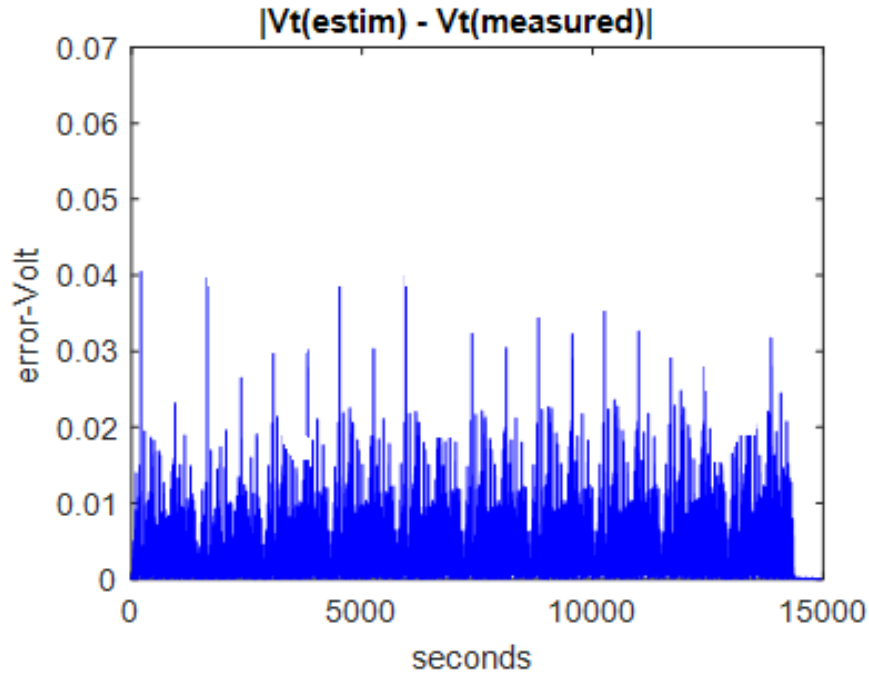


Figure 4-11 Error of terminal voltage

Observation noise and process noise directly affect errors and RMSE. Therefore, by tuning the values the best amount for them is set as follows:

$$Q = \begin{bmatrix} 1.0e^{-4} & 0 & 0 \\ 0 & 1.0e^{-5} & 0 \\ 0 & 0 & 1.0e^{-5} \end{bmatrix} \quad R = 10^{-5} \quad (4-31)$$

Figure 4.11 shows the error of terminal voltage that is defined as estimated terminal voltage take away measured terminal voltage.

The first RC pair shows transient effects in the short-term transient condition, and the second pair shows the long-term transient characteristic and has a larger time constant and consists of concentration polarization and electrochemical effects. These effects consist of diffusion, charge transfer effect. Figure 4.11 shows the real time data for Internal Resistance, polarization resistance and electrochemical resistance.

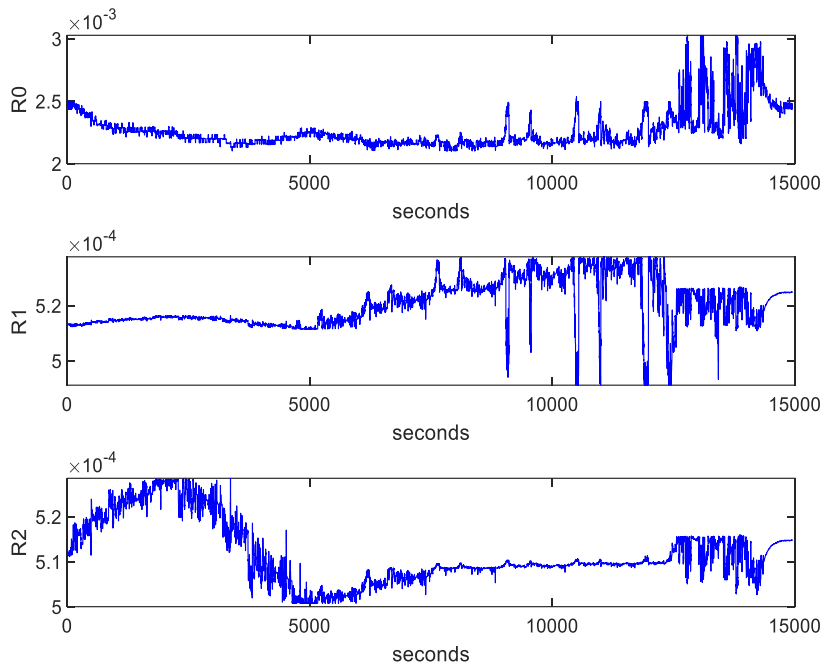


*Figure 4-12 Battery internal Resistances ( $\Omega$ )*

Figure 4.13 illustrates 2 capacities included in battery second order Tevenin model consists of electrochemical capacitor and diffusion capacitor.

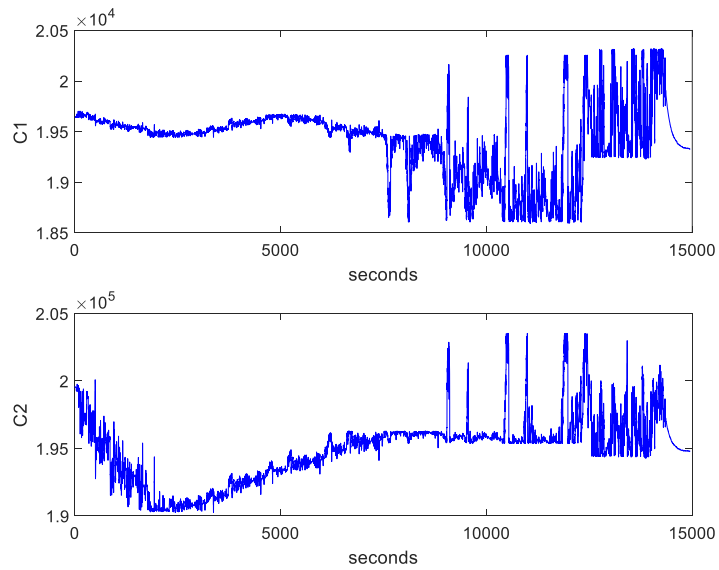


*Figure 4-13 Battery internal Capacities*

#### ***4.4 RMSE values for Terminal Voltage and SOC in UKF***

In this study, the UKF method is used to estimate the SOC and terminal voltage of a Lithium ion battery. The state space analysis is calculated using the 2 RC Lithium ion electrical equivalent model. The Open Circuit Voltage (OCV) 3-dimensional curve as a function of SOC and T is calculated using the Hybrid Pulse Power Characterization (HPPC) test data acquired at 40°C, 25°C, 10°C, 0°C, and -10°C. It can be seen that the UKF method of battery SOC estimation is more accurate than the coulomb counting approach, according to a comparison of the two methods. The inaccuracy in the UKF results is less than 1%, indicating that UKF is a trustworthy method for estimating battery states. Moreover, The Root Mean Square Error (RMSE) is utilized as the assessment index to quantify the estimation error of techniques. RMSE values for Terminal Voltage and SOC are 4% and 1.6% respectively.

## 5. Conclusion

Lithium-ion batteries are preferred more than other types of batteries in electric vehicle applications due to their inherent safety, fast charge capacity, and long life (Martins et al., 2021). To create an accurate battery model, it is important to be able to identify health factors such as charge and health. Using LA92 drive cycle experimental data, the typical lithium-ion battery charge state estimation algorithm has been improved. First, we created a mathematical model of an analogue circuit battery to accurately mimic the behavior of a lithium-ion battery (Khalfi, Boumaaz and Soulmani, 2021) . The Thevenin model consists of two RC branches developed to identify model parameters and by an extended Kalman filter and Unscented Kalman filter were applied to the battery model. The three-dimensional curve of SOC as a function of SOC and T using hybrid pulsed power characteristic (HPPC) test data achieved at 5 degrees from 40°C to -10°(Dees et al., 2008). A comparison of the three methods (Coulomb Counting, UKF, and EKF) is showing that the UKF method for battery SOC assessment is more reliable than the traditional method CC (Coulomb counting).

The inaccuracy in the EKF results is less than 1%, indicating that EKF is a trustworthy method for estimating battery states. Moreover, RMSE is utilized for the assessment index to quantify the estimation error of techniques. RMSE values for Terminal Voltage and SOC are 5% and 1.7% respectively. UKF is a reliable approach for determining battery states because the error in the results is less than 1%. Additionally, The Root Mean Square Error (RMSE) is used as an evaluation metric to express the estimation error of methodologies. Terminal Voltage and SOC have RMSE values of 4% and 1.6%, respectively. The error observed in the UKF results is less than 1%, indicating that the UKF can reliably estimate battery condition. So, in Li-ion batteries as being deeply nonlinear the UKF is more accurate and reliable among other methods.

### 5.1 Further Work

Although the Kaman Filter family is an acceptable method for estimating the state of charge of the battery, it has some week points such as numerically instability. In further works it can be improved by adding an algorithm. On the other hand, it is important to predefine the Sv and Sw (process noise and measurement noise) correctly. In case of inaccurate values, we will have high errors and high RMSE value. Definition of an algorithm for optimizing those matrixes would be helpful.

In this study the Hybrid Pulse Power Characterization (HPPC) test data acquired at 40°C, 25°C, 10°C, 0°C, and -10°C. The next improvement could be done by is to take the temperature effect to the account in more degrees.

## 6. References

1. Beckmann, U., Gillies, D.M., Berenholtz, S.M., Wu, A.W. and Pronovost, P. (2004) Incidents relating to the intra-hospital transfer of critically ill patients: an analysis of the reports submitted to the Australian Incident Monitoring Study in Intensive Care. *Intensive care medicine*, 30, 1579-1585.
2. Bergveld, H.J., Kruijt, W.S., Notten, P.H., Bergveld, H.J., Kruijt, W.S. and Notten, P.H. (2002) *Battery management systems*. Springer.
3. Botsford, C. and Szczepanek, A. (2009) Fast charging vs. slow charging: Pros and cons for the new age of electric vehicles. *International Battery Hybrid Fuel Cell Electric Vehicle Symposium of Conference*.
4. Cai, C., Du, D. and Liu, Z. (2003) Battery state-of-charge (SOC) estimation using adaptive neuro-fuzzy inference system (ANFIS). *The 12th IEEE International Conference on Fuzzy Systems, 2003. FUZZ'03. of Conference*.
5. Chan, C.C. (2007) The state of the art of electric, hybrid, and fuel cell vehicles. *Proceedings of the IEEE*, 95 (4), 704-718.
6. Chatzakis, J., Kalaitzakis, K., Voulgaris, N.C. and Manias, S.N. (2003) Designing a new generalized battery management system. *IEEE transactions on Industrial Electronics*, 50 (5), 990-999.
7. Cheng, K.W.E., Divakar, B., Wu, H., Ding, K. and Ho, H.F. (2010) *Battery-management system (BMS) and*
8. Chiang, Y.-H., Sean, W.-Y. and Ke, J.-C. (2011) Online estimation of internal resistance and open-circuit voltage of lithium-ion batteries in electric vehicles. *Journal of power sources*, 196 (8), 3921-3932.
9. Collins, J., Li, X., Pletcher, D., Tangirala, R., Stratton-Campbell, D., Walsh, F.C. and Zhang, C. (2010) A novel flow battery: A lead acid battery based on an electrolyte with soluble lead (II). Part IX: Electrode and electrolyte conditioning with hydrogen peroxide. *Journal of power sources*, 195 (9), 2975-2978.
10. Dees, D., Gunen, E., Abraham, D., Jansen, A. and Prakash, J. (2008) Electrochemical modeling of lithium-ion positive electrodes during hybrid pulse power characterization tests. *Journal of The Electrochemical Society*, 155 (8), A603.
11. Dunik, J., Simandl, M. and Straka, O. (2012) Unscented Kalman filter: aspects and adaptive setting of scaling parameter. *IEEE Transactions on Automatic Control*, 57 (9), 2411-2416.
12. Dürr, M., Cruden, A., Gair, S. and McDonald, J. (2006) Dynamic model of a lead acid battery for use in a domestic fuel cell system. *Journal of power sources*, 161 (2), 1400-1411.
13. Gu, W. and Wang, C. (2000) Thermal-electrochemical modeling of battery systems. *Journal of The Electrochemical Society*, 147 (8), 2910.
14. Haq, I.N., Leksono, E., Iqbal, M., Sodami, F.N., Kurniadi, D. and Yulianto, B. (2014) Development of battery management system for cell monitoring and protection. 2014

international conference on electrical engineering and computer science (ICEECS)of Conference.

15. Harlow, J.E., Ma, X., Li, J., Logan, E., Liu, Y., Zhang, N., Ma, L., Glazier, S.L., Cormier, M.M. and Genovese, M. (2019) A wide range of testing results on an excellent lithium-ion cell chemistry to be used as benchmarks for new battery technologies. *Journal of The Electrochemical Society*, 166 (13), A3031.
16. Hasan, M.K., Mahmud, M., Habib, A.A., Motakabber, S. and Islam, S. (2021) Review of electric vehicle energy storage and management system: Standards, issues, and challenges. *Journal of Energy Storage*, 41, 102940.
17. He, H., Xiong, R. and Guo, H. (2012) Online estimation of model parameters and state-of-charge of LiFePO<sub>4</sub> batteries in electric vehicles. *Applied Energy*, 89 (1), 413-420.
18. Horiba, T. (2014) Lithium-ion battery systems. *Proceedings of the IEEE*, 102 (6), 939-950.
19. Huang, G.P., Mourikis, A.I. and Roumeliotis, S.I. (2008) Analysis and improvement of the consistency of extended Kalman filter based SLAM. 2008 IEEE International Conference on Robotics and Automation of Conference.
20. Iwai, T. (2019) The Degradation Mechanisms of Nickel Metal-Hydride Battery and Lead Acid Battery during Open Circuit.
21. Jang, Y.-I., Dudney, N.J., Tiegs, T.N. and Klett, J.W. (2006) Evaluation of the electrochemical stability of graphite foams as current collectors for lead acid batteries. *Journal of power sources*, 161 (2), 1392-1399.
22. Jongerden, M. and Haverkort, B. (2008) Battery modeling. Enschede, January, 38.
23. Kamali-Heidari, E., Kamyabi-Gol, A., Heydarzadeh Sohi, M. and Ataie, A. (2018) Electrode materials for lithium ion batteries: a review. *Journal of Ultrafine Grained and Nanostructured Materials*, 51 (1), 1-12.
24. Khalfi, J., Boumaaz, N. and Soulmani, A. (2021) An electric circuit model for a lithium-ion battery cell based on automotive drive cycles measurements. *International Journal of Electrical and Computer Engineering*, 11 (4), 2798.
25. Kroeze, R.C. and Krein, P.T. (2008) Electrical battery model for use in dynamic electric vehicle simulations. 2008 IEEE Power Electronics Specialists Conference of Conference.
26. Lelie, M., Braun, T., Knips, M., Nordmann, H., Ringbeck, F., Zappen, H. and Sauer, D.U. (2018) Battery management system hardware concepts: An overview. *Applied Sciences*, 8 (4), 534.
27. Li, M., Lu, J., Chen, Z. and Amine, K. (2018) 30 years of lithium-ion batteries. *Advanced Materials*, 30 (33), 1800561.
28. Lin, F.-J. (1996) Robust speed-controlled induction-motor drive using EKF and RLS estimators. *IEE Proceedings-Electric Power Applications*, 143 (3), 186-192.
29. Lotfivand, A., Yu, D. and Gomm, B. (2022) State Of Charge estimation using Extended Kalman Filter in Electric Vehicles. 2022 27th International Conference on Automation and Computing (ICAC) of Conference.
30. Lu, L., Han, X., Li, J., Hua, J. and Ouyang, M. (2013) A review on the key issues for lithium-ion battery management in electric vehicles. *Journal of power sources*, 226, 272-288.

31. Manenti, A., Abba, A., Merati, A., Savaresi, S.M. and Geraci, A. (2010) A new BMS architecture based on cell redundancy. *IEEE transactions on Industrial Electronics*, 58 (9), 4314-4322.
32. Martins, L.S., Guimarães, L.F., Junior, A.B.B., Tenório, J.A.S. and Espinosa, D.C.R. (2021) Electric car battery: An overview on global demand, recycling and future approaches towards sustainability. *Journal of environmental management*, 295, 113091.
33. Mekonnen, Y., Sundararajan, A. and Sarwat, A.I. (2016) A review of cathode and anode materials for lithium-ion batteries. *SoutheastCon 2016*, 1-6.
34. Mirzaei, A., Leonardi, S. and Neri, G. (2016) Detection of hazardous volatile organic compounds (VOCs) by metal oxide nanostructures-based gas sensors: A review. *Ceramics international*, 42 (14), 15119-15141.
35. Morita, Y., Saito, Y., Yoshioka, T. and Shiratori, T. (2021) Estimation of recoverable resources used in lithium-ion batteries from portable electronic devices in Japan. *Resources, Conservation and Recycling*, 175, 105884. SOC development for electrical vehicles. *IEEE transactions on vehicular technology*, 60 (1), 76-88.
36. Ng, K.S., Moo, C.-S., Chen, Y.-P. and Hsieh, Y.-C. (2009) Enhanced coulomb counting method for estimating state-of-charge and state-of-health of lithium-ion batteries. *Applied Energy*, 86 (9), 1506-1511.
37. Nikdel, M. (2014) Various battery models for various simulation studies and applications. *Renewable and Sustainable Energy Reviews*, 32, 477-485.
38. Pop, V., Bergveld, H.J., Danilov, D., Regtien, P.P. and Notten, P.H. (2008) Battery management systems: Accurate state-of-charge indication for battery-powered applications. Springer Science & Business Media.
39. Ren, L., Dong, J., Wang, X., Meng, Z., Zhao, L. and Deen, M.J. (2020) A data-driven auto-CNN-LSTM prediction model for lithium-ion battery remaining useful life. *IEEE Transactions on Industrial Informatics*, 17 (5), 3478-3487
40. Scavongelli, C., Francesco, F., Orcioni, S. and Conti, M. (2015) Battery management system simulation using SystemC. 2015 12th International Workshop on Intelligent Solutions in Embedded Systems (WISES) of Conference
41. Seaman, A., Dao, T.-S. and McPhee, J. (2014) A survey of mathematics-based equivalent-circuit and electrochemical battery models for hybrid and electric vehicle simulation. *Journal of power sources*, 256, 410-423.
42. Sun, F., Hu, X., Zou, Y. and Li, S. (2011) Adaptive unscented Kalman filtering for state of charge estimation of a lithium-ion battery for electric vehicles. *Energy*, 36 (5), 3531-3540.
43. Severson, K.A., Attia, P.M., Jin, N., Perkins, N., Jiang, B., Yang, Z., Chen, M.H., Aykol, M., Herring, P.K. and Fraggedakis, D. (2019) Data-driven prediction of battery cycle life before capacity degradation. *Nature Energy*, 4 (5), 383-391.
44. Shen, M. and Gao, Q. (2019) A review on battery management system from the modeling efforts to its multiapplication and integration. *International Journal of Energy Research*, 43 (10), 5042-5075.
45. Shrivastava, P., Soon, T.K., Idris, M.Y.I.B. and Mekhilef, S. (2019) Overview of model-based online state-of-charge estimation using Kalman filter family for lithium-ion batteries. *Renewable and Sustainable Energy Reviews*, 113, 109233.

46. Zakiyya, H., Distya, Y. and Ellen, R. (2018) A review of spent lead-acid battery recycling technology in indonesia: comparison and recommendation of environment-friendly process. IOP Conference Series: Materials Science and Engineering of Conference.
47. Zhang, Z., Yu, L., Dai, C. and Yan, Y. (2014) Investigation and development of a new brushless DC generator system for extended-range electric vehicle application. 2014 IEEE Energy Conversion Congress and Exposition (ECCE) of Conference.

## 7. Appendix

### 7.1 MATLAB CODES FOR EXTENDED KALMAN FILTER

```
1- Fitting OCV and SOC:
2- clc
3- clear
4- close all
5-
6- load 'Z_BatteryModel.mat'; % Load the battery parameters
7-
8- T_data = param.T;
9- SOC_data = param.SOC;
10-
11- R0_data = param.R0;
12- R1_data = param.R1;
13- R2_data = param.R2;
14- C1_data = param.C1;
15- C2_data = param.C2;
16-
17- clear param
18-
19- % Z_R0_xy = fit([T_data,SOC_data],R0_data,'poly45');
20- % R0fit = feval(Z_R0_xy,[T_data,SOC_data]);
21- %% R0
22- %%
23- Fancion_R0 = scatteredInterpolant(T_data,SOC_data,R0_data);
24- R0_estim = Fancion_R0(T_data,SOC_data);
25-
26- figure
27- hold on
28- plot3(T_data,SOC_data,R0_data,'ob');
29- plot3(T_data,SOC_data,R0_estim,'*r');
30-
31- stem3(T_data,SOC_data,R0_data,'ob');
32- stem3(T_data,SOC_data,R0_estim,'*r');
33-
34- legend('Real','Estimation')
35- xlabel("T")
36- ylabel('SOC')
37- zlabel('R0')
38- box on
39- grid on
```

```

40- view(-45, 45)
41-
42- %% R1
43- %%
44- Fancion_R1 = scatteredInterpolant(T_data,SOC_data,R1_data);
45- R1_estim = Fancion_R1(T_data,SOC_data);
46-
47- figure
48- hold on
49- plot3(T_data,SOC_data,R1_data,'ob');
50- plot3(T_data,SOC_data,R1_estim,'*r');
51-
52- stem3(T_data,SOC_data,R1_data,'ob');
53- stem3(T_data,SOC_data,R1_estim,'*r');
54-
55- legend('Real','Estimation')
56- xlabel('T')
57- ylabel('SOC')
58- zlabel('R1')
59- box on
60- grid on
61- view(-45, 45)
62-
63- %%
64- %% R2
65- %%
66- Fancion_R2 = scatteredInterpolant(T_data,SOC_data,R2_data);
67- R2_estim = Fancion_R2(T_data,SOC_data);
68-
69- figure
70- hold on
71- plot3(T_data,SOC_data,R2_data,'ob');
72- plot3(T_data,SOC_data,R2_estim,'*r');
73-
74- stem3(T_data,SOC_data,R2_data,'ob');
75- stem3(T_data,SOC_data,R2_estim,'*r');
76-
77- legend('Real','Estimation')
78- xlabel('T')
79- ylabel('SOC')
80- zlabel('R2')
81- box on
82- grid on
83- view(-45, 45)
84- %% C1
85- %%

```

```

86- Fancion_C1 = scatteredInterpolant(T_data,SOC_data,C1_data);
87- C1_estim  = Fancion_C1(T_data,SOC_data);
88-
89- figure
90- hold on
91- plot3(T_data,SOC_data,C1_data,'ob');
92- plot3(T_data,SOC_data,C1_estim,'*r');
93-
94- stem3(T_data,SOC_data,C1_data,'ob');
95- stem3(T_data,SOC_data,C1_estim,'*r');
96-
97- legend('Real','Estimation')
98- xlabel('T')
99- ylabel('SOC')
100-      zlabel('C1')
101-      box on
102-      grid on
103-      view(-45, 45)
104-      %%
105-      %% C2
106-      %%
107-      Fancion_C2 = scatteredInterpolant(T_data,SOC_data,C2_data);
108-      C2_estim  = Fancion_C2(T_data,SOC_data);
109-
110-      figure
111-      hold on
112-      plot3(T_data,SOC_data,C2_data,'ob');
113-      plot3(T_data,SOC_data,C2_estim,'*r');
114-
115-      stem3(T_data,SOC_data,C2_data,'ob');
116-      stem3(T_data,SOC_data,C2_estim,'*r');
117-
118-      legend('Real','Estimation')
119-      xlabel('T')
120-      ylabel('SOC')
121-      zlabel('C2')
122-      box on
123-      grid on
124-      view(-45, 45)
125-      %%
126-      %%
127-      Name_fun='Z_batrrey_info_lotfi';
128-      save(Name_fun,'Fancion_R0','Fancion_R1',...
129-          'Fancion_R2','Fancion_C1','Fancion_C2');
130-      %%
131-

```

```

132-
133-      %%

2-

clc
clear
close all

load 'Z_BatteryModel.mat'; % Load the battery parameters

T_data = param.T;
SOC_data = param.SOC;

R0_data = param.R0;
R1_data = param.R1;
R2_data = param.R2;
C1_data = param.C1;
C2_data = param.C2;

clear param

% Z_R0_xy = fit([T_data,SOC_data],R0_data,'poly45');
% R0fit = feval(Z_R0_xy,[T_data,SOC_data]);
%% R0
%%
Ffunction_R0 = scatteredInterpolant(T_data,SOC_data,R0_data);
R0_estim = Ffunction_R0(T_data,SOC_data);

figure
hold on
plot3(T_data,SOC_data,R0_data,'ob');
plot3(T_data,SOC_data,R0_estim,'*r');

stem3(T_data,SOC_data,R0_data,'ob');
stem3(T_data,SOC_data,R0_estim,'*r');

legend('Real','Estimation')
xlabel('T')
ylabel('SOC')
zlabel('R0')
box on
grid on
view(-45, 45)

```

```

%% R1
%%
Faction_R1 = scatteredInterpolant(T_data,SOC_data,R1_data);
R1_estim = Faction_R1(T_data,SOC_data);

figure
hold on
plot3(T_data,SOC_data,R1_data,'ob');
plot3(T_data,SOC_data,R1_estim,'*r');

stem3(T_data,SOC_data,R1_data,'ob');
stem3(T_data,SOC_data,R1_estim,'*r');

legend('Real','Estimation')
xlabel('T')
ylabel('SOC')
zlabel('R1')
box on
grid on
view(-45, 45)

%%
%% R2
%%
Faction_R2 = scatteredInterpolant(T_data,SOC_data,R2_data);
R2_estim = Faction_R2(T_data,SOC_data);

figure
hold on
plot3(T_data,SOC_data,R2_data,'ob');
plot3(T_data,SOC_data,R2_estim,'*r');

stem3(T_data,SOC_data,R2_data,'ob');
stem3(T_data,SOC_data,R2_estim,'*r');

legend('Real','Estimation')
xlabel('T')
ylabel('SOC')
zlabel('R2')
box on
grid on
view(-45, 45)
%% C1
%%
Faction_C1 = scatteredInterpolant(T_data,SOC_data,C1_data);
C1_estim = Faction_C1(T_data,SOC_data);

```

```

figure
hold on
plot3(T_data,SOC_data,C1_data,'ob');
plot3(T_data,SOC_data,C1_estim,'*r');

stem3(T_data,SOC_data,C1_data,'ob');
stem3(T_data,SOC_data,C1_estim,'*r');

legend('Real','Estimation')
xlabel('T')
ylabel('SOC')
zlabel('C1')
box on
grid on
view(-45, 45)
%%
%% C2
%%
Faction_C2 = scatteredInterpolant(T_data,SOC_data,C2_data);
C2_estim = Faction_C2(T_data,SOC_data);

```

```

figure
hold on
plot3(T_data,SOC_data,C2_data,'ob');
plot3(T_data,SOC_data,C2_estim,'*r');

stem3(T_data,SOC_data,C2_data,'ob');
stem3(T_data,SOC_data,C2_estim,'*r');

legend('Real','Estimation')
xlabel('T')
ylabel('SOC')
zlabel('C2')
box on
grid on
view(-45, 45)
%%
%%
Name_fun='Z_batrey_info_lotfi';
save(Name_fun,'Faction_R0','Faction_R1',...
      'Faction_R2','Faction_C1','Faction_C2');
%%

%%

```

```

3- EKF:
clc
clear
close all
%-----
load('Z_measurment.mat')
%-----
sampel_time=10;
% -----

% Resample input data
data.RecordingTime      = meas.Time (1: sampel_time: end);
data.Measured_Voltage   = meas.Voltage(1: sampel_time: end);
data.Measured_Current   = meas.Current(1: sampel_time: end);
data.Measured_Temperature = meas.Battery_Temp_degC(1: sampel_time: end);
% -----
data.Ah                  = meas.Ah(1: sampel_time: end);
% -----
Ah=data.Ah ;

% Nominal capacity of the Battery in Ah obtained from database.
nominalCap = 4.81;

% Obtain the SOC with C-C for comparing with EKF
data.Measured_SOC      = (nominalCap +Ah).*100./nominalCap;

Qn_rated  = 3600*4.81; % Transforming Ah to Amp-seconds
% -----
load('Z_OCV_estim_Lotfi.mat')
% [VOC_fit,df_VOC_SOC,df_VOC_T]= Estim_Voc(SOC,T);
% -----
load('Z_batrrey_info_lotfi.mat')
% -----
% -----
%process noise
% Sw=[1.0e-6  0    0
%  0    1.0e-5  0
%  0    0    1.0e-5]; %cov

Sw=[1.0e-4  0    0
    0    1.0e-5  0
    0    0    1.0e-5]; %cov
%-----
%-----

```

```

%observation noise
Sv=0.004; %cov.
% Sv=10^-5; %cov.
%-----
%-----
%Being Prepared for starting filtering
%creating some space
Nf=1;
P=zeros(3,3,Nf);
M=zeros(3,3,Nf);
K=zeros(3,Nf);
%-----
% creating some space er(n), xe(n)
rx=zeros(3,Nf);
rer=zeros(3,Nf);
%-----
%process noise jacobian
% W=eye(3,3);
W = [1  0  0
      0  1  0
      0  0  1];

% noise of observation' Jacobian
V=1;
%-----
%Following system's Behavior filter after starting state
% SOC V1 V1
x = [1
      0
      0]; % state space x parameter intializations

%-----

xe=x; % filter state
xa=xe; % starting for middle state
%-----
nn=1;
DeltaT = 1; % sample time in seconds

eta=1;

Nf=numel(data.Measured_Current)-10;
%time
tim=0:DeltaT:(Nf-1)*DeltaT;

y_estim=zeros(1,1);

```

```
RMSE_Vt = sqrt((sum((data.Measured_Voltage - y_estim).^2))
/(length(data.Measured_Voltage))) % mV
```

```
while nn<Nf+1
```

```
%-----
% recording the estimation
rx(:,nn)=xe; %states
% rer(:,nn)=x-xe; %calculating errors
%-----
%system
% rx(:,nn)=x; %state calculating
% Calculate RMSE and MAX of Vt and SOC
```

```
T = data.Measured_Temperature(nn); % C
U = data.Measured_Current(nn); % A
```

```
if U > 0
    eta = 1; % in the discharging step
elseif U <= 0
    eta = 1; % in the discharging step
end
```

```
SOC = xe(1);
V1 = xe(2);
V2 = xe(3);
%
```

```
=====
====
%
```

```
=====
====
%system output
%measurement
Voltage_sensor = data.Measured_Voltage(nn);
ym=Voltage_sensor;
%
```

```
=====
====
%
```

```
=====
====
%Prediction
%a priori state
```

```
R0_estim = Fancion_R0(T,SOC);
R1_estim = Fancion_R1(T,SOC);
R2_estim = Fancion_R2(T,SOC);
```

```
C1_estim = Fancion_C1(T,SOC);
C2_estim = Fancion_C2(T,SOC);
```

```
Tau_1 = C1_estim * R1_estim;
Tau_2 = C2_estim * R2_estim;
```

```
a1 = exp(-DeltaT/Tau_1);
a2 = exp(-DeltaT/Tau_2);
```

```
b1 = R1_estim * (1 - exp(-DeltaT/Tau_1));
b2 = R2_estim * (1 - exp(-DeltaT/Tau_2));
```

```
B = [-(eta * DeltaT/Qn_rated)
      b1
      b2];
```

```
A = [1 0 0;
      0 a1 0;
      0 0 a2];
```

```
xa = (A * xe) + (B * U);
```

```
%
```

```
=====
```

```
=====  
%a priori cov.
```

```
F = [1 0 0;
      0 a1 0;
      0 0 a2];
```

```
%-----
```

```
%obtaining Jacobian of states
```

```
M(:,:,nn+1)=(F*P(:,:,nn)*F')+(W*Sw*W');
```

```
%-----
```

```
%Updating
```

```
%-----
```

```
[VOC_fit,df_VOC_SOC,df_VOC_T]= Estim_Voc(SOC,T);
```

```
ya= VOC_fit - R0_estim * U - V1 - V2;
```

```
y_estim(nn)=ya;
```

```

%measurement jacobian
H=[df_VOC_SOC -1 -1];
%
=====
====
% 3*1 = (3*3 3*1) * [ 1*3 3*3 3*1 + 1*1 1*1 1*1]

% K(:,nn+1)=( M(:,,nn+1)*H' ) /
(V* Sv *V') (H * M(:,,nn+1) *H')* +);
%Replace b*inv(A) with b/A || Replace inv(A)*b with A\b

K(:,nn+1)=(M(:,,nn+1)*H') / ((H * M(:,,nn+1) *H') + (V* Sv *V'));

P(:,,nn+1)=M(:,,nn+1)-(K(:,nn+1)* M(:,,nn+1) * H);

xe= ( K(:,nn+1) ) * (ym-ya) +xa ; %estimating the next state
% -----

nn=1+nn;
end
% -----

%Gaphs
figure(1)
subplot(1,3,1)
hold on

plot(tim,rx(1,1:Nf)*100,'r');
plot(tim, data.Measured_SOC(1:Nf),'b');

title('SOC');
xlabel('seconds')
box on
legend('EKF','CC')

%-----
subplot(1,3,2)
hold on

plot(tim,rx(2,1:Nf),'r');
title('V1');
xlabel('seconds');
box on
legend('EKF')

```

```

%-----
subplot(1,3,3)
hold on

plot(tim,rx_e(2,1:Nf),'r');
title('V2');
xlabel('seconds');
box on
legend('EKF')
%
=====
=====

%display
figure(2)
hold on

plot(tim,y_estim(1,1:Nf),'r');
plot(tim, data.Measured_Voltage(1:Nf),'b');

title('V_{t}');
xlabel('seconds')
ylabel('Volt')
box on
legend('EKF','measured')

%
=====
=====

```

## 7.2 MATLAB CODES FOR UNSCENTED KALMAN FILTER

```

clc

clear
close all

load 'Z_BatteryModel.mat'; % Load the battery parameters

T_data = param.T;
SOC_data = param.SOC;

```

```

R0_data = param.R0;
R1_data = param.R1;
R2_data = param.R2;
C1_data = param.C1;
C2_data = param.C2;

clear param

% Z_R0_xy = fit([T_data,SOC_data],R0_data,'poly45');
% R0fit = feval(Z_R0_xy,[T_data,SOC_data]);
%% R0
%%
Fanction_R0 = scatteredInterpolant(T_data,SOC_data,R0_data);
R0_estim = Fanction_R0(T_data,SOC_data);

figure
hold on
plot3(T_data,SOC_data,R0_data,'ob');
plot3(T_data,SOC_data,R0_estim,'*r');

stem3(T_data,SOC_data,R0_data,'ob');
stem3(T_data,SOC_data,R0_estim,'*r');

legend('Real','Estimation')
xlabel('T')
ylabel('SOC')
zlabel('R0')
box on
grid on
view(-45, 45)

%% R1
%%
Fanction_R1 = scatteredInterpolant(T_data,SOC_data,R1_data);
R1_estim = Fanction_R1(T_data,SOC_data);

figure
hold on
plot3(T_data,SOC_data,R1_data,'ob');
plot3(T_data,SOC_data,R1_estim,'*r');

stem3(T_data,SOC_data,R1_data,'ob');
stem3(T_data,SOC_data,R1_estim,'*r');

legend('Real','Estimation')
xlabel('T')

```

```

ylabel('SOC')
xlabel('R1')
box on
grid on
view(-45, 45)

%%
%% R2
%%
Fanction_R2 = scatteredInterpolant(T_data,SOC_data,R2_data);
R2_estim = Fanction_R2(T_data,SOC_data);

figure
hold on
plot3(T_data,SOC_data,R2_data,'ob');
plot3(T_data,SOC_data,R2_estim,'*r');

stem3(T_data,SOC_data,R2_data,'ob');
stem3(T_data,SOC_data,R2_estim,'*r');

legend('Real','Estimation')
xlabel('T')
ylabel('SOC')
zlabel('R2')
box on
grid on
view(-45, 45)
%% C1
%%
Fanction_C1 = scatteredInterpolant(T_data,SOC_data,C1_data);
C1_estim = Fanction_C1(T_data,SOC_data);

figure
hold on
plot3(T_data,SOC_data,C1_data,'ob');
plot3(T_data,SOC_data,C1_estim,'*r');

stem3(T_data,SOC_data,C1_data,'ob');
stem3(T_data,SOC_data,C1_estim,'*r');

legend('Real','Estimation')
xlabel('T')
ylabel('SOC')
zlabel('C1')
box on
grid on

```

```

view(-45, 45)
%%
%% C2
%%
Faction_C2 = scatteredInterpolant(T_data,SOC_data,C2_data);
C2_estim = Faction_C2(T_data,SOC_data);

figure
hold on
plot3(T_data,SOC_data,C2_data,'ob');
plot3(T_data,SOC_data,C2_estim,'*r');

stem3(T_data,SOC_data,C2_data,'ob');
stem3(T_data,SOC_data,C2_estim,'*r');

legend('Real','Estimation')
xlabel('T')
ylabel('SOC')
zlabel('C2')
box on
grid on
view(-45, 45)
%%
%%
Name_fun='Z_batrey_info_lotfi';
save(Name_fun,'Faction_R0','Faction_R1',...
      'Faction_R2','Faction_C1','Faction_C2');
%%

%%

OC Fit

clc
clear
close all

load 'Z_BatteryModel.mat'; % Load the battery parameters

T_data = param.T;
SOC_data = param.SOC;

R0_data = param.R0;
R1_data = param.R1;
R2_data = param.R2;

```

```

C1_data = param.C1;
C2_data = param.C2;

clear param

% Z_R0_xy = fit([T_data,SOC_data],R0_data,'poly45');
% R0fit = feval(Z_R0_xy,[T_data,SOC_data]);
%% R0
%%
Fanction_R0 = scatteredInterpolant(T_data,SOC_data,R0_data);
R0_estim = Fanction_R0(T_data,SOC_data);

figure
hold on
plot3(T_data,SOC_data,R0_data,'ob');
plot3(T_data,SOC_data,R0_estim,'*r');

stem3(T_data,SOC_data,R0_data,'ob');
stem3(T_data,SOC_data,R0_estim,'*r');

legend('Real','Estimation')
xlabel('T')
ylabel('SOC')
zlabel('R0')
box on
grid on
view(-45, 45)

%% R1
%%
Fanction_R1 = scatteredInterpolant(T_data,SOC_data,R1_data);
R1_estim = Fanction_R1(T_data,SOC_data);

figure
hold on
plot3(T_data,SOC_data,R1_data,'ob');
plot3(T_data,SOC_data,R1_estim,'*r');

stem3(T_data,SOC_data,R1_data,'ob');
stem3(T_data,SOC_data,R1_estim,'*r');

legend('Real','Estimation')
xlabel('T')
ylabel('SOC')
zlabel('R1')
box on

```

```

grid on
view(-45, 45)

%%
%% R2
%%
Fanction_R2 = scatteredInterpolant(T_data,SOC_data,R2_data);
R2_estim = Fanction_R2(T_data,SOC_data);

figure
hold on
plot3(T_data,SOC_data,R2_data,'ob');
plot3(T_data,SOC_data,R2_estim,'*r');

stem3(T_data,SOC_data,R2_data,'ob');
stem3(T_data,SOC_data,R2_estim,'*r');

legend('Real','Estimation')
xlabel("T")
ylabel('SOC')
zlabel('R2')
box on
grid on
view(-45, 45)
%% C1
%%
Fanction_C1 = scatteredInterpolant(T_data,SOC_data,C1_data);
C1_estim = Fanction_C1(T_data,SOC_data);

figure
hold on
plot3(T_data,SOC_data,C1_data,'ob');
plot3(T_data,SOC_data,C1_estim,'*r');

stem3(T_data,SOC_data,C1_data,'ob');
stem3(T_data,SOC_data,C1_estim,'*r');

legend('Real','Estimation')
xlabel("T")
ylabel('SOC')
zlabel('C1')
box on
grid on
view(-45, 45)
%%
%% C2

```

```

%%
Faction_C2 = scatteredInterpolant(T_data,SOC_data,C2_data);
C2_estim = Faction_C2(T_data,SOC_data);

figure
hold on
plot3(T_data,SOC_data,C2_data,'ob');
plot3(T_data,SOC_data,C2_estim,'*r');

stem3(T_data,SOC_data,C2_data,'ob');
stem3(T_data,SOC_data,C2_estim,'*r');

legend('Real','Estimation')
xlabel('T')
ylabel('SOC')
zlabel('C2')
box on
grid on
view(-45, 45)
%%
%%
Name_fun='Z_batrrey_info_lotfi';
save(Name_fun,'Faction_R0','Faction_R1',...
      'Faction_R2','Faction_C1','Faction_C2');
%%

%%

```

